Representing local dynamics within water resource systems through a data-driven emulation approach

Shahin Zandmoghaddam

A Thesis

in

The Department

of

Building, Civil and Environmental Engineering

Presented in Partial Fulfillment of the Requirements

For the Degree of

Master of Applied Science in Civil Engineering at

Concordia University

Montreal, Quebec, Canada

November 2018

CONCORDIA UNIVERSITY

School of Graduate Studies

This is to certify that the thesis prepared

By: Shahin Zandmoghaddam

Entitled: Representing local dynamics of water resource systems through a data-driven emulation approach

and submitted in partial fulfillment of the requirements for the degree of

Master of Applied Science (Civil Engineering)

complies with the regulations of the University and meets the accepted standards with respect to originality and quality.

Signed by the final Examining Committee:

_____ Chair

Prof. S. Samuel Li

_____ Examiner

Prof. Luis Rodrigues

_____ Examiner

Dr. Mazdak Nik-Bakht

_____ Supervisor

Dr. Ali Nazemi

Approved by _____

Chair of Department or Graduate Program Director

December 2018 _____

Dean of Faculty

Representing local dynamics within water resource systems through a data-driven emulation approach

Shahin Zandmoghaddam

Abstract

Growing population and socio-economic activities along with looming effects of climate change have led to enormous pressures on water resource systems. To diagnose and quantify potential vulnerabilities, effective tools are required to represent the interactions between limited water availability and competing water demands across a range of spatial and temporal scales. Despite significant progresses in integrated modeling of water resource systems, the majority of existing models are still unable to fully describe the contemplating dynamics within and between elements of water resource systems across all relevant scales and/or variables. Here, a data-driven approach is suggested to represent local details of a water resource system through emulating an existing water resource system model, in which these details have been missed. This is through advising a set of interconnected functional mappings, i.e. integrated emulators, parameterized using the simulation results of the existing model at a common scale and/or variable but can support process representation with finer resolution and/or details. The proposed approach is applied to a complex water resource system in Southern Alberta, Canada, to provide a detailed understanding of the system's dynamics at the Oldman Reservoir, which is the key to provision of effective water resource management in this semi-arid and already stressed cold region. By proposing a rigorous setup/falsification procedure, a set of alternative hypotheses for emulators describing the local dynamics of local irrigation demand and withdrawals along with reservoir release and evaporation is developed. Findings show that emulators formed using Artificial Neural Networks mainly outperform simpler emulators developed for the variables considered. The non-falsified emulators are then coupled to represent the local dynamics of the water resource system at the reservoir location, considering the underlying interplays with hydro-climatological conditions and human decision on the irrigation area. It is found that emulators with input variables identified through expert knowledge can outperform fully data-driven emulators in which proxies were selected based on an input variable selection method. The top non-falsified coupled models are able to capture the dynamic of lake evaporation, water withdrawal, irrigation demand, reservoir release and storage with coefficient of determination of 0.80 to 0.82, 0.45 to 0.55, 0.52 to 0.59, 0.98 to 0.99

and 0.72 to 0.88, respectively. The practical utility of the proposed approach is demonstrated through an impact assessment study by analysing four performance criteria, corresponding to reservoir's storage, local irrigation demand, number of spill events and median reservoir release, in three stress-tests. These stress tests asses the local sensitivity of water resource system at the Oldman reservoir at three different levels, corresponding to (1) changing incoming streamflow to the basin in a bottom-up approach; (2) joint scenario of changing streamflow and warming climate, using a coupled bottom-up/top-down approach; and (3) specific changes in incoming streamflow, climate and irrigation area in a heuristic approach. For the first experimentation, weekly realizations for possible water availability are stochastically reconstructed and fed into the top non-falsified integrated emulator. By defining warm/dry, historical and cold/wet flow conditions, we found through alteration from dry to wet regime condition, the expected number of low storage duration is not changed, and expected annual water deficit is declined. Moreover, the expected number of spill events increases whereas median reservoir release increases. In the next impact assessment study, different scenarios of warming climate obtained from NASA-NEX downscaled global climate projections and the joint impact of changing streamflow and temperature on the system's behaviour is evaluated. This assessment demonstrated that in warmer climate, the expected number of low storage duration in dry condition increases whereas in historical and wet conditions, the low storage duration does not change. In addition, the expected annual water deficit increases while the expected number of spill events decreases in the three flow regime conditions. Moreover, the expected median reservoir release increases in the dry, historical and wet regime conditions. In the final level of assessment, vulnerability of the system under changing streamflow, climate including temperature and precipitation and changing irrigation area is assessed. Results show that increasing irrigation area combined with declining inflow can considerably increase the duration of low reservoir storage in the Oldman Reservoir. Increasing temperature can lead to decline in both reservoir storage and outflow. In addition, when combined with declining inflow, increasing temperature can severely increase the annual water deficit for irrigation sector. Furthermore, it is noted that although the performance of unfalsified models are identical in representing the dynamics of the Oldman Reservoir under the historical data, but assessment can be slightly to moderately different depending on the defined scenarios of change. This is due to the choice of model configuration and can address the uncertainty regarding the system's behaviour. Our study shows the promise of data-driven emulation approach as a tool for developing more enhanced water resource system models to face emerging management problems in the era of change.

Acknowledgment

I would like to thank my supervisor Professor Nazemi for his support and encouragement throughout the study and research. In fact I was honored to learn and experience a lot during the time I was doing this program.

Moreover, it was a great pleasure to have the support of Professor Elmira Hassanzadeh who was involved in this research. Without her passionate participation and input, the research could not have been successfully conducted.

In addition, this research was partially supported by Government of Quebec in terms of loan and bursary that provided to the author. The author also received funding from National Science and Engineering and Research Council through Discovery Grant obtained by my supervisor, Dr. Ali Nazemi. I also would like to thank Concordia University for funding this study through FRS and Concordia teaching award. Without these funding supports this research would have been remained undone.

Table of Contents

List of Figures

List of Tables

List of abbreviations

Artificial Neural Network	(ANN)
Bayesian Information Criterion	(BIC)
Bayesian network	(BN)
California Value Integrated Network	(CALVIN)
Coefficient of Determination	(R^2)
Cubic Meter per Second	(CMS)
Decision Support System	(DSS)
Dynamic Emulation Modelling	(DEMo)
Feed Forward Neural Networks	(FFNNs)
Global Climate Models	(GCM)
Groundwater Flow Model	(GFM)
Generalized Likelihood Uncertainty Estimation	(GLUE)
Gaussian Process	(GP)
Hydrological Models	(HMs)
Ideal Point Error	(IPE)
Integrated Emulators	(IEs)
Integrated Water Resources Management	(IWRM)
Integrated Water Resource Models	(IWRMs)
k-nearest neighbour	(kNN)
Linear Programming	(LP)
Logarithmic *RMSE*	$(LRMSE)$
Million Cubic Meter	(MCM)
Multiple Linear Regression	(MLR)
Nash-Sutcliffe Efficiency	(NSE)
Lethbridge Northern Irrigation District	(LNID)
Oldman River Basin	(OMRB)
Partial Correlation Input Selection	(PCIS)
Radial Basis Function	(RBF)
Relative Error	(REV)
Relative Error in Peak	(REP)
Root Mean Square of Errors	$(RMSE)$

South Saskatchewan River Basin	(SSRB)
System Dynamic	(SD)
Water Evaluation And Planning system	(WEAP)
Water Resource Management	(WRM)
Water Resource Management Model	(WRMM)

List of symbols

Emulator function for irrigation demand per unit of area	(dem)
Emulator function for lake evaporation	(eva)
Emulator function for reservoir release	(rel)
Emulator function for water withdrawal per unit of area	(wwd)

Chapter 1: Introduction

1.1 Background

Freshwater scarcity is now turning into a threat for the sustainable development of human society. In terms of potential impact, water crisis are currently considered as the largest global risk (Mekonnen and Hoekstra 2016). Most importantly, both water demand and water demand per capita, have increased drastically over the past few decades due to rapid population and socio-economic growth (Vörösmarty et al. 2010; McDonald et al. 2011). In parallel, climate change has significantly altered the regional characteristics of water availability (Arnell 2004; Falkenmark et al. 2007; Parry et al. 2007; Hurrell and Deser 2010; Beck and Bernauer 2011; Falkenmark 2013; Kundzewicz et al. 2018) and water demand (Vörösmarty and Sahagian 2000; Jackson et al. 2001; Kirk et al. 2002; Oki and Kanae 2006; Krausmann et al. 2009; Brownson et al. 2011). Human activities related to land and water management have also affected water availability across various scales (Nazemi and Wheater 2015a; b), which in some cases resulted into increasing imbalances between water availability and demand. The combination of these stressors, endanger water security (Döll 2002; Werritty 2002; Solomon 2007; Bates et al. 2009; Sušnik et al. 2015), which is often politically sensitive (Nazemi and Madani 2017) and may trigger national and international conflicts (Gemenne et al. 2014; Petersen-Perlman et al. 2017).

As stated in IPCC (2007), vulnerability is defined as the degree to which a system is not able to manage the unfavorable effects of water scarcity. Regionally, the imbalances between water demand and water availability are much more severe in semi-arid and arid regions. In these areas, along with natural water shortages due to specific climate and hydrological conditions, the ineffectiveness of water recourse management itself can be a major cause for vulnerability (AghaKouchak et al. 2015b; Lemieux et al. 2015). Under future climate change, precipitation is projected to decrease whereas temperature is expected to increase, which can in turn result in severe natural water shortage (Lee and Wang 2014; Vasseur et al. 2014). There are already relevant examples indicating the increase in water security crisis in arid and semi-arid regions, such as South Asia, the Middle East, Mexico, North East Brazil, Canadian Prairies and Africa, affecting agriculture, energy production, and water quality and quantity (Kusangaya et al. 2014; Selby and Hoffmann 2014). This issue results in significant amounts of economic and environmental losses in these regions (Bergstrom and Randall 2016; Carleton and Hsiang 2016; Hsiang et al. 2017).

To investigate the future challenges, decision makers require effective tools in order to take into account various scenarios for changing in climate, water availability and water demand at local and regional scales, and to foresee their potential impacts on water resource systems. Developing such models are urgent needs in the face of changes in natural and anthropogenic systems as they can help water managers to understand how different sectors would be affected under different scenarios of change and therefor can contribute in to development of sustainable water management strategies (Herrera-Pantoja and Hiscock 2015).

1.2. Statement of the problem

Effective water resource management should ensure the satisfaction of all of the water sectors with their demands, prevent water-related damages related to extreme events (e.g. floods and droughts) and maintain the resources for future human and environmental use. In many cases, these diverse objectives are in conflict and the goal of 'integration' demonstrates that resources management should be tackled from a broad perspective which includes conflicting objectives and competing water demands. The aim of integrated water resource management is therefore representing all potential trade-offs in system objectives and performance across different spatial and temporal scales (Pahl-Wostl 2007). Although various, so-called Integrated Water Resource Models (IWRMs) have been developed, current models include different levels of simplifications that result in inability to explicitly represent some of the details within water resource systems. For instance, water availability and demand are fed into IWRMs as prescribed inputs and as a result the physical processes behind these processes are not clear. As another example, evaporation is provided to models as constant input values and the link between available stored water and temperature is missing. One way to tackle this issue is developing new IWRMs which can address all the required details within water resource systems. This can be a time consuming approach and increases the model complexity. On top of that IWRMs are problem-oriented and they could be outdated when new details are required to be tackled. An alternative approach is to develop some sub-models that can be coupled with the original IWRM and are able to add the required details to the main model. These modules can be developed by replicating the results of the original model at common variables/scales and can address the required details within and between the main model.

The focus of this research is to reveal the local details within a complex water resource system located in a semi-arid region. Here, the specific goal is to represent the local interplay between water availability, water demand and water withdrawals, and their interactions with climate conditions and human decisions which are missed in the original integrated water resource model. A comprehensive model development protocol is proposed to configure a wide range of add-on modules to the original model. Then their performance is rigorously tested individually or in a coupled setting mode when non-falsified models for each variable are linked with one another. Then the practical utility of this approach is tested through stress-test analysis to reveal the impact of changes in natural and human conditions on the performance of the water resource system. Different scenarios of impact assessment are employed to evaluate the performance of the system to changing natural and anthropogenic changes that are taking place outside or within the selected water resource system.

1.3 Research purpose and objectives

The purpose of this research is to provide a detailed understanding of the dynamics within a complex water resource system located in a semi-arid region. This is done through developing and adding add-on modules to the original model that are able to address the required details that are missing in the main model. The specific objectives are:

1. Developing a wide range of add-on modules that are able to address specific details regarding local lake evaporation, water withdrawal and demand as well as reservoir release within the selected water resource system. A two data-driven approach, i.e. Artificial Neural Networks and Multiple Linear Regression, is used to develop add-on modules.
2. Coupling the developed modules with one another to establish a wide range of models that can represent the local behaviour of the selected system.
3. By applying a reductionist approach, coupled models are falsified and top non-falsified models are selected to assess the vulnerability of the system.
4. Through defining various scenarios of change in hydroclimatic and anthropogenic variables the impact of changing scenarios on the system's performance is investigated. The impact assessment is run in three levels using bottom-up, coupled top-down/bottom-up and bottom-up approaches:

4.1. In the first level of scenario assessment, the sensitivity of the system to changing streamflow is evaluated.

4.2. In the second level, changing scenarios of temperature are included in the impact assessment study. By obtaining temperature data from NASA-NEX downscaled global climate projections, the joint scenarios of changing streamflow and temperature are defined and the response of the system to changing hydroclimatic variables is assessed.

4.3. The third scenario assessment is related to analysing the system's performance under changing streamflow, climate (temperature and precipitation), and human intervention manipulated in irrigation area. In other words effects of changing hydroclimate and anthropogenic conditions is evaluated in this scenario assessment.

5. The last objective of this thesis is to compare the performance of nan-falsified models under the same scenarios of change and to check the uncertainty regarding the performance of top selected integrated emulators.

1.4 Expected contribution

This research aims at developing a tool with which it would be possible to address the missing details within a water resource system where and when needed. These details are missed in the main water resource management model that is currently used in this water system. With the approach applied in this study the missing details are found without developing new models. This approach can be used until an improved integrated model would be available. In addition, this tool is a transitional solver which can be used to assess the impact of unseen drivers on a water system behaviour which cannot be addressed in the main model. Moreover, the contribution of this research in water resource engineering is that the developed model can be used for long term planning and management, understanding the risk of a water resource system under natural (climate variability and change) and anthropogenic (human decision on changing the area of irrigation districts) stressors on the behaviour of a water system. As an example, with the developed model, it would be possible to assess the effect of changing streamflow, temperature and irrigation area on behaviour of a water resource system.

1.5 Layout of the thesis

Chapter 2 reviews water security issues due to the imbalance between water availability and demand, discusses how IWRMs are developed, and demonstrates the logic behind emulation approach. Chapter 3 introduces the case study, along with available data and existing IWRM, for which emulation models are developed to better represent the local details at a critical part of the system. Chapter 4 provides a rationale for developing emulators for such applications and briefly introduces methodological elements used in this thesis for setting up these models. In Chapter 5, the model development protocol is proposed to systematically build alternative emulation models for different water sectors, and to falsify them based on their performance in individual and coupled modes. Chapter 6 provides the results of modeling attempts, which leads to a suite of non-falsified surrogate models for representing the local dynamics within and between water sectors at the Oldman Reservoir. Chapter 7 uses these emulation models for impact assessment study and in the context of stress-test analysis, and shows the influence of various scenarios of (1) changing water availability (2) changing water availability along with climate and (3) changing water availability, climate and human management on the system's performance. Finally, Chapter 7 concludes the study and provides further remarks.

Chapter 2: Literature review

In this chapter the focus is on water resources system vulnerability due to imbalances between water availability and demand, in particular in arid and semi-arid regions and the assessment of the impact of changing conditions on water security. This leads to the urgent need for diagnosing and proposing improved management strategies to achieve food and water security. For this purpose, the concept of Integrated Water Resources Management (IWRM), which is the process of development and management of freshwater supply and demand and understanding their interplay with natural and human conditions is introduced. The last part reviews the approach used through which the required details within a water resource system can be addressed. In addition, this section illustrates the theories, methods, and implementations of this approach in environment and water resource management modeling.

2.1. Vulnerability in water resource systems

Regional water resource systems are under an unprecedented pressure due to changing climate and anthropogenic conditions (Elliott et al. 2014; Haddeland et al. 2014; Schewe et al. 2014). This pressure arises from water scarcity, which by definition means lack of available freshwater compared to existing water demand. This can result in extensive ecological and human livelihood crises (Gleick 1998). Natural and anthropogenic factors are considered as key drivers of water scarcity (Falkenmark et al. 2007; Falkenmark 2013). Climate variability and change are natural sources of water scarcity. Climate variability is change in naturally-occurring, often periodic, patterns of atmospheric and oceanic variability, such as El Niño-Southern Oscillation and the North Atlantic Oscillation, which is leading to significant variations in weather and climate throughout a great part of the earth over inter-annual timescale (Hurrell and Deser 2010). Temperature and precipitation change are caused by climate variability which have effects on droughts and floods. A relevant example is Sahel droughts, in which Sahel region of West Africa is faced with a multi-decadal decline in total annual rainfall (Janicot et al. 1996). Also, in case of warming condition climate variability can have significant consequences in the regions where snowpack is the main source of water budget (Barnett et al. 2004). Stewart et al. (2005) showed that in Pacific Northwest where snowmelt dominates river flows, temperature rise increased runoff in winter whereas less runoff was occurred in summer. In addition, earlier peak snowmelt, runoff and soil moisture recharge in spring were other consequences of climate variability. According to Merritt et al. (2006) in Okanagan River Basin, Canada the major consumptive water use is irrigation while

increased temperature as a result of climate variability has resulted in significant environmental and economy costs for the region. This study showed warming climate make imbalances between water availability and demand.

Human and natural factors are main drivers of change in atmospheric greenhouse gasses and aerosols, land surface properties and solar radiation which affect the energy balance of the climate system resulting in climate change. Human activities such as fossil fuel use and land-use change as well as agricultural activities and natural drivers due to solar activity and volcanoes have increased the global atmospheric concentration of carbon dioxide, methane and nitrous oxide contributing to climate change (Climate change 2007; Parry et al. 2007). Potential regional impacts of climate change are considered as increased magnitude and duration of floods and droughts, changes in precipitation, temperature, humidity, soil moisture and duration of accumulated snowpack (Solomon 2007). Climate change increases temperature which directly affect evapotranspiration and atmospheric water storage. Therefore, this leads to potential change in magnitude, frequencies and intensities of rainfall. In addition, the seasonality and inter-annual variability and spatial distributions of rainfall are affected due to climate change.

Climate change have effects on water availability and demand. Schewe et al. (2014) used an ensemble of global hydrological models as well as the latest greenhouse-gas concentration scenarios to assess the effect of climate change on water availability. They concluded that climate change exacerbates the regional and global water scarcity remarkably and showed that in case of climate warming of 2 °C above present, additional 15% of population of the world will be faced with severe water shortage and will live under the absolute water scarcity. Studies have carried out to understand the impact of climate change on irrigation water demand in various spatiotemporal scales. Al-Najar and Ashour (2013) analysed the impacts of temperature and precipitation change on irrigation water demand in an orchard crops (olive, palm, grapes, citrus and guava) in Gaza Strip, Lebanon. They concluded that increased temperature by 1 or 2 °C rises the annual average evapotranspiration by 45 or 91 mm leading to 3.28 or 6.68% growth in irrigation requirements. In addition, Wada et al. (2013) used seven global hydrological models to assess the effect of projected global climate change on irrigation water demand. Their results showed an increasing trend in the future irrigation water demand while the increase is substantially dependent on global warming and regional precipitation patterns. Based on their findings, under the highest greenhouse gas emission scenario, irrigation

water demand increases during the summer in the Northern Hemisphere and the maximum demand shifts almost a month or more. Accordingly, it can be concluded that irrigation water demand increases due to increased evapotranspiration and decreased soil moisture which occurs under warmer climate conditions.

In addition to irrigation water demand, climate change affects industrial, domestic and ecological water demand. The majority of industrial water need is used for cooling purposes while due to climate change and warming climate condition, water temperature rises and its efficiency in cooling process declines. This results in the additional need for water supplies in order to compensate for decreased efficiencies of cooling systems. Residential purposes, in-house water use for drinking, bathing, etc., is considered as domestic water demand which is supposed to increase due to projected rising temperature and evapotranspiration. However, this change is not significant in many regions due to increased precipitation resulting from climate change. Moreover, water demand for ecological system protection and environmental maintenance is defined as ecological water demand which is subject to increase due to increased evapotranspiration and water temperature. In general, it can be concluded that climate change increases different sectors' water demand (Wang et al. 2016).

In addition, climate change can considerably affect human health, energy supply, fisheries, forestry, etc., (Olmstead 2014). The dryer and warmer a region becomes, the water is less available and the amount of water demand is higher. This will influence irrigation, which is the largest water use sector, and affects future water and food security (Döll 2002; Werritty 2002; Solomon 2007; Bates et al. 2009; Change 2014; Sušnik et al. 2015).

Anthropogenic factors putting pressure on water resource systems are considered as developing socio-economic activities, population growth, land use and land management as well as human intervention in terrestrial water cycle. Intensive socio-economic development, such as agricultural and industrial activities, energy production, and municipalities are sectors of water consumption facing rapid expansion which heightens water demand (Tilman 1999; Kirk et al. 2002; Brownson et al. 2011). Moreover, during the 20th century, there was a significant increase in population and the size of the global economy. In brief, the global population hit 6.2 billion and global economic output was raised over 20-fold (Jackson et al. 2001; Oki and Kanae 2006; Krausmann et al. 2009). Vörösmarty et al. (2000) conclude that the future relationship between water supply and demand is greatly dependent on the forthcoming change in global-scale

population and economic development. Land use and land management have also altered the global environment. Almost half of the ice-free land surface have been transformed into agricultural and urban systems globally. Deforestation, as an example of land transformation, has raised the concentration of atmospheric carbon dioxide, which contributes to climate warming (Vitousek et al. 1997; Carpenter et al. 1998; Chapin Iii et al. 2000). Another anthropogenic factor affecting global water supply is human intervention in terrestrial water cycle. Through construction of dams and water withdrawals for agricultural, industrial and domestic purposes (water resource management), human significantly changes the local or regional dynamics of water cycle. In brief, human intervention in terrestrial water cycle, in particular alters the timing of the released flow from man-made reservoirs (Nazemi and Wheater 2015a). In addition, construction of dams and reservoirs is leading to the trapping of freshwater runoff, loss of surface runoff to groundwater, corresponding to impoundment, increased evaporation from reservoirs and the changing of the overall water budget of catchments (Vörösmarty and Sahagian 2000). Haddeland et al. (2014) analysed direct human and climate change impacts on terrestrial water cycle using seven hydrological models that had been forced with multiple climate projections. Results showed that in some regions such as parts of Asia and western United States, the direct human impacts on water cycle is the same or even more severe than moderate levels of global warming. Moreover, a research conducted by Fekete et al. (2010) showed that the impact of human intervention through construction of dams in some water systems is equal or even more severe that the impact of climate change in the next 40 year period.

Water scarcity is more evident in arid and semi-arid regions where precipitation is less than potential evapotranspiration. In these regions there is a significant pressure on water supplies and the competition is severe between different sectors such as agriculture, domestic and industry to satisfy their water needs. In addition, historical land use has degraded soil in arid and semi-arid regions resulted into low soil quality and its poor structure. Salinity, erosion, degradation due to human activity and loss of soil water storage are major threats to soils in these regions (Garcia-Franco et al. 2018). In fact, semi-arid and arid regions are facing disastrous consequences of water shortage such as declined standard of life, biodiversity loss, land degradation and migration (Azarnivand and Chitsaz 2015). Moursi et al. (2017) used a probabilistic assessment of changing climate on water shortage in the Sevier River Basin of Utah, USA. This semi-arid region is faced with high agricultural water demands and the water supply in the basin is mostly snowmelt-driven. Thirty one general circulation models have been

used to assess the vulnerability to water scarcity in the study area for the whole twenty-first century. Results demonstrated that off-season precipitation and temperature are the most sensitive factors which affect water shortage in the basin. In addition, a considerable probability of water shortage was found for the period 2025 to 2049. Faramarzi et al. (2017) analyzed uncertainties in water supply in another semi-arid region, Alberta, Canada. Major geo-spatial heterogeneity and hydrological features were included in the study. They assessed the effects of climate, vegetation and glaciers as natural factors as well as irrigation, dams and industrial development as anthropogenic factors on water scarcity in water resources in the basin. They found severe water scarcity in spring and summer months due to agricultural activities while in winter months the scarcity is resulted from demands of petroleum or other industries. In addition, their results showed over exploitation of the groundwater in southern sub-basins.

The mentioned stressors and pressures on water supplies coupled with the increasing trend on water demand make water resource systems vulnerable and create serious water security threats and introduce challenges to water resource management. In particular, these threats are more highlighted in complex water resource systems that include a great amount of details. This results in the need for assessment of the vulnerability of water resource systems to climate change and is aimed at development of policies in order to reduce the risks resulting from climate change. The two crucial responses from the vulnerability impact assessment studies are limiting global climate change by controlling and reducing the related stressors and moderating the effects of unavoided consequences by applying a wide range of policies that are targeted at a vulnerable system. As an example, Gosain et al. (2006) conducted an impact assessment study on the water resources of Indian River systems and showed that under the different greenhouse gas emission scenarios a general reduction in the available runoff is expected. In another study on the Yakima River Reservoir system in USA, (Vano et al. 2010) simulated the effects of climate change on irrigated agriculture and found increased water shortage for the short, middle and long temporal perspectives under different scenarios of climate warming.
The above mentioned discussions on the limited water availability and increasing water demand are resulted in vulnerability of water resource systems as well as some serious water security threats which indicates concerns regarding potential harmful states of both human and natural water systems (Hall and Borgomeo 2013). A majority of the world's population confronts a high-level of water security which by definition is an acceptable level of water-related risks to humans and ecosystems. Based on this definition, we need adequate quantity of water with acceptable quality to support livelihoods, ecosystems, human health and national

security (Bakker 2012). Therefore, it brings about a crucial need for water resource planning and management in particular in arid and semi-arid regions in order to decrease water scarcity, increased water and food security and assessment of changing conditions on water security. In order to manage water resource systems, decision makers need practical tools to simulate the systems' behavior and analyse the potential threats under different scenarios of change. Next section introduces the need for water resource management and explains different methods which are widely taken for assessment of water resource systems.

2.2. Integrated water resource management models

Loucks et al. (2005) argue that limited water quantity and deteriorating water quality have constrained countries around the world to revise their development policies based on the management of their finite sources of water. This means that Water Resource Management (WRM), which has been considered as a supply-oriented, engineering-based approach, has been experiencing a change to a demand-oriented, multispectral approach, which can be described as integrated water resources management. In other words, IWRM has evolved from a water master planning to a comprehensive water policy planning. The previously used method is a top-down management approach, whose main focus is on water availability and development, whereas the more recent method concentrates on comprehensive water policy planning, which addresses the dynamic between subsectors, explores priorities, and builds management capacity.

During 1990s members of water professions began to appreciate that water problems are multi-dimensional, multi-sectorial and multi-regional. This is due to the fact that water raises interest in multiple sectors that have multiple causes and/or agendas. As a result, water as a natural resource should be considered holistically and be managed across sectors, with wide participation in decision making (Giordano and Shah 2014). This resulted in the idea of integrated water resource management and more refined definition for IWRM (Biswas 2004). The Global Water Partnership (2000) defines integrated water resource management as "a process which promotes the coordinated development and management of water, land and related resources, in order to maximize the resultant economic and social welfare in an equitable manner without compromising the sustainability of vital ecosystems".

In order to practically implement the integrated management strategy in a water system, practical tools that integrate knowledge about all the components of the system are required. This have resulted in developing integrated water resource management models. In brief, integrated assessment is an approach for assessing the trade-offs within components of a water resource system such as water and land related management options and stakeholders engagement. With this approach, water managers are provided with information that is required for diagnosing potential vulnerabilities and advising improved management strategies for facing future water security threats and decision making processes (Pahl-Wostl 2003). Nikolic et al. (2013) explained that in order for these model to totally fulfill the thorough definition and displayed standards, the IWRM modeling process requires (1) formation of feedback system structure to understand the dynamic of water resource system's nature, (2) having adequate temporal and spatial scales and (3) engaging stakeholders in the decision making process.

So far, substantial progresses has been made by the integrated assessment strategy. For this purpose various integrated water resource management models have been developed and employed around the world. These models are able to integrate knowledge from different disciplines to address multiple cause effect relationships within a water system. IWRM modeling needs a generic, multi-faced modeling approach and it is more valuable when economic and environmental objectives are combined. Harou et al. (2009) explained that models that integrate different aspects of a water systems, such as hydrology, environment, engineering and economy, are called hydro-economic models. In brief, these models are able to capture the interaction between water and economy. Moreover, hydro-economic models assess the effects of economic water use on water availability and quality in the both short and long run (Brouwer and Hofkes 2008). These progresses in IWRM modeling resulted in capability of models to include various aspects and components of water systems such as water quantity and quality, environment, economy and stakeholder's participation in decision making processes.

To implement integrated water resource management, simulation, optimization or coupled simulation/optimization models are applied. Various methodologies have been widely used to develop optimization and simulation models such as System Dynamics (SD), Bayesian networks, coupled component models, agent-based models and knowledge-based models (Kelly et al. 2013). These methods are widely used mainly due to their simple modification characteristic. To be more precise, based on the structure of these models, when inclusion of

new components to the model is required it is possible to modify the model with affordable necessities. Table 1, presents the integrated models that have been developed so far and explains the techniques and methodologies used for model development and demonstrates the components that have been included in models.

Table 1. Techniques, methodologies and components applied to develop integrated water resource management models.

Author (Year)	Location	Model type	Method	Components
Graveline et al. (2014)	Gállego catchment, Spain	Simulation	Linear programming algorithm	Water quantity, economy
Varela-Ortega et al. (2011)	Upper Guadiana, Spain	Simulation	Linear programming algorithm (weap)	Water quantity, economy
Gober et al. (2010)	Phoenix, USA	Simulation	System dynamic	Water quantity, stakeholder participation
Schreinemachers and Berger (2011)	Chile, Germany, Ghana, Thailand, Uganda, and Vietnam	Simulation	Agent-based model	Environment, water quantity, economy
Lam et al. (2004)	Seymour reservoir, Canada	Simulation	knowledge-based model	Environment, water quantity, water quality
Guan and Hubacek (2008)	North China	Simulation	System dynamic	Water quantity, water quality, economy
Molina et al. (2010)	Murcia, Spain	Simulation	Object-Oriented Bayesian Networks	Water quantity, economy, stakeholder participation
Qin et al. (2011)	Shenzhen, China	Simulation	System dynamic	Environment, water quantity, water quality
Xue et al. (2017)	Northwest China	Simulation	Bayesian networks	Environment, water quantity, stakeholder participation
Molina et al. (2011)	South east Spain	Simulation	Bayesian networks	Environment, water quantity, economy, stakeholder participation
Van Delden et al. (2009)	Guadalentín, Spain	Simulation	Coupled component models	Environment, water quantity, water quality, economy, stakeholder participation

Cai et al. (2002)	Syr Darya River Basin, central Asia	Optimization	Genetic algorithm and linear programming	Environment, water quantity
Wang et al. (2009)	Haihe River basin, China	Optimization	Hybrid genetic algorithm	Environment, water quantity, economy
Draper et al. (2003)	South California water system, USA	Optimization	Linear programming algorithm	Environment, water quantity, economy
Cai et al. (2003)	Maipo River Basin, Chile	Optimization	General Algebraic Modeling System	Environment, water quantity, water quality, economy
George et al. (2011)	Krishna Basin, India	Simulation-optimization	Linear programming algorithm	Water quantity, economy
Ferreyra et al. (2008)	Ontario, Canada	Simulation-optimization	Linear programming algorithm	Water quantity, water quality, stakeholder participation

Simulation models address "what-if" scenario situations to assess design or operating strategies. Simulation models are relatively precise tools for the investigation of various conditions such as different scenario assessment. They are ideally suited to explore specific management strategies and are of quantitative understanding and have the capability of simulating field behaviour. If properly designed in a common framework, it is possible to develop, test and employ simulation models of components of a larger water resource system and then compile or link them together to investigate more integrated decisions and behaviours. To be more precise, simulation models can assess the effects of alternative water management strategies (Loucks et al. 2005). One critical characteristic for simulation models is that they permit the examination of the impact of future changes in the water resources systems (Heinz et al. 2007) which have resulted in numerous examinations of water resources systems under various scenarios and policies (Marques et al. 2006; Kalbus et al. 2012). As an example of integrating water quantity and economy components of a catchment, Varela-Ortega et al. (2011) conducted a research in the Upper Guadiana basin located in a central arid region of Spain, for the purpose of conserving groundwater resources. The competition for water between different sectors has risen social conflicts over the years in this arid region. The developed simulation based model was able to integrate an economic and a hydrology model, WEAP (Water Evaluation And Planning system), to evaluate the spatiotemporal effects of water and agricultural policies regarding different climate scenarios. Their model was able to predict the response of the system at local and regional scale and in both short and long run.

Their results showed that under current water withdrawal policy water supplies are not able to satisfy rural communities' water demand. In another study, Graveline et al. (2014) proposed an integrated hydro-economic model which couples physical (hydrology) and economic processes (agricultural water demand, reservoir operation) to assess the effect of global climate change and policy options on water scarcity and the agricultural economy in the Gállego catchment in Spain. A linear programing algorithm was the method applied in the simulation model and the authors evaluated different scenarios of ongoing changes in climate conditions, hydrology and agriculture. They found that in order to mitigate the negative impacts of climate change on irrigation districts, modernization of irrigation technology would be a practical approach. In addition, their findings showed the ineffectiveness of a planned reservoir extension project.

Gober et al. (2010) used WaterSim, a system dynamic based simulation model, to study the role of climatic and uncertainty about the consequences of climate change in the water management process in Phoenix, USA. This study assessed the impact of different climate scenarios on the catchment's water budget and identified various policy options to confront climate uncertainties. Their model included participation of policy makers and stakeholders in decision making process. The article argued that instead of searching for the optimal solution for a single reasonable set of future outcomes, actions should be taken to look for adaptive behaviors to manage the risk regarding the uncertainty around future climate. Results of the study showed that under most of the defined scenarios, per capita water use could not be supported anymore and that prompt action must be taken since Phoenix's water security was under serious threat, due to global warming and population growth. Schreinemachers and Berger (2011) extended the integration concept by including environment, water quantity, and economy component of water systems and developed a software package, which is an agent-based simulation model, and is built on a decision-making platform in agricultural systems. The model has an empirical application and has been used in different study sites such as Germany, Thailand and Vietnam. The purpose of this study was to understand how agricultural technology, environmental change and management policies affect the population of households. The combination of microeconomic modeling approach and the choice of alternative biophysical modules make this software package unique.

Lam et al. (2004) developed a knowledge-based model for watershed management to evaluate the water quality consequences regarding various proposed policy strategies. The model was

able to integrate environment, water quantity, and water quality components by integrating hydrological, agricultural, hydrodynamic, transport and dispersion, and water quality modules to simulate sediment transportation and water quality for the Seymour reservoir, B.C., Canada. Using a simulation model, Guan and Hubacek (2008) presented an analytical approach that linked an economic system with a hydrological system in North China, with the ability of analysing interactions between the two systems. Their hydro-economic analytical framework allowed tracking the amount of input water to the catchment, which was being consumed, and the pollution, which was leaving the catchment. This model was developed to assess water quantity, water quality and economy elements of the system. In another study, Molina et al. (2011) included other aspects of integrated modeling by developing an integrated model to assess the issue of water management in an overexploited aquifer in south east Spain, where interdisciplinary examinations, in view of integrated methodologies, were required. To evaluate the hydrological behaviour of the system, a groundwater flow model was used. In parallel, to determine the impacts of various management scenarios on environmental, economic, and social aspects in the study area, a decision support system using Bayesian networks was built. This integrated model created a robust tool to assess sustainable alternatives for the damaged aquifer. Then management strategies were selected to evaluate their possible impact in future water management scenarios. Their results suggested a drastic change in the groundwater abstraction to long term sustainability of the aquifer. This model was developed to look at water quantity, economy and stakeholder participation in decision making processes within the water resource system. To understand the integrated socio-economic and water management system in Shenzhen River catchment in China, Qin et al. (2011) developed an integrated model that incorporated environment, water quantity and water quality components with the system dynamic platform. The model was able to assess the effects of the growing population and the socio-economic development for the succeeding 10 years on both water resources and water quality. The model was capable of replicating the interactions between social, economic, supply, and environmental issues, plus the pollutant convection in the river.

In order to couple ecosystem services into integrated water resource management, Xue et al. (2017) proposed an ES–based IWRM framework, based on a Bayesian network approach. The model was developed, evaluated, and applied with the participation of stakeholders, water managers, water management experts, and the research team in Qira oasis area, Northwest China. The area is faced with an intense competition between human activities and natural

ecosystems. Results demonstrated that the model could successfully integrate ecosystem services into the IWRM framework with the engagement of different water users. Molina et al. (2010) developed an integrated simulation model for a semi-arid water system in the Altiplano region of Murcia in south east Spain. In this area, agriculture and tourism are the main consumer sectors of water, while the region relies on groundwater resources. In addition, water deficit is extreme and water abstraction exceeds recharge. The aim of the study was to build a Decision Support System (DSS) using Object-Oriented Bayesian Networks technique in order to improve decision making to engage stakeholders, enabling water managers to identify water supply scenarios to find the best policies for the area and integrating hydrological, economy, and social factors. The study assessed the impact of a range of management interventions and showed efforts should be made for Stakeholder participation in decision making processes. Van Delden et al. (2009) increased the number of assessing components of a water system including environment, water quantity, water quality, economy, and stakeholder participation to developed a flexible modelling framework (DeSurvey IAM) for Guadalentín river basin in Spain, which incorporated various pre-existing model components such as hydrology, climate, water management, erosion, salinization, land use, irrigation, (coupled component models). This model had various spatiotemporal scales with a temporal resolution varying between minutes and years and spatial scale from regional to local (1 ha) levels. The model was able to capture the non-linear behaviour of a system, had the flexibility to configure integrated models while highly improving user interaction. This tool has been developed for strategic planning and supporting long-term development of integrated visions within the basin or for the region. By increasing the number of options, simulation models are not able to evaluate all possible alternatives and the number of required runs increases drastically. Even by using the most efficient simulation software, reducing the time and cost of a simulation run will not solve this issue. To find a solution in a large complex space of various combinations, optimization models are required. They usually benefit from simpler formulations of the system, in comparison to simulation models.

To maximize financial proficiency (Alvarez et al. 2004; Moghaddasi et al. 2010) and/or potentially minimize the hazard in environmental protection (Fang et al. 2010; Chang et al. 2011), the optimization method is regularly applied. Optimization method addresses “what’s best” scenarios and the system objectives are formulated as an optimization problem. Optimization models may be useful in recognizing the decision-variable values, which address the best plan, considering assumptions included in the model. As an example, in order to find

sustainable development patterns in irrigative basins, Cai et al. (2002) used quantified sustainability criteria to form a new optimization modeling framework of the Syr Darya River Basin in central Asia. The method used to develop the model was a hybrid genetic algorithm and linear programming method. The model ensured long-term and flexible water supply capacity in order to satisfy crop water demands as well as industrial and municipal water needs with minimized negative environment consequences due to irrigation. Using the model's output, they proposed long-term reservoir operations, facility improvement and crop pattern change. Moreover, they showed that long-term water and soil salinity are quite sensitive to irrigation expansion and even a small development in irrigation area without investments in infrastructure advancement can have negative impacts on environment. Their model was considering water quantity and environment whereas IWRM needs a broader modeling approach.

Wang et al. (2009) developed a nonlinear optimization model to allocate water resources among competing users at the basin scale that also accounted for environmental water demand. The model was developed using a hybrid genetic algorithm and applied to the Haihe River basin in China. Implementing this approach they were able to consider economic, social and eco-environmental objectives and provide better results in comparison to other simple linear programming solutions through the integration of all the objectives simultaneously. They also proposed a forecasting method in order to predict industrial and domestic water needs and at the same time, the model performed better results in comparison to previously developed models due to incorporation of various forecasting methods. Another economic-engineering model (California Value Integrated Network - CALVIN) was created by Draper et al. (2003) for the South California water system, USA. This is a large-scale optimization model that uses linear programing algorithm to optimally allocate available water to demands in a great spatial scope. Having considered the physical, environmental and policy aspects of the state, the model allocated surface and groundwater resources over the historical hydrologic record, to maximize the economic indices of agricultural and urban water use. The model was created for providing of planning information that previously was not available due to loosely knitted mix of separate models whereas by its integration policy and including various components of the water system, this model showed much greater spatial scope and detail in comparison with previously developed models. The model included environment, water quantity and economy components of the water system. Cai et al. (2003) included water quality component and developed an optimization model implementing general algebraic modeling system method to integrate

hydrologic-agronomic-economic components for the Maipo River Basin, a key agricultural region in central Chile. To have a better understanding and management of the basin, the model had several components. Flow and pollutant transport, irrigation and drainage processes, investment on infrastructure and institutional management governing water policies and environmental water use were the main aspects that the model was able to address. Results of the study proved that in order for farmers to have more economic proficiencies, investment in improvement of irrigation technologies and selling surplus water to urban areas is required.

Nevertheless, optimization models have their own limitations and require simplifications, in order to take optimization solution algorithms into consideration. Joint simulation-optimization strategies permit optimization models to recognize promising mixes of choices, to test and refine the results of the simulation model (Heinz et al. 2007). In Addition, in some cases, it is necessary that the solutions of optimization models be examined in more details through the use of simulation models. As an example, in order to assess different policy scenarios for the water allocation to some sources of demand, George et al. (2011) linked a simulation-based model (network allocation model which uses a fast network linear programming algorithm) with an economic model (Cost Benefit economic model), in the Krishna Basin, India. Their study showed that the coupled models present a more complete analysis and is capable of supporting decision making, in comparison to other previously used uncoupled models. In fact, the model results was superior to other models due to considering the concept that water should be looked at as an economic good and should be allocated with respect to its value. With this approach, policy managers can make judgments in terms of both water security and economic value. They concluded that in the basin, completion for water amongst different sectors is very high and is getting more intense in the future due to the low value of water in agricultural zones resulting in high tendency to transfer water to urban users. To analyse agro-environment policies to secure water quality in the Province of Ontario, Canada, Ferreyra et al. (2008) applied an integrated framework. In this study, the strategy included participant observations, document analysis, and semi-structured interviews. They concluded that exploration and examination of new ways to link watershed needs to current socially and politically meaningful scales in agricultural areas was warranted. Water quantity, water quality and stakeholder participation were integrating components of the model.

As presented above, simulation, optimization or coupled simulation optimization techniques with different methodologies used to develop integrated water resource management models

and were used to tackle a specific problem. For any specific case and problem, a unique model was developed and used while for the assessment of a new sort of details within a system a different model was being developed. This presents that IWRMs are mainly developed based on a specific problem or particular details. In the requirement of any new details, the models should be redesigned from scratch and the already available models are not able to be applied. In addition, despite substantial progress, integrated water resource models often undergo various levels of simplifications, which results in the ignoring of some of the existing details in representing water resource systems (McIntosh et al. 2011; Simonovic 2012). For instance, information related to water availability and demand are often provided to integrated water resource models as prescribed inputs; therefore, physical processes driving these variables are not considered. Also, the dynamic between some processes within a water system may not be known. As an example, the link between water supply and water demand/withdrawal may be unknown or the effect of climate on some processes in a system (e.g. irrigation water demand and withdrawal) may be unexplained. In addition, water can be used for in-stream e.g. hydropower generation and recreation, or off-stream purposes e.g. agricultural, industrial and municipal demands. These processes have different time resolutions. For instance from hydropower generation to agricultural activities time scale varies from hourly to weekly or monthly. In order to incorporate these processes in integrated water resource models, the processes with finer resolutions are often lumped in a way to have the same resolution as the processes with coarse resolution. Moreover, these models are regularly developed to analyse water systems regionally or globally (including various number of lakes and reservoirs), whereas it may be necessary to assess the behaviour of a local reservoir or lake in a basin. To overcome these and other limitations in IWRMs, one approach is to develop new models that take into account all of the required details, which is obviously time consuming and substantially increases the modeling complexity. In some cases, the simulation process takes a great amount of time due to unavailability of adequate computational hardware. In addition, as IWRMs are often problem-oriented, they become outdated when a new process and/or detail needs to be represented (Sterman 2000).

An alternative approach would be to build new generic sub-models, that can be coupled with the original IWRM, to describe the required details only where and when needed. These modules include new functionalities to represent the required details at the scale of interest. This is done with emulation approach which its definition and application is discussed in the next subsection.

2.3. Emulation Approach

To tackle the shortcomings of IWRMs and having better representation of water systems, emulation approach can be applied. By using this approach, new sub-models are developed that are coupled with the original model and are able to add required details of interest to the original model. These "adds-on" modules can be seen as model emulators that replicate the result of the original IWRM at a common scale and/or variable; but, they include new functionalities to represent the required details at the scale of interest (Castelletti et al. 2011; Hamilton et al. 2015). In brief, the aim of emulation is to establish trackable surrogate models that adequately represent the main dynamics of the original model (Castelletti et al. 2012a; Castelletti et al. 2012b; Machac et al. 2016). Ratto et al. (2012) argue that emulation is a vital and extending zone of research and represents one of the real advances in the investigation of complex mathematical models, with applications ranging from model reduction to sensitivity analysis or increasing details within a system.

The application of this approach can be traced back to Blanning (1975), who argued that it is possible to utilize the information produced by past simulations for developing a new model that addresses some of the limitations in the past model, particularly with respect to reducing complexity and/or adding new details. In the context of water resource systems, this can be achieved through two distinct approaches based on emulating the structure (i.e. structure-driven) or the simulation results (i.e. data-driven) of the original model. The structure-driven method is based on manipulating the high-dimension equations of the process-based model, onto simplified lower-dimension space. This method is mostly used for linear and weakly non-linear models (Rudnyi and Korvink 2002; Phillips 2003). In addition, Castelletti et al. (2012b) argue that structure-driven emulator is basically used in management problems. In addition, due to the strong non-linearity of the environment field, structure-driven dynamic emulation modeling has been restrictively adopted (Crout et al. 2009; Siade et al. 2010).

In a data-driven approach, the emulator is defined based on a data set of input and output samples which have been generated by the main model. The data-driven emulation technique is more powerful and flexible, in comparison to a structure-driven technique, due to its ability to deal with the non-linear relationship between input and output (Ratto et al. 2007). In comparison to the structure-driven technique, this method has been explored largely for environment modeling purposes. As an example, van der Merwe et al. (2007) adopted this

framework to develop neural network based emulators that could represent the dynamic of a large-scale circulation model, extremely fast and accurately. The original model had a thousand degrees of freedom and was highly non-linear. Emulators provided accurate simulation of the original model, 1000 times faster.

Emulation approach has been increasingly used in recent water resources applications (Castelletti et al. 2010; Razavi et al. 2012). To implement this approach, Gaussian process (GP), Polynomials, kriging, k-nearest neighbour (kNN), Multiple Linear Regression (MLR), Artificial Neural Network (ANN), System Dynamics (SD) and Radial Basis Function (RBF) are some methods adopted to develop emulation models. As an example, Hassanzadeh et al. (2014) developed an integrated water resource model using system dynamics for scenario assessment in the Saskatchewan River Basin, Canada. By emulating an existing water resource management model (WRMM), an irrigation and an economic sub-models developed to estimate dynamic irrigation demand and the value of water use for various sectors of economy. Their results showed that the water system is sensitive to expansion of the irrigation area. Through this approach they added required details to the already available model. In another study, Di Pierro et al. (2009) used a non-dynamic approach stipulating that designing of water distribution systems is a non-linear optimization problem with a great amount of complexities which should be tackled through the use of network design models. Global stochastic search methods have been used for the design purposes, and since this approach requires a huge number of iterations to achieve a satisfactory solution, it is computationally expensive. To remedy this issue, in Southern Italy, a metamodeling approach with two multi-objective, hybrid algorithms, ParEGO and LEMMO, was implemented to design a medium size network. Results of the study suggested that both algorithms are effective tools to design large-scale water distribution networks. The use of this approach in their study was for model simplification. In addition, Shaw et al. (2017) emulated a hydrodynamic and water quality model (CE-QUAL-W2) using an artificial neural network and integrated the emulator into a genetic algorithm optimization approach in order to maximize hydropower generation conditional to constraints on water quality. This method applied to a multipurpose reservoir in Tennessee, USA. The model was able to increase hydropower production value with improved water quality. The emulation approach was implemented in their study in order for model simplification and adding details to the original model. In another study, Castelletti et al. (2010) applied a structure-driven emulation approach for iterative approximation of a complex process-based simulation model for scenario assessment in Googong Reservoir, Australia. They integrated

science-oriented and engineering-oriented sub-models in order to improve water quality in the study area. Their results indicated significant improvements by changing the location of already installed mixers. In the mentioned study, the application of emulation was for reducing model complexity, identifying the underlying mechanism of the system and adding details to the already available model.

This thesis suggests a data-driven emulation approach, applied to an optimization-based water allocation model in order to reveal the local details within a complex water resource system with a greater goal of representing local interplay between water availability, water demand and water withdrawals, and their interactions with climate conditions and human decisions. Due to intensive socio-economic activities in the region, there are intensive competition for water amongst different water use sectors. In addition, due to looming effects of climate change in the region, (i.e. declining streamflow, rising temperature and decreasing precipitation), the stress on available water in the system is and will be intensified. Applying this approach will provide water managers with tools through which they would be able to (1) have better understanding regarding water allocation, (2) assess the behaviour of the system under different scenarios of change and (3) by having knowledge regarding response of the system to changing condition water managers can come up with practical decision making for the system.

Chapter 3: Case study and available water resource model

3.1. Oldman River Basin

The focus of this study is on Oldman River basin which is a cold climate catchment (27,600 km2), located in southern Alberta, Canada. The catchment initiates from mountainous headwaters in eastern slopes of the Canadian Rockies and extends eastward into the prairies towards Alberta/Saskatchewan border. In this region, mountain streams have the fundamental role of providing reliable water resource for both nature (aquatic ecosystems) and human needs (settlement, food production and industrial activities). Having the mean annual precipitation of 580 mm to 380 mm and the mean annual potential evapotranspiration of 350 mm to 600 mm from west to east, the basin is marked as semi-arid cold region. In semi-arid areas, imbalances between water availability and demand is more highlighted and local water availability is insufficient to satisfy all demands.

The Oldman River basin has been under enormous pressures during the recent past and the extent of water demand in the basin is high relative to the water availability. As discussed above, incoming streamflow to this region initiates from Rocky Mountains and is subject to change. This change is attributed in two certain characteristics of the headwater streams, namely the timing of the annual peak and the annual volume. These characteristics are the main factors in order to develop regional water resource management. These components have been traditionally assumed to be unchanged in time. This makes management practices sensitive when increased variability and change in streamflow characteristics are occurred (Fleming and Sauchyn 2013). AghaKouchak et al. (2015a) argue that the variability and change in streamflow characteristics are due to changes in natural (climate) and anthropogenic (human management practices) systems. In western North America climate variability is mainly due to various large-scale climate circulation patterns, in particular the Pacific Decadal Oscillation which results in increased variability in streamflow in this region (Doney and Sailley 2013). It is expected that warming climate due to climate change and variability causes more decline in winter snow pack in the Rocky Mountains resulting in changing flow characteristics (Prowse et al. 2006; Schindler and Donahue 2006; Hipel et al. 2011). This can largely affect the interplay between natural and anthropogenic drivers of water resources at this basin and beyond (Nazemi and Wheater 2014).

In the study area, increased variability has been emerging from recent past and highly variable streamflow characteristics included extreme events such as droughts and floods with substantial socioeconomic impacts. A major 5-year drought from 2000 to 2004 resulted in a $5.8 billion drop in Canada's gross domestic product. During this period, the Oldman Reservoir was depleted to its minimum level within 1.5 years (South Saskatchewan Regional Plan 2010). This was followed by the flooding in 2013 in which the peak flow reached to 2370 CMS at Lethbridge (Alberat Environement 2013) with an estimated cost of at least $5.0 billion (Bonsal and Regier 2007; Wheaton et al. 2008; Nazemi et al. 2017).

In addition, in this semi-arid region due to climate warming temperature is increasing. Warmer climate increases irrigation water demand and decreases soil moisture. This contributes to heighten the vulnerability of this complex water resource system (Tanzeeba and Gan 2012). Moreover, plus changes in temperature the form and amount of precipitation are also changing. This is considered as other climatic sources of change in the streamflow regime and is attributed to global warming (Forbes et al. 2011). Moreover, Climate variability and change can indirectly impact streamflow regime through changing the controlling mechanisms of vegetation (Ireson et al. 2015). Evapotranspiration dynamics is dependent on natural vegetation and consequently have indirect effect on streamflow regime. Due to human intervention in the region's landscape through forest cuts, urbanization and change in the type of vegetation from natural grassland to farms, evapotranspiration pattern has changed in time and space resulting in indirect effects on streamflow regime (Wheater and Gober 2013). In this region, decreased annual mean streamflow combined with the earlier occurrence of the annual peak flows make water resource systems vulnerable with significant policy implications (Nazemi et al. 2013).

In addition, in this region water resource management have significant direct impact on streamflow characteristics through regulating the natural streamflow regime with large networks of dams which store and redistribute natural flows mostly for irrigation purposes. Direct human-driven impact on streamflow characteristics is due to abstraction and storage of streamflow for consumptive use, resulting in manipulating flow peak, increased evaporation and its feedbacks on climate (Nazemi and Wheater 2015b).

Although this is a semi-arid area, the region is one of the main producers of Canada's irrigated agriculture and a majority of the available water is consumed by irrigation activities. This shows the importance of headwater streams to determine the water availability in this area

(Nazemi et al. 2017). The water resource system in this basin is complex, including more than 100 clusters of demands, along with irrigation, hydropower, industrial, municipal, environmental and recreational water demands that are mainly supported by the surface water (Alberta Environment 2002b). 88% of the licensed water use is related to irrigated agriculture, which are supported by several man-made reservoirs, built since early 20th century. Although the basin is currently considered as over-allocated (Nicol and Klein 2006), water withdrawals are expected to increase due to socio-economic growth and recognition of environmental needs in the system (Alberta Environment 2002a; Gober and Wheater 2014). Among the existing reservoirs, the Oldman Reservoir is the largest, with the storage capacity of approximately 490 Million Cubic Meter (MCM), and plays a key role in regulating the flows and meeting downstream water demands. Constructed in 1984 as a multipurpose reservoir (Shpyth 1991), the Oldman Reservoir is located downstream of the confluence of the Oldman, Castle and Crowsnest Rivers, which respectively have the mean annual discharge of 13.1, 15.9 and 4.9 Cubic Meter per Second (CMS) just upstream of the confluence (Rood and Tymensen 2001). Oldman Reservoir, is responsible for providing agriculture, industry and municipality sectors with their water needs. Lethbridge Northern Irrigation District (LNID) with the area of 92,000 hectare is irrigated with the stored and regulated water in the Oldman Reservoir. Thirteen irrigation districts are forming the Alberta Project Association and the LNID comprises almost 82% of the irrigation land in the Province. This highlights the importance of the Oldman Reservoir in providing LIND with its water demand. In particular, looking at the history of droughts in this region illustrates the importance of this reservoir in drought mitigation through a practical management. In addition, city of Lethbridge with the population of 93,000 people is located downstream of the reservoir which is prone to floods. Again, according to history of flooding in this region, Oldman Reservoir can play an important role in flood mitigation. For these reasons Oldman Reservoir is the key to provision of the effective water resource management in this already-stressed semi-arid cold basin and is selected as the case of this study.

The dynamics of the storage at the Oldman Reservoir can be described by the inflow to the reservoir, losses through lake evaporation, local water withdrawals as well as the reservoir release. The reservoir release supplies the water for the LNID and passes through the city of Lethbridge. Figure 1 shows the schematic of the Oldman River up to downstream of Lethbridge.

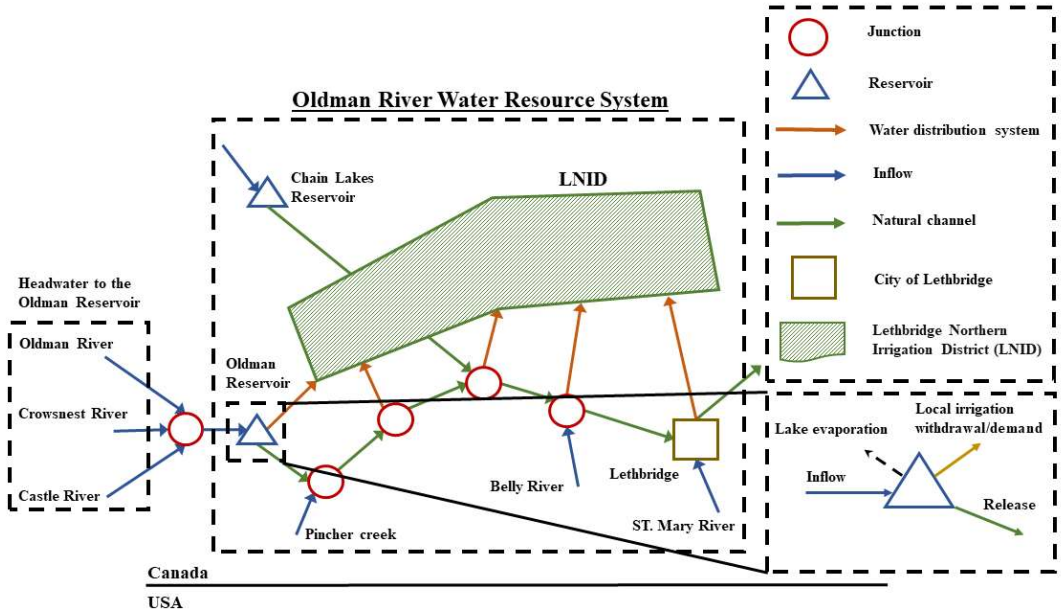

Fig. 1. A schematic look at the water resource system developed around Oldman River in southern Alberta, Canada, up to city of Lethbridge with the focus on the Oldman Reservoir.

Figure 1 presents the three streamflows to the Oldman Reservoir including Oldman River, Crowsnest and Castle River which are joining at UPRES215 junction and enter the Oldman Reservoir. The area and length of the reservoir are 17 km^2 and 15 km respectively. The river passes through the city of Lethbridge which is located at 40 km downstream of the dam. LNID was formed in 1919 and located on the northern side of Oldman River and city of Lethbridge. 57% of cultivated irrigation area goes to forage while cereal, oils, specialty crops and miscellaneous are limited to 22%, 15%, 4% and 2%. The figure also shows the loss through lake evaporation, the water which is withdrawn to satisfy the local demand and the outflow which is released to meet the regional water demand. Based on the available data, expected annual lake evaporation, local water withdrawal and reservoir release are 14, 13 and 836 MCM at the Oldman reservoir, respectively. These values show the importance of these processes because a considerable amount of water is evaporated, allocated to local irrigation networks or released for downstream environmental needs, agricultural or other water-based activities.

In Alberta province in order to allocate water to all sub-basins a Water Resource Management Model (WRMM) has been developed by Alberta Environment. This model is used for water resource management and planning in this semi-arid region and simulates river flows and water uses under different current and future scenarios. A description of WRMM is presented in the

next section. Using this model, a lot of important water management decisions have been made. The model and its application is demonstrated in the next sub-section.

3.2. Water Resource Management Model (WRMM)

Water Resource Management Model (WRMM) is an operational IWRM, developed for planning, decision-making and management purposes for water resources utilization in southern Alberta. WRMM is an optimization-based water allocation model that uses the Linear Programming technique (LP) to allocate available water to the competing demands, given the water allocation priorities and the state of the system. The early versions of the WRMM go back to the 1980s, but the model has been continuously updated to accommodate new demands and operational policies in the system - See (Alberta Environment 2002a; Nazemi and Wheater 2014) for more information on the WRMM model used in this study.

WRMM is a surface water allocation model, and in the modelling procedure, a river basin is the fundamental unit of the study. The model is able to be run repeatedly, in order to account for the response of the river system to changing natural conditions or planning alternatives. Application of the model has developed in two forms: basin planning and operational planning. The former is applied to assess long term water use alternatives in future with respect to the historical data, whereas the latter is employed to assess the short-term future consequences of various operational strategies. The basin planning model have been used in this study.

The model has the ability to apply various operating policies/priorities in order to allocate water to different sources of demands within a system. In this model, water allocation priorities are characterized by a penalty point system and the purpose is to limit the overall system penalty. The system topology is represented by a standard set of components. These components are: reservoir, hydropower, natural channel, appointment channel, diversion channel, irrigation network, junction, and major and minor withdrawal. The model simulates different choices of planning by allocating supply to current or projected demands. The model has the ability to represent: (a) water supplies, such as headwater, runoff, in-diversion, (b) reservoir storage, outflow, precipitation, and evaporation, (c) diversion channels, (d) irrigation consumption, (e) hydropower production, (f) major and minor consumption demands from large cities or industries, to small municipalities and industrial uses. The model application may vary from a simple system, including some of the above mentioned processes, to an extensive complex

system comprising hydroplants, diversion canals, in-stream channels, irrigation, and other consumptive uses.

The system operating policy is based on a defined ideal state and a number of zones corresponding to derivations above and below the ideal state. In the case that enough water is available, the model satisfies all ideal requirements. Otherwise, the needs are satisfied in the order of priorities, which have been assigned by the user. These priorities are specified by penalty values that represent derivation from ideal levels. The higher penalty represents the higher priority of allocation. In the simulation procedure, deviations initially happen in those zones that have low penalty values, and after that, continues to zones having higher penalty amounts.

In order to clarify how the model works mathematically, a simple water system, as an example, is explored – see Figure 2. This system includes a single reservoir with two penalty zones corresponding to maximum and minimum water level/storage, an urban centre, an irrigation district, and a natural channel. Except for the reservoir, all other components have one penalty zone. The values of the penalty zones are: 1000 when the water level in the reservoir stands beyond minimum and maximum limits, 900 for natural channel, 650 for urban centre, and 600 for irrigation district. Water demand for the natural channel, urban centre and irrigation district are 10, 20 and 15 cubic meter per week, respectively. In this system the reservoir is the source of water allocation to all of the components. However, the water level/storage should not go beyond the minimum or maximum levels, otherwise a penalty of 1000 is applied. Therefore, the objective function of this simple system would be as presented in Equation 1.

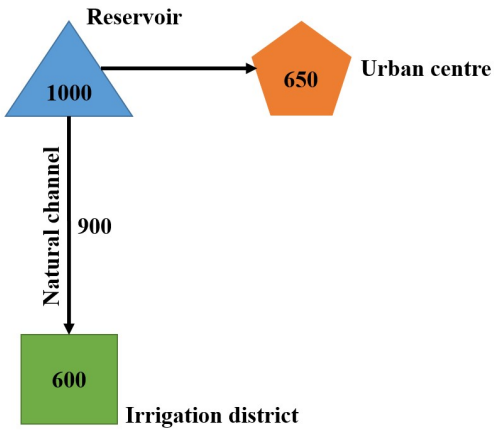

Fig. 2. A schematic of a water system to explain WRMM operation mechanism (Hosseini Safa 2015).

$$Objective = min\big(900 \times (|10 - x_1|) + 650 \times (|20 - x_2|) + 600 \times (|15 - x_3|)\big) \quad (1)$$

where x_1, x_2 and x_3 are the volume of water allocated to the natural channel, urban centre, and irrigation district, respectively. In the case that water level goes under or above the minimum or maximum level, a penalty of 1000 is applied to the equation. If the system has enough water to allocate to all the defined needs, the objective function would be zero. However, at the water scarcity condition, the model allocates more volume of water to natural channel to minimize the objective function. The reason is that the penalty value of this component is higher than others. The second and third priorities go to the urban center and irrigation district as they are of less penalty value.

WRMM has successfully been applied to the South Saskatchewan River Basin with the greater goal of project planning. This model has been used to analyse: (a) a broad range of networks of rivers and reservoirs, (b) various water use options, and (c) several water allocation priorities. Alberta Environment has used this model to make decisions on irrigation licensing, reservoir operation, and instream flow allocations. This model has also been applied to analyse the consequences of operating strategies in dry years. The new versions of this model are able to capture the behaviour of the modelled system in weekly time-steps which raise the accuracy of the simulations.

The model used in this study, operates at the weekly scale and requires streamflow, water demands, license priorities, operational policies, in-stream flow needs, and the apportionment requirements, along with physical characteristics of the reservoirs, as prescribed inputs. Therefore, the model has limited application if some input variables such as irrigation water demand or lake evaporation are subject to change; or understanding the interactions between these variable and their natural and anthropogenic drivers are sought. For instance, irrigation demand is a prescribed input to WRMM and the model does not consider the dynamic interactions between the irrigation demand, local climate, and antecedent water availability (Hassanzadeh et al. 2014). Similarly, reservoirs' gross evaporation are provided to the model as prescribed inputs; therefore, the effects of changing temperature and/or lake storage on reservoir evaporation are not represented. In addition, the dynamic interplay between water demand and water withdrawal is determined through a complex optimization procedure; hence,

the effects of relevant drivers on changing the demand-withdrawal dynamics is not explicitly characterized. Here the aim is representing these details at the Oldman Reservoir through the proposed emulation framework, with the greater goal of understanding the integrated performance of the Oldman Reservoir under changing inflow, climate, and irrigated area.

3.2. Available data

The aim of this study is to represent local details within Oldman Reservoir which are missed in the main water resource system model (WRMM) and to evaluate the behaviour of the system in different defined scenarios through an impact assessment study. To develop sub-models that address the required details, the data is derived from WRMM. Precisely, the inputs/output pairs of the weekly WRMM model are used to develop our models. The data consists of lake evaporation, precipitation, water withdrawal, irrigation water demand, reservoir release and storage available for 63 years spanning from January 1938 to December 2000. In addition to agriculture, Oldman Reservoir allocates water to other sectors such as industry and municipality. Since here the focus is on irrigation, water demand related to other sectors are treated as must-meet constant values. In this case, the data related to industry and municipality water demand are obtained from WRMM and lumped together and is added to estimated irrigation demand to find total water demand. In addition temperature time series obtained from Environment Canada's historical climate archive (http://climate.weather.gc.ca). The biweekly time series of the data used in this study is presented in the Supplementary Information (Appendix).

Having the required data, a comprehensive model development protocol is proposed to configure a wide range of alternative hypotheses for emulation models. Then their performance is rigorously tested, individually and in coupled settings, where non-falsified emulators for each variable of interest are linked with one another. To showcase the practical utility of the proposed emulation approach, sensitivity analyses are performed to reveal the impact of changes in natural and human conditions (i.e. inflow, temperature, precipitation and irrigation area) on the reservoir's performance.

Chapter 4. Rationale and Methodology

As discussed previously, water resources are under enormous pressure. Due to natural and anthropogenic stressors, imbalances between water availability and demand is heightened. This makes water resource systems vulnerable and brings about needs for managing water system. To examine the future challenges, practical tools are required in order to investigate different scenarios of changing climate, water availability and water demand at different spatial and temporal scales and understand their potential impact on water resource systems. These tools can help water experts to understand the effect of scenarios of change on different sectors and develop sustainable water management strategies. As integrated water resource management models are often problem-oriented, they focus only on those processes, variables and/or scales that are relevant to the problem in hand. In many cases, therefore, a new model is needed if a new process and/or detail needs to be represented in the model structure. A good example in that regard is the issue of water demand, which is given to water allocation models mainly as prescribed inputs. As a result, the effects of local climate and/or human management cannot be directly seen by the model. Here, instead of building up a new IWRM model to support more details, it would be more efficient to develop adds-on modules that can represent more details only when and where needed. These sub-models include new parametric functionalities to support representing new processes, variables and/or scales and can be identified in a way that replicate the results of the already available integrated water resource management model at a common scale and/or variable.

As a result, the key assumption here is that the existing IWRM (and/or its prescribed inputs) can sufficiently represent the system dynamics at larger scales and/or lower resolutions. Therefore, using surrogate models (or emulators) for developing these adds-on modules is suggested. Referring back to the example of water demand, the emulator can include a procedure for calculating water demand from climate (e.g. by incorporating temperature in the emulator) and anthropogenic proxies (e.g. by considering human intervention embedded is changing irrigation area) and can be parameterized in a way that can replicate the prescribed water demands of the existing IWRM. Emulators can also include new functionalities to represent the processes that take place within the simulation time-step of the existing IWRM. For instance, the common scale of the existing IWRM can be monthly, including for the water allocation for hydropower production. In such cases, the emulator can represent the water allocation for hydropower at finer daily or hourly scale and can be parameterized in a way that

can replicate the monthly hydropower allocations, represented by the original IWRM. Parameterized emulator can be then used to explore the behaviour of the water resource system where more details are needed either individually or in relation to other system components. Figure 3 shows the general idea behind the proposed emulation framework, in which the emulator can be parameterized using the input-output relationships of the original IWRM.

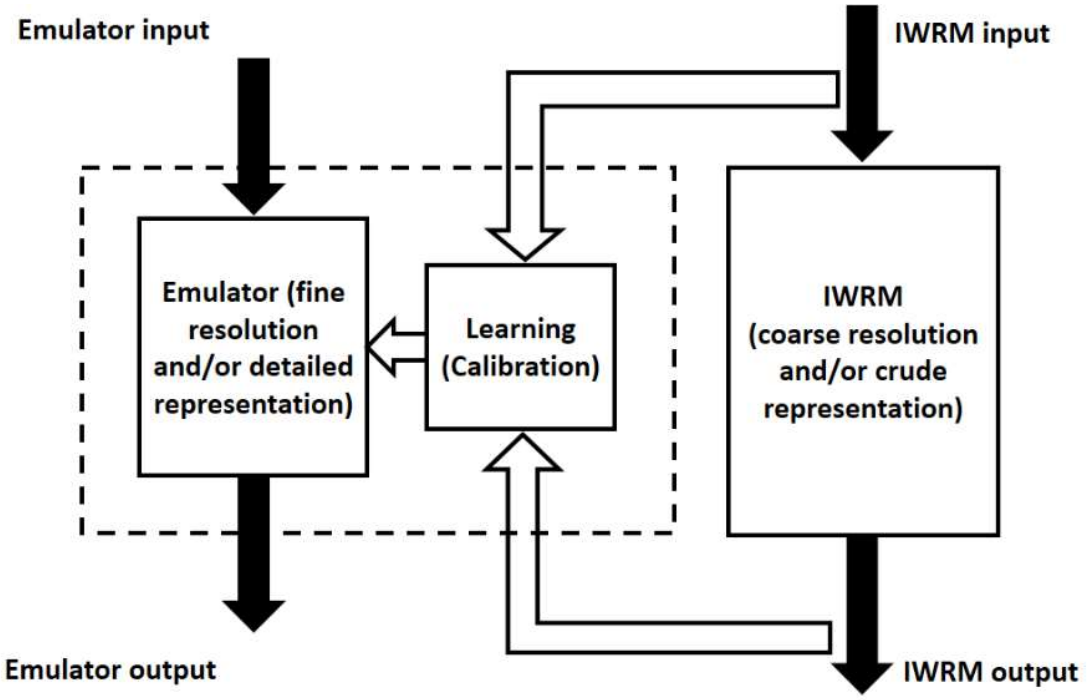

Fig. 3. A schematic view to the proposed data-driven emulation framework for supporting detailed representation in an existing IWRM. The emulator is calibrated in a way that replicates the result of an existing IWRM at a common scale and/or variable.

Wheater et al. (1993) classified modeling techniques based on their model structure, spatial distribution, and spatial-temporal application in three clusters namely, metric, conceptual and physics-based models. Characteristics of metric models are found based on observations. In brief, the system response is established from the available data. Therefore, this approach is essentially empirical. The simplicity of this technique has allowed it to be applied in different fields, in particular hydrological modeling. However, metric models are dependent on the range of available data with which they have been developed and although they have been used for extrapolating (e.g. extreme events or ungauged catchments), results are not often reliable. Data-driven is a metric modeling approach and is applied for time series analysis and simulation. The model structure is an empirical transfer function developed based on the available input-

output data. The advantage of this technique is its ability to determine the structure of the model without prior hypothesis. In contrast, in conceptual models the structure is described before any modeling being undertaken. In addition, not all the model parameters have physical interpretation. Hence these parameters should be estimated through calibration using observed data. In terms of complexity, these models can vary from simple to highly complex levels. Moreover this modeling technique perform less accuracy in comparison with metric models. Physic-based models are developed based on continuum mechanics. In these models, equations are solved numerically using a finite difference or a finite element scheme. Therefore, the complexity of these models are rather high. The physics behind the model structure are based on small-scale experiments. The parameters of physics-based models are found at a point. Then model uses averaged parameters at grid scale which is greater than the scale of variation of the process. This affects the accuracy of this method. These models perform less accuracy and highest uncertainty in comparison with the other two models (Pechlivanidis et al. 2011).

Since the metric technique is a simple and accurate data modeling approach, is applied in this research. Here, statistical modeling (data modeling) technique in time domain is applied in order to develop metric models (hereafter data-driven models). Data modeling procedure often include a standard approach:

1- Determining independent variables that can affect dependent variables.
2- Examining any significant time lag between dependent and independent variables.
3- Finding potential mathematical functions that can map from independent to dependent variables.
4- Finding the parameters of the chosen model.
5- Evaluating the accuracy and uncertainty of parameterized models.
6- Testing the parameterized models.
7- Falsifying developed models to fine top non-falsified options that can properly describe the dependent variable.

Here, using the data-driven approach for developing emulators is suggested. Mathematically, the structure of a data-driven emulator can be described using a functional mapping as the following:

$$\hat{V}(t) = F(\boldsymbol{X}(\boldsymbol{\Theta}^*)) \quad (2)$$

where $\hat{V}$ is the emulated results of the existing IWRM model at a common scale and/or variable; $F(.)$ is the functional mapping; $\boldsymbol{X}$ is the vector of emulator inputs and $\boldsymbol{\Theta}^*$ demonstrates the matrix of time signatures, for which inputs to emulators are provided. As an example, if $Y = f\big(X_1(t-1), X_2(t)\big)$, $\mathbf{X} = \begin{bmatrix} X_1 \\ X_2 \end{bmatrix}$ and $\boldsymbol{\Theta}^* = [1 \;\; 1].\begin{bmatrix} t-1 \\ t \end{bmatrix}$. In this equation $\mathbf{X}$ is the matrix of predictors, $X_1 \; and \; X_2$, in time $t-1 \; and \; t$, respectively.

The procedure of developing emulators involves finding the optimal inputs, structures and/or parameters of the functional mapping in a way that emulated results replicate the simulations of the existing IWRM. Here, the focus is on two data-driven methodologies, i.e. Multiple Linear Regression (MLR) and Artificial Neural Networks (ANNs) to form the structure of the emulators. These approaches represent the two ends of the data-driven modeling spectrum in terms of transparency and complexity. The input variables to emulators are identified either through expert knowledge (i.e. prescribed inputs) or through a formal input variable selection (i.e., Partial Correlation Input Selection – hereafter PCIS). Below these methodologies are briefly introduced.

4.1 Multiple Linear Regression

Multiple Linear Regression (MLR) is a generalized form of Linear Regression, by including many terms in a function rather than one intercept and a slope. The MLR represents the linear association of a set of independent variables to one predictand – see Draper and Smith (2014). The MLR with response Y and terms $X_1, X_2, \ldots$ to X_p has the general form of:

$$E(Y|X) = \beta_0 + \beta_1 \times X_1 + \cdots + \beta_p \times X_p + \varepsilon \qquad (3)$$

where $E(Y|X)$ means that Y is conditioned to Xs. the βs are unknown parameters that need to be estimated. Ɛ is the remaining unexplained noise in the data, or the related error. The equation is a linear function of the parameters. When $P = 1$, the simple linear regression function is obtained. At the time $P = 2$, the response surface is in a three dimensional plane. When $P > 2$ the response surface changes to a hyperplane in a $P + 1$ dimensional space.

The null hypothesis in linear regression technique is that the coefficient relating independent variables to dependent variable is zero. In other words, there is no relationship between predictand and predictors. Whereas the alternative hypothesis is that this coefficient is not equal to zero, meaning that there is some kind of relationship between independents and dependent variables. In linear regression technique there are some underlying assumptions, such as: (a) the constant variance of residuals, (b) no existence of outliers and (c) normal distribution of residuals. These assumptions can be assessed by examining the residuals. By plotting the predicted values against the residuals it would be possible to assess the constant variance between model estimations and residuals. In addition, from the plot it is possible to look for outliers in the data. To check the third assumption, it is possible to produce a normal probability plot. The ordered values of residuals are plotted against the expected values from the normal distribution. In the case that residuals are normally distributed, they lie on the diagonal approximately (Tranmer and Elliot 2008).

The statistical regression is the simplest form of data modeling and is one of the most widely used statistical methods in different fields. It is normally the first approach adopted for statistical modeling and is considered as a benchmark modeling approach due to its simplicity. Here, both independent and dependent variables are normalized using their observed range in the scale of [0.1 0.9]. Having the normalized values they are used to develop emulation models. This makes equations dimensionless and considered buffers would facilitate accommodating outliers and extreme events. Then observed data ranges are used to rescale estimations obtained from dimensionless equations into their actual domain (Hsu et al. 1995). MLR is associated with powerful parameterization schemes such as the Maximum Likelihood Method, with which the associated parametric confidence interval and predictive uncertainty can be quantified (Beven and Smith 2014; Giles et al. 2016). Due to its simplicity, the MLR has been widely used to find functional mappings in the context of emulation models (House 2011; He et al. 2014; He et al. 2015; Malik and Kumar 2015; Mogaji et al. 2015).

4.2 Artificial Neural Networks

ANNs are robust tools that can be used for the modeling of complex non-linear relationships between inputs and outputs by simulating the functional aspects of biological neural networks (Bishop 1995; Russell and Norvig 2016). ANNs behave similarly to statistical methods and learn from the empirical samples. The structure of ANNs is not specified prior to any modelling

being undertaken and this makes the method a non-rule-based technique. The network consists of a number of neurons as information processing units, which are linked to input variables, a central processing unit and outputs – see Figure 4. Inputs are received through the links from outside the network or other neurons (X). Each link is assigned a weight (W) which represents the strength of the connection between two nodes. The information is processed in each neuron by adding up the weighted inputs and bias (b) – see Equation 4, and is passed through the activation function $f(t)$ – see Equation 5. The activation function is a mathematical transfer operator that maps predictors to target variables and forms the output of the nodes. There are various types of activation functions, i.e. sigmoid, linear, threshold, Gaussian, or hyperbolic tangent function, that can be chosen based on the network's type and the training algorithm. One of the most commonly used functions that has been employed in this study is log-sigmoid because it is continuous, its derivatives are simple to find, and it provides non-linear response (ASCE 2000). ANNs have the ability of learning through training. This requires a set of data which consists of series of input and corresponding output vectors. During training, the weights in the network are adjusted to find desired output. The estimation may not equal the desired output. In this case an error signal (difference between actual and desired output) is defined and the network uses this signal to justify the weights to minimize the error signal (Gardner and Dorling 1998).

$$t = \sum_{i=1}^{n} W_i X_i + b \tag{4}$$

$$f(t) = \frac{1}{1 + e^{-t}} \tag{5}$$

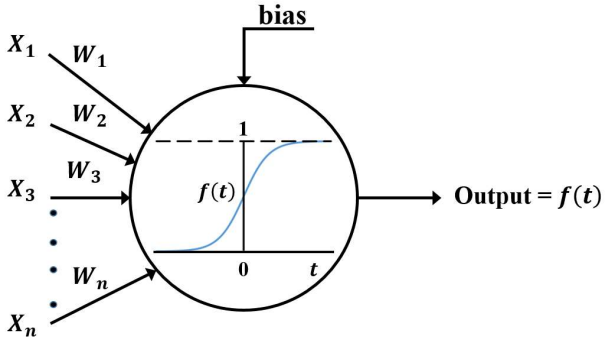

Fig. 4. Schematic diagram of an artificial neuron (Gardner and Dorling 1998).

In water resource problems, one of the most popular types of ANNs is the feed forward neural networks (FFNNs). In the structure there are input layers with different numbers of neurons, one or more hidden layers, and an output layer – see Figure 5. In FFNNs the information flows in one direction, from input layer through hidden layer, and finally goes to the output layer. In this process the neurons are fully connected. Each neuron in the hidden layer receives the information from the input layer through the weighted connection links. Then the signals is processed in each hidden layer and the output is passed to the output layer.

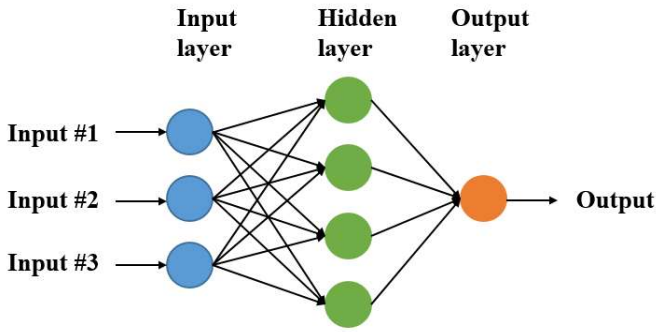

Fig. 5. Configuration of three-layer feed forward ANN with three neurons in input layer, four neuron in hidden layer and one output (Gardner and Dorling 1998).

When developed models are running with different initial conditions (weights and biases), the results are different estimations of observed output. Ensemble of estimations is known as the uncertainty regarding developed modes. The uncertainty reflects the inability to determine exact values of model parameters, process understanding and model approximations. Various techniques such as Generalized Likelihood Uncertainty Estimation (GLUE), frequentist approaches, and standard Bayesian approach have applied to quantify the uncertainty in hydrologic predictions. Having knowledge regarding the uncertainty of model estimation will help decision makers to assess the behaviour of systems under possible scenarios (Renard et al. 2010). Here, to address the predictive uncertainty, each developed ANN-based model is trained under a certain number of iterations with different initial conditions, resulting in different estimations of the target value. The ensemble of all estimations represents an envelope which shows the predictive uncertainty of the developed model.

Neural networks have been considered an effective alternative to traditional statistical techniques. It has been shown that this technique can approximate any smooth and measurable function. It has the capability of modeling highly non-linear functions and if properly trained

can accurately generalize with new unseen data. These characteristics make this technique attractive alternative to numerical models and other statistical approaches (Gardner and Dorling 1998). Moreover, there are various neural networks architectures which are being used in environment science, e.g., static-feedforward and dynamic-feedback neural networks (Chiang et al. 2004), hierarchical neural networks (Schaap et al. 1998), and hybrid neural networks (Jain and Kumar 2007).

Here, a feed-forward neural networks, equipped with Levenberg-Marquardt back propagation learning algorithm, is used (Riedmiller and Braun 1993). The back propagation algorithm is the most widely recognized training algorithm in the FFNNs in water resource modeling (Maier and Dandy 2000). This method is a gradient descent technique that adjusts system weights and biases in a way that minimizes network error. This algorithm benefits from iterative processes that lead to minimization of the error between network output and targeted output. Initially, the data goes through the network to the output unit. Then the network error is computed and is fed backward to the network towards the input layer depending on the magnitude of the error. This process continues until the output data reaches an acceptable level – see Deswal and Pal (2008). This ANN structure has been extensively applied in hydrological modeling literature (Dawson and Wilby 2001; Mekonnen et al. 2015).

4.3 Partial Correlation Input Selection

The performance of statistical models considerably depends on input variable selection. Linear correlation-based selection algorithms are among the most widely used input variable selection schemes in hydrology (Wu et al. 2014). Partial Correlation Input Selection (PCIS), proposed by May et al. (2011), is a popular linear correlation-based scheme and is used in this study in order to select best models' proxies form a potential pool of variables. The PCIS adopts a forward selection strategy looking at the linear relationship between predictors and predictand. The methodology is based on the residual information from a new predictor and is terminated when adding new predictors causes no improvement in BIC value (see Equation 17) obtained for predictand residuals. The Sum of Squared Errors is considered as the error density function for BIC calculation. This will provide a trade-off between goodness-of-fit and model complexity by penalizing more complex models. Here the proxies that can improve the BIC value for predictand residual more than 10% are considered.

In simple PCIS, the linear correlation coefficient (i.e. Pearson correlation coefficient) is utilized to measure the strength of the relationship between predictors and predictand, and MLR is used to estimate the residuals. However, a sensitivity analysis is also carried out by implementing Spearman's rho and Kendall's tau dependence coefficients in the input variable section scheme in this research, instead of Pearson correlation coefficient – see Genest and Favre (2007) for information about Spearman's rho and Kendall's tau dependence coefficients. In brief, given a candidate set, S, and output variable, Y, the PCIS proceeds at each iteration by finding the new candidate, C, that minimizes the BIC value with respect to output variable, conditioned on the previously selected input. If adding the candidate C, improves the performance of the model by decreasing the BIC evaluation criterion, the selection continues, otherwise, there are no more significant candidates remaining and the algorithm terminates (Fernando et al. 2009; May et al. 2011).

4.4 Impact assessment

So far, different methodologies have been adopted to address vulnerability of water resource systems (Conway 1996; Sheffield et al. 2009). Two top-down and bottom-up approaches are taken in order to apply the vulnerability assessment studies in a water resource system. In the top-down approach, different climate scenarios are obtained from Global Climate Models (GCM). However, the climate variables need to be bias corrected (Piani et al. 2010) and using downscaling techniques their spatial resolution adjusted to the scale of interest prior to their use in hydrological models (Wilby et al. 2002). Then based on downscaled climate projections, Hydrological Models (HMs) are used to estimate different scenarios of streamflow. This data, in the next stage is fed into a water resource system model to estimate the performance of a water resource system under the projected scenarios of streamflow (Vicuna et al. 2010). However, both climate models and downscaling techniques are uncertain (Jenkins and Lowe 2003; Smith et al. 2009). In parallel, hydrological models translate climate projections to streamflow with a large uncertainty which later propagates in the impact assessment analysis of a water resource system (Nazemi and Wheater 2014).

An alternative approach for water resource system vulnerability assessment is analyzing the response of the systems without using downscaled GCMs projections (Prudhomme et al. 2010). In other words, in this approach in order to implement vulnerability assessment study, the focus is not only on the future states of the system. this makes a difference between this approach

and the previously introduced top-down vulnerability assessment method (Wiley and Palmer 2008). Instead of predicting the future risks, the bottom-up approach identifies the critical conditions under which the system is vulnerable (Brown and Wilby 2012). In order to implement assessment studies using bottom-up approach, initially a set of critical variables to which water resource systems are sensitive are defined. Then a feasible range is determined for each critical variable which reflects different possibilities for future climate scenarios. A large number of climate projections or stakeholders' needs can be considered in order to identify the range associated to each climate variable (Stainforth et al. 2007; Brown et al. 2011). Then using the defined range for critical variables, the response of the water resource systems can be assessed through water resource system models. Since this approach covers a wider range of scenarios, therefore is able to address better understanding of possible systems' response to changing conditions (Herman et al. 2015).

Chapter 5. Model development

5.1 Variables and data support

Here, the objective is to represent local details which are missed in the existing water resource system model (WRMM). To add these details, a set of sub-models are developed through which it would be possible to describe the required local dynamics. The sub-models determine the dynamics of the storage at the Oldman Reservoir. These elements include (1) reservoir evaporation, which is the local loss of the available water; (2) local water withdrawal, which is the water uptake for local irrigation demands; and (3) regional water withdrawal, which is manifested as the reservoir outflow, released for various purposes downstream. Detailed understanding of the water withdrawals requires characterizing the water demand, with which water deficit can be estimated. Having knowledge regarding water deficit will enable water managers to take measures for effective decision making in order to manage, plan and minimize the consequences of water shortage. As here the aim is understanding the local details of the water resource system at the Oldman Reservoir, the focus is to consider characterizing (4) local water demand for irrigated agriculture. It should be noted that there are other non-irrigative water withdrawals at the reservoir related to local municipal and industrial demands. These withdrawals however are minor and related to constant must-meet demands that can be considered as known losses at each time-step.

Here, building up a suite of MLR- and ANN-based emulators for each of the variables identified above is considered, using the inputs/output pairs of the weekly WRMM model, available for 63 years spanning from January 1938 to December 2000. Then using a reductionist bottom-up approach various emulation models are built, in which the available data is split into three time episodes for calibration (i.e., 1938 to 1975), testing (1976 to 1988) and validation (1989 to 2000). By taking the reductionist bottom-up approach a group of alternative hypothesis are defined, developed and refined to adopt the choices that are more efficient to represent the required information. Calibration period is exclusively for setting up and parameterizing a wide range of competing emulators (i.e. alternative hypotheses) for the four variables identified above. The competing alternatives are defined in order to be compared with one another and to find models that are describing the required details in the system with higher efficiencies. In addition, having a suite of alternatives it would be possible to address the uncertainty regarding the variables that are being modeled. The behaviour of emulators developed for each of the variables are explored and intercompared based on their optimality

and complexity by defining and using goodness-of-fit measures during the testing period, in which some emulators are falsified based on their relative performance in tracking the corresponding WRMM time series. The selected emulators are then able to represent the dynamic of the variables based on which they have been developed with highest efficiency. But these individual emulators do not depict interactions between variables and cannot be used individually to assess the behaviour and dynamic of the whole system. In order to have the required understanding regarding the dynamic of the system, the non-falsified emulators for the considered variables are then mixed-and-matched to provide a suite of competing Integrated Emulators (IEs). These IEs not only are used for representing the interactions between system's components but based on the underlying concept behind their development, thy have the ability for including the effect of climate and human actives (coupled dynamics) on water allocation at the Oldman Reservoir. The performance of the IEs are further investigated during validation phase and some of the IE alternatives are falsified based on their relative performance in tracking the WRMM simulations. The non-falsified IEs are then used for impact assessment at the reservoir location. Below the procedure of model development is outlined.

5.2 Emulators with known and unknown input variables

Both MLR- and ANN-based emulators require a set of proxies (predictors) with which the four variables of interest, in particular lake evaporation, water withdrawal, irrigation demand and reservoir release can be quantified. Three different scenarios with respect to the *priori* knowledge (based on expert knowledge and literature) about the necessary inputs of the emulators are considered. In addition, to examine the expert knowledge regarding related proxies, the correlation between inputs of each model and the target variables is assessed. In the first scenario of input selection, it is assumed that a perfect knowledge about the necessary input variables and their associated time signatures is available and therefore the inputs to each emulator are fully known. Second and third scenarios are related to different levels of partial knowledge about the emulator inputs. In the second scenario, the complexity of predictor selection is increased. In this scenario, it is assumed that a pool of potential variables in their relevant time signatures is available for each emulator, from which a set of input variables can be selected. For each emulator, the pool of potential inputs include same proxies considered based on perfect *priori* along with various nonlinear transformations of these variables (e.g. inverse, square root, squared, cubed, logarithm and exponential). In brief, in this scenario,

predictors of emulators are unknown but their relevant time signatures are known. In other words a partial knowledge regarding the inputs of models is available. In the third scenario, the complexity of predictor selection is even heightened. In this level, it is assumed that not only the inputs of emulators are unknown but their relevant time signatures are also unexplained and therefore they should be identified from a pool of relevant time signatures. In the third scenario, similar variables and functional transformations that had been used in the second scenario of predictor selection considered. Moreover, the variables with one-step time lag are also included in the pool of potential inputs. When emulators' inputs are unknown, the PCIS chooses an optimal set of predictors from a pool of potential input variables.

Here, the input variables and the functional mapping for each emulator related to the first scenario (i.e. perfect *priori*) is outlined and extended to the second and third scenarios for input selection. Considering a perfect *priori* for input variables for emulators, the gross evaporation from the Oldman Reservoir at the end of each week as E (mm/week), can be linked through a MLR- or ANN-based mapping eva to the initial reservoir storage S (MCM/week) at the beginning of the week and the average temperature (℃) during the week:

$$E_t = eva(S_{t-1}, T_t) \tag{6}$$

In developing this equation it is assumed that evaporation throughout the lake area is the same. In other words, the effect of water depth in evaporation procedure is ignored. This emulator is a continues mathematical function with a negative and positive range. Negative numbers are due to winter snow deposit (e.g. blowing snow or sublimation) which is not precipitation related. Weekly gross reservoir evaporation at the Oldman Reservoir is a prescribed input in the WRMM, with which the parameters of the mapping G can be identified. The storage information can be obtained through WRMM simulation and the weekly temperature data at the Oldman Reservoir is taken from the climate station at the City of Lethbridge. The time series of lake evaporation, temperature and reservoir storage are shown in Figures A2, A4 and A8 (Appendix), respectively. This representation allows assessing the effect of climate on the evaporation amount. To examine the correlation between lake evaporation and selected predictors, the time series of these variables are plotted and presented. Figure 6 shows the correlation between evaporation as the predictand and storage and temperature as predictors of the model. In this figure, x-axis shows storage in MCM/week (Panel- a) and temperature in °C

and y-axis belongs to lake evaporation in mm/week. The range of storage in Pane-a, is from 0 to 490 MCM and the range of temperature in Panel-b, is from -31 °C to +25 °C.

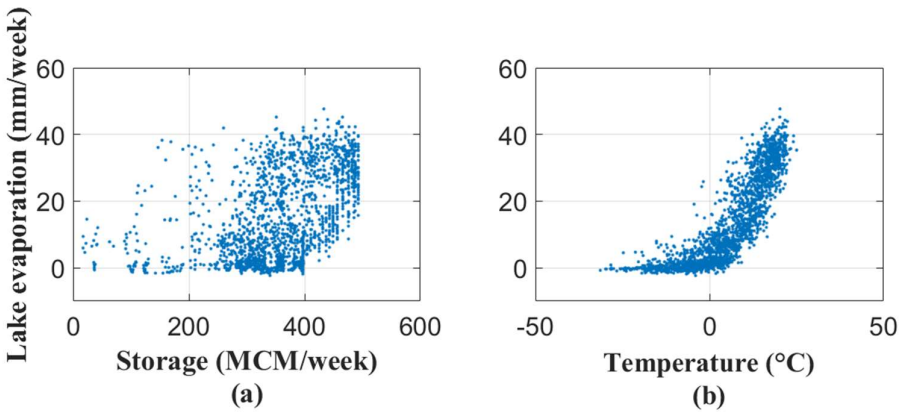

Fig.6. Correlation between dependent variable (lake evaporation) and independent variables (storage- Panel a, and temperature- Panel b) at Oldman Reservoir.

Panel (a) shows the correlation between storage and lake evaporation and Panel (b) demonstrates the dependency between temperature and lake evaporation. Both Panels show a significant correlation between predictors and the predictand. Based on Panel (a), lake evaporation is more significant when reservoir storage is more than 250 MCM. Panel (b) also shows the strong dependency between the two variables. Increasing temperature results in higher evaporations values. In particular, when the temperature is positive, the evaporation exacerbates. Based on these panels, the maximum lake evaporation is 50 mm/week.

Since agriculture is a developing activity and is of high priority and interest in this region, water withdrawal WD (mm/week/hectare) is considered per unit of area in this study. Inclusion of area will enable the assessment of response of the system to developing irrigation networks in this area. Water withdrawal per unit of area is linked through MLR- or ANN-based mapping wwd to irrigation demand per unit of area D (mm/week/hectare), irrigation area $Area$ (hectare) and the reservoir storage S at the beginning of allocation week (MCM/week):

$$WD_t = wwd(Area \times 10 \times D_t, S_{t-1}) \,/(Area \times 10) \quad (7)$$

This equation links the dynamics of water withdrawal to the storage condition and total irrigation demand. The multiplier of 10 is for unit conversion. Such inclusion of irrigation area in this equation can assist analyzing the sensitivity of the water withdrawal to changes in irrigation area. In developing this emulator, we assumed that water withdrawal is constant and will not change during an operational week. This equation is a continues mathematical function with a positive range. The time series of water withdrawal and irrigation demand derived from WRMM are shown in Figures A5 and A6 (Appendix), respectively. Figure 7 demonstrates the correlation between water withdrawal as the dependant variable and irrigation demand and storage as independent variables of the model.

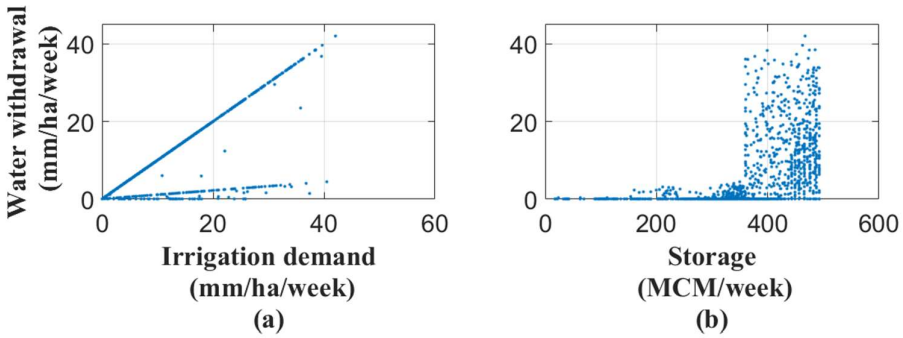

Fig.7. Correlation between dependent variable (water withdrawal) and independent variables (irrigation demand- Pane a, and storage- Pane b) at Oldman Reservoir.

Panel (a) shows the correlation between water withdrawal and irrigation demand and the dependency between water withdrawal and storage is demonstrated in Panel (b). The figure presents a strong dependency in both Panels. In panel (a) two lines belong to irrigative and non-irrigative demands for which water was withdrew from the reservoir. Also Panel (b) shows that the major withdrawal takes place when reservoir storage is more than 350 MCM. Throughout a typical year, water withdrawal can range from 0 to 40 mm/ha/week.

Irrigation demand D (mm/week/hectare) is also being looked as per unit of area because of enabling the model for assessing the consequences of irrigation development in this region. Irrigation demand per unit of area is considered as a MLR- or ANN-based mapping dem as the following:

$$D_t = dem(P_{t-1}, WD_{t-1}, T_t) \quad (8)$$

P (mm/week) and WD (mm/week/hectare) are local precipitation and the water withdrawal per unit of area at the previous time-step. Temperature T (℃) during the week is a proxy for evaporative need of crops during the week, in which the withdrawal is scheduled. In developing this emulator it is assumed that during a week irrigation demand is constant and will not change. This equation is a continues mathematical function with a positive range. The time series of precipitation derived from WRMM is shown in Figures A3 (Appendix). Consideration of precipitation and water withdrawal is to accommodate for the antecedent soil moisture condition. Such dynamic calculation of irrigation demand based on water supply and climate conditions not only allows more realistic estimation of irrigation demand (Hassanzadeh et al. 2014) but also assist in quantifying the potential climate control through direct consideration of temperature and precipitation. Here, it is assumed that the crop and irrigation practice is uniform across the land as a result the total demand can be calculated simply by multiplying *D* to *Area*. Figure 8 illustrates the correlation between irrigation water demand as the predictor and precipitation, and temperature. The dependency between water withdrawal and irrigation demand was shown in Figure 7.

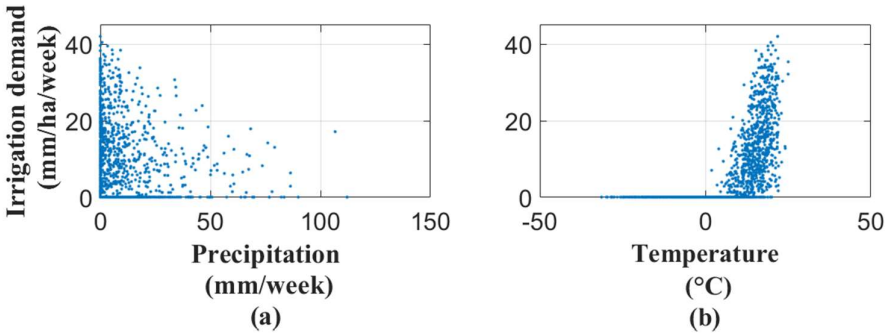

Fig.8. Correlation between dependent variable (irrigation demand) and independent variables (precipitation- Panel a, and temperature- Panel b) at Oldman Reservoir.

In this figure, Panel (a) shows the dependency between irrigation demand and precipitation. Panel (b) also presents the correlation between irrigation demand and temperature. Based on this figure, irrigation demand and precipitation have negative correlation while irrigation demand and temperature have direct relationship. In other words, when precipitation increases, irrigation demand decreases. Moreover, in warmer temperature, irrigation demand goes up. Based on these panels, maximum irrigation demand is 40 mm/ha/week.

Reservoir release R (CMS/week), which is the lumped representation of all withdrawals from the Oldman Reservoir for downstream needs, can be described as a MLR- or ANN-based mapping of *rel* as the following:

$$R_t = rel(I_t, S_{t-1}, (E-P)_t, D_t \times Area \times 10) \quad (9)$$

I, S, E and P are inflow to reservoir (CMS/week), reservoir storage (MCM/week), reservoir evaporation (mm/week) and local precipitation (mm/week) respectively. D and $Area$ represent irrigation demand per unit of area (mm/week/hectare) and irrigation area (hectare). The multiplier of 10 is used to convert the unit of irrigation demand from (mm/hectare) to (m^3). Our assumption in developing this equation is that reservoir release is constant during an operational week. This equation is a continues mathematical function with a positive range. The time series of inflow to reservoir and reservoir release obtained from WRMM are shown in Figures A1 and A7 (Appendix), respectively. Figure 9 shows the correlation between reservoir release as the dependent variable and reservoir storage, inflow to reservoir, lake evaporation, precipitation and irrigation demand as independent variables.

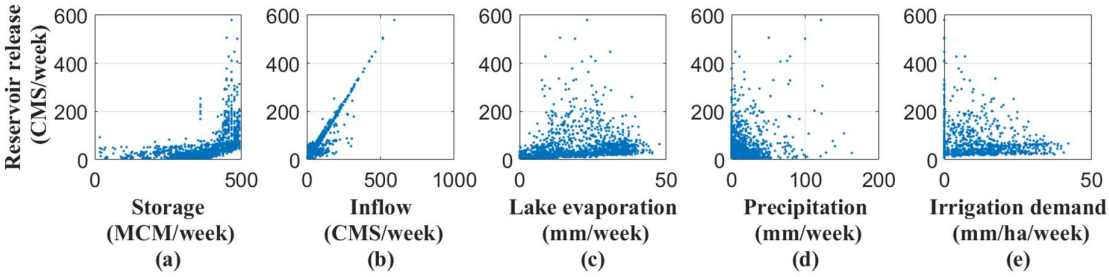

Fig.9. Correlation between dependent variable (reservoir release) and independent variables (reservoir storage- Panel a, inflow to reservoir-Panel b, lake evaporation-Panel c, precipitation-Panel d and irrigation demand-Panel e) at the Oldman Reservoir.

Figure 9 shows the correlation between reservoir release and storage (Panel-a), inflow (Panel-b), lake evaporation (Panel-c), precipitation (Panel-d) and irrigation demand (Panel-e). Based on the panels, reservoir release has a direct relation with storage, inflow, lake evaporation and irrigation demand whereas there is a negative correlations between reservoir release and precipitation. Panel (a) shows that the reservoir release exponentially increases when reservoir storage is more than 450 MCM. Panel (b) explains the significant correlation between inflow

and reservoir release. Panel (c) shows that lake evaporation and reservoir release have positive correlation. In other words in warmer climate, when the reservoir is under pressure, higher amount of water evacuates to downstream. Panel (d) explains that in case of precipitation, operators are more intended to store water in the reservoir. In this case, precipitation provides environment or downstream irrigation district with their water demands. Based on these panels, maximum reservoir release is 600 CMS.

Figure 10, panels (a) to (d) show the functional mappings proposed based on the perfect *priori* about the emulators' inputs. These emulators can be integrated through the mass balance equation (Panel- e), which estimates the change in storage (m^3/week) based on the inflow (m^3/week), net evaporation (m^3/week), local withdrawal (m^3/week) and reservoir release (m^3/week):

$$S_t = S_{t-1} + (I_t - R_t) \times 604{,}800 - (E_t - P_t) - area \times 10 \times WD_t \quad (10)$$

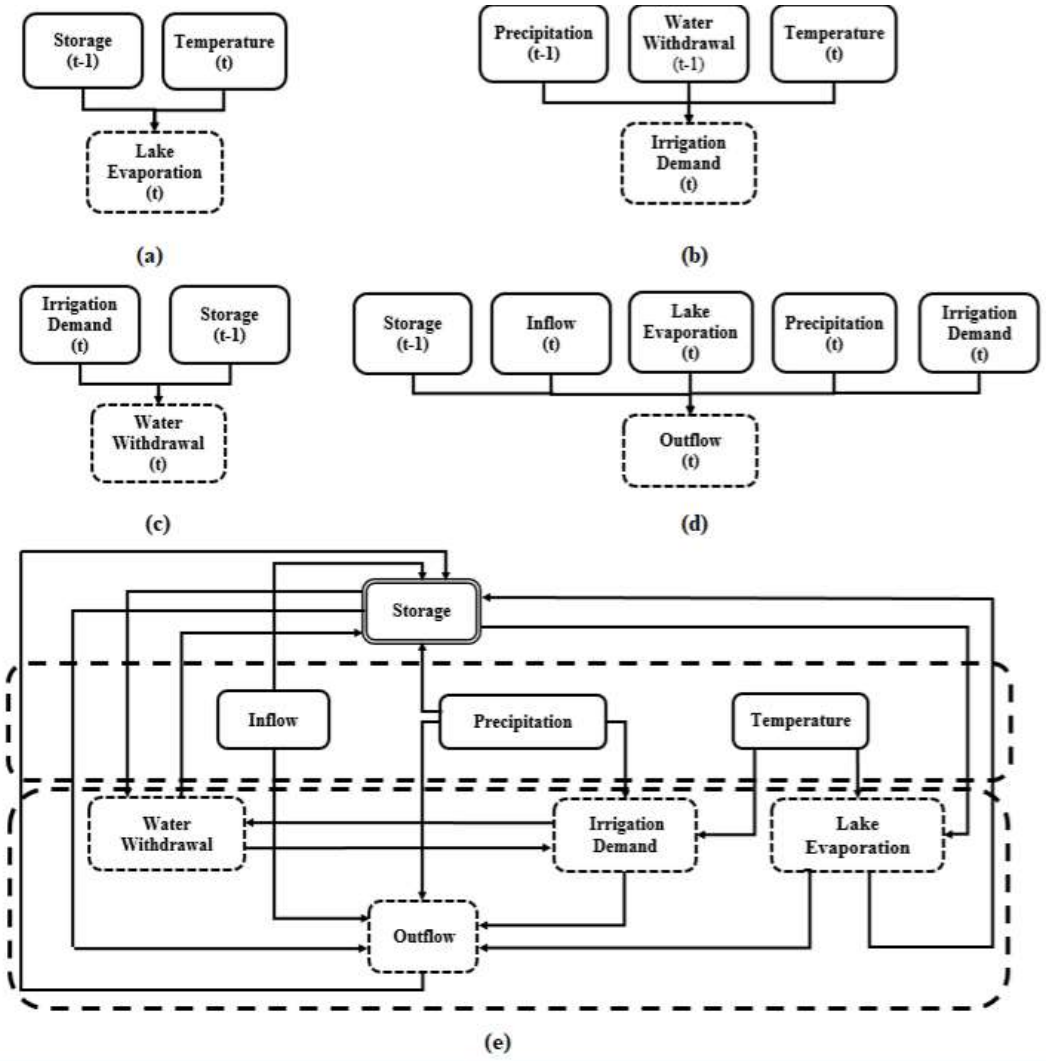

Fig. 10. The predictor/predictand relationships for emulators developed assuming perfect *priori* for (a) Reservoir evaporation, (b) local irrigation demand, (c) local water withdrawal, and (d) reservoir release. Panel (e) shows the integrated emulator obtained by coupling individual emulators shown in panels (a) to (d).

Panel (e) shows how the developed emulators are integrated to represent the state of the system (storage). This panel presents three levels. The lower and middle dashed rectangulars are input variables with which emulators are developed. The lower dashed rectangular shows the individual emulators, developed for the four variables and their interactions. For instance, here the link between water demand and withdrawal is presented. Irrigation demand emulator uses precedent water withdrawal estimations and observed precipitation data as well as current time-step observed temperature as its inputs to update water withdrawal in the current time-step. Whereas Irrigation demand emulator itself in the current time-step along with previous time-

step storage are the inputs of water withdrawal emulator to update this variable in the current time-step. As another example, lake evaporation emulator gets its input variables from previous time-step storage and current time-step observed temperature and is fed to reservoir release emulator to estimate current time-step reservoir release with current time-step of inflow to reservoir, precipitation and irrigation demand. In the third level the water withdrawal, evaporation and reservoir outflow estimations as well as observed inflow to reservoir and precipitation at the current time-step are also fed into mass balance equation to update current time-step of reservoir storage. This procedure continues throughout all the period with which the emulators have been developed or can be applied to test or validation periods to evaluate the performance of the system. With this approach it is possible to assess the link between variables within the system and their interactions. In addition, by including climate data and irrigation area in emulators' equations, it is possible to evaluate the effect of changing climate or human intervention in irrigation area on the performance of the system.

5.3 Alternative hypotheses for setting up and falsifying emulators

For each predictand, a set of alternative hypotheses for emulators is set up by matching MLR and ANN mappings with three scenarios outlined above for emulator input selection. Here, the two mentioned mapping techniques are used in order to have the capability to compare models and find the emulators that can better represent the dynamic of their target variables. Figure 11 shows the development hierarchy for setting up emulators for the four emulation cases noted above and introduce the model IDs for reservoir evaporation (E), local withdrawals (WD), local demand (D) and reservoir release (R).

Considering the MLR for developing functional mappings, it would be seven emulators in total: One emulator is related to perfect *priori* and the other six emulators correspond to considering the two input variable pools with three setups of the PCIS algorithm using three measures of dependence, i.e. Kendall's tau, Pearson's correlation coefficient and Spearman's rho respectively. Similar configurations are considered for ANN structures, but each ANN structure have been established with 1 to 10 neurons, configured in one hidden layer.

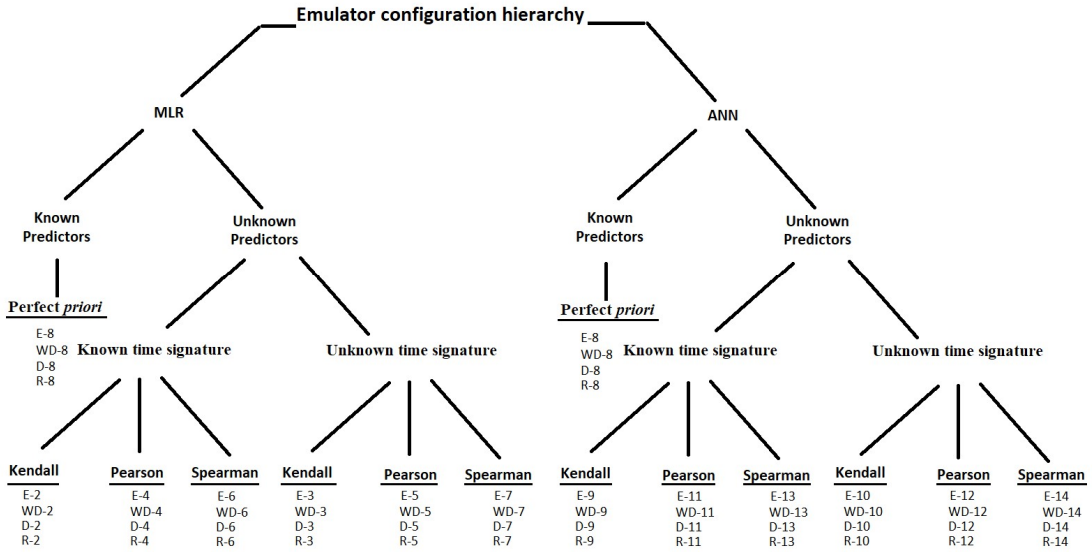

Fig. 11. Development hierarchy and the IDs for individual emulators developed for reservoir evaporation (E-1 to E-14), local withdrawal (WD-1 to WD-14), local demand (D-1 to D-14) and reservoir release (R-1 to R-14) at the Oldman Reservoir.

Simulations with different neuron configurations can address uncertainty regarding developed models. In addition, based on Coulibaly et al. (2005) the number of training examples can be found using Equation 11.

$$N > \frac{|W|}{(1-a)} \tag{11}$$

where N is number of training examples, W is total number of weights and biases of the network and a is required accuracy.

Based on the number of available data for training ANN-based emulators, weights and biases corresponding to the most complex model and the considered 97.5 percent confident interval, here, maximum 10 neurons are examined. This characteristic stays the same for developing other ANN-based emulators with lower level of complexity, mainly due to respect homogeneity in model development. Also, The only hidden layer for developing networks is considered with respect to Hornik et al. (1989) suggestion that a feedforward ANN with enough neurons in one hidden layer is a universal approximator.

As noted above, the parameters of MLR emulators with associated confidence intervals and predictive uncertainty can be obtained by the Maximum Likelihood Method. In this regard, the parameters of emulators which are developed with MLR approach are found with 95% level of confidence. Here, the range of each parameter is divided to four segments resulting in five different realizations for each parameter of the equations. Having the different realizations for all the parameters, equations are run with mixed and matched realizations. The ensemble of estimations can create the uncertainty regarding the emulation variable. For ANN-based emulators (70 in total for each emulation variable – 7 input configurations matched with 1 to 10 hidden neurons), the training is repeated 100 times using different initial conditions to provide an ensemble of 100 independent sets, with which parametric and predictive uncertainty can be characterized. Figure 12 shows five realizations of one parameter of reservoir release MLR-based emulator and 100 different weights that link storage values as an input to a neuron in hidden layer for water withdrawal ANN-based emulator.

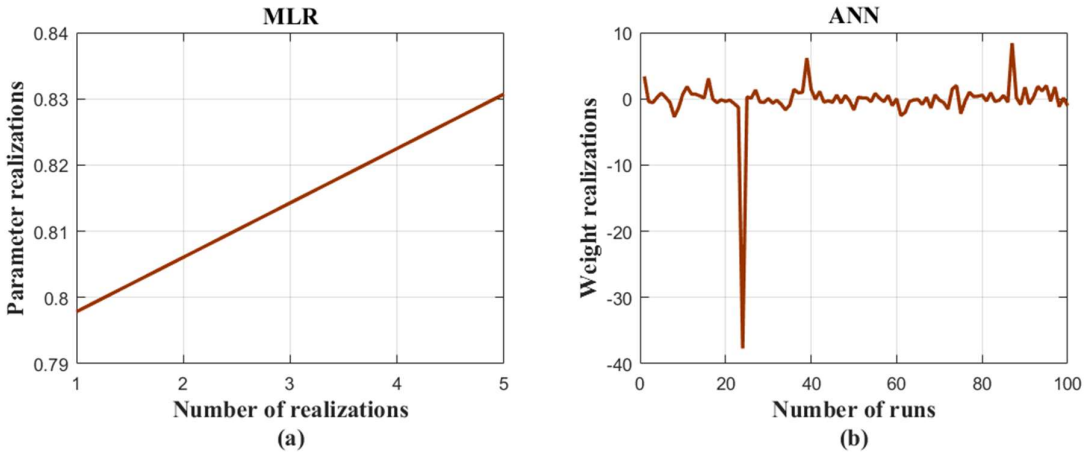

Fig. 12. Different realizations of parameters and weights for (a) MLR-based emulator of reservoir release and (b) ANN-based emulator of water withdrawal.

Panel (a) shows different realizations of a parameter in reservoir release emulator developed by MLR approach. The lower and upper bounds have been found with 95% confidence interval and other values have been uniformly distributed between these limits. In other words, with 95% level of confidence, the parameters of MLR emulator are 0.797 and 0.83. Three other values generated between these values as shown in the panel. Panel (b) also presents weights in an ANN-based emulator of water withdrawal. The weights link an input variable (storage) to one neuron in a hidden layer.

To assess the performance and to discriminate between different emulators, a set of goodness-of-fit measures are used. These measures include Coefficient of Determination (R^2), Root Mean Square of Errors ($RMSE$), Logarithmic *RMSE* ($LRMSE$), Nash-Sutcliffe Efficiency (NSE), Relative error in Peak (REP), Ideal Point Error (IPE) and Bayesian Information Criterion (BIC). The definitions and formulations of these error measures are described as bellow:

The coefficient of determination (R^2) can be described as:

$$R^2 = \left(\frac{\sum_{i=1}^{n}(O_i - \bar{O})(P_i - \bar{P})}{\sqrt{\sum_{i=1}^{n}(O_i - \bar{O})^2}\sqrt{\sum_{i=1}^{n}(P_i - \bar{P})^2}} \right)^2 \quad (12)$$

where O is the simulated values of the WRMM model; P is the simulated values of the surrogate model; and n is the number of data points. The range of R^2 lies between zero and one and representing the ratio of variance in O that is described by P.

The overall (dis)agreement between the simulations of WRMM and surrogate models (O and P, respectively) can be measured by the *RMSE* – see Equation S1-2. The higher the difference between O and P is, the higher value of $RMSE$ is.

$$RMSE = \sqrt{\frac{\sum_{i=1}^{n}(O_i - P_i)^2}{n}} \quad (13)$$

As *RMSE* considers the squares of errors, it tends to minimize larger errors that are normally associated with high data points. In order to reduce the sensitivity of the error measure to higher data points, we calculated the *RMSE* of the logarithmically transformed data, i.e. *LRMSE*. The logarithmic transformation results in flattening the higher values, which makes lower values more influential in assigning the goodness-of-fit.

The Nash-Sutcliffe efficiency (NSE) proposed by Nash and Sutcliffe (1970) is defined as Equation S1-3. This coefficient is between –∞ and 1.

$$NSE = 1 - \frac{\sum_{i=1}^{n}(O_i - P_i)^2}{\sum_{i=1}^{n}(O_i - \bar{O})^2} \quad (14)$$

The negative values of NSE indicate accuracies below the long-term mean of the time series. Zero means the accuracy equal to the long term mean of the time series and one means a perfect fit. The Relative Error of Peak (REP) is defined as:

$$REP = \frac{mean(max\ annual\ observed\ value - max\ annual\ estimated\ value)}{max\ annual\ observed\ value} \quad (15)$$

The REP indicates the expected magnitude of error in estimating the annual peaks.

In order to combine the effect of $RMSE, LRMSE, EV$ and REP measures in one indicator, Elshorbagy et al. (2010) defined the Ideal Point Error (IPE) as define below. The lower values for the IPE correspond to higher level of accuracy and it means that the model is closer to the ideal point with coordinates of $RMSE = 0, LRMSE = 0, REP = 0$.

$$IPE = \sqrt{.25 \times \left[\left(\frac{RMSE}{\max(RMSE)}\right)^2 + \left(\frac{LRMSE}{\max(LRMSE)}\right)^2 + \left(\frac{REP}{\max(REP)}\right)^2\right]} \quad (16)$$

The BIC is a likelihood measure that assesses the accuracy and complexity of a model. Lower values of BIC corresponds to higher level of efficiency meaning that results are more accurate and parsimonious (Mekonnen et al. 2015). The *BIC* can be quantifies as below:

$$BIC = nlog(MSE) + klog(n) \quad (17)$$

In which, n is the total number of observations and k is the model parameter. The MSE is the mean of squared errors, and is defined as:

$$MSC = \frac{\sum_{i=1}^{n}(O_i - P_i)^2}{n} \quad (18)$$

The first level of falsification takes place when the optimal number of neurons for each ANN configuration is found. In the first level of falsification, the best parametric set among 100 training trials based on the *RMSE* during the calibration period is selected. By having ten ANN trained structures, corresponding to 1 to 10 hidden neurons, then the ANN emulator that has the lowest *BIC* value during the calibration period is selected and therefore this makes an optimal trade-off between the model complexity and accuracy. The second level of falsification takes place when some of the 14 emulators configured for each variables (see Figure 11) are selected based on their relative performance compared to others. Here, emulators are evaluated based on their optimality and uncertainty which is characterized by the *BIC* during the testing period. For each emulator, the optimality is represented by the *BIC* of the best fit during the testing period. In parallel, the uncertainty is quantified based on the 95% confidence interval of the empirical cumulative distribution of BIC values during the testing phase (between 0.025% and 0.0975% percentiles corresponding the 95% parametric confidence interval). For each variable, (1) best emulator configured based on perfect *priori* along with other emulators that have (2) the highest accuracy, (3) the least uncertainty, and (4) the least trade-off between accuracy and uncertainty are selected. Having the non-falsified emulators for each variable, various configurations for IEs can be set up through mix-and-match. The IEs are then tested in two different periods, i.e. semi- and fully-coupled modes. In brief in the semi-coupled evaluation, which is performed during the testing phase, the storage time series is not updated through integrated simulation; therefore, errors propagate between emulators (and represent in the storage time series) only at any given time-step. In the fully-coupled mode, in contrast, the storage at every time-step is updated through simulation; therefore, errors can propagate from one time-step to another. The fully-coupled evaluation of IEs are take place during the validation phase, in which IEs are discriminated based on their performance in tracking the weekly time series of storage according the *IPE* criterion. In the next chapter, the result of model development procedure is presented.

5.4 Alternative hypothesis for impact assessment study

Having developed integrated emulators, it is possible to assess the performance of the system under changing scenarios. Based on declining streamflow, increasing temperature and developing socio-economic activities in the region, three scenarios is defined:

In the first level of scenario assessment, a bottom-up impact assessment method is applied. Due to changing incoming flow to the region, here changing two main characteristics of streamflow, namely the annual flow volume and annual flow peak are considered. For annual flow volume 11 scenarios of change (from 75% to 125% of historical flow volume in increments of 5%) and for annual flow peak 14 scenarios (from -5 to +8 weeks change in historical annual peak in increments of 1 week) are defined. In total 154 different scenarios of changing both annual flow volume and peak are considered. For each scenario, 100 realizations for streamflow generated by applying Ensemble generation scheme, introduced by Nazemi et al. (2013). All the scenarios of change are fed into best integrated emulator and the response of the system to changing scenarios is assessed.

In the second vulnerability study, a joint bottom-up/top-down approach applied. As discussed previously, temperature is getting warmer in the study area which not only puts pressure on water availability but can significantly increase water demand. For this reason using NASA-NEXT downscaled global climate projections daily temperature data for the period of 1950 to 2100 is obtained. Then the resolution of this data is changed to weekly format. By defining a 30 year window and moving it throughout the whole time series, expected annual temperature for each window is found. In the next stage these realizations are clustered in pools corresponding to no change in expected historical temperature to +3 °C change in historical temperature in increments of 0.5 °C. From each pool 100 realizations are randomly chosen. Having scenarios of changing temperature (7 × 100) and scenarios for changing streamflow (154 × 100) it would be possible to assess the behaviour of the system under joint changing scenarios of streamflow and temperature. Due to the extensive computational runs, instead of evaluating the selected IE for all 154 scenarios of changing the annual flow volume and peak, the focus is on dry (-4, 75%), historical (0, 0) and wet (+4, 125%) regime conditions.

In the third level of vulnerability assessment study, a heuristic impact assessment is applied. Based on developing socio-economic activities in the region, there is a serious competition for water by different sectors of water use such as agriculture, industry and municipality. In particular, agriculture is of high importance in this region because Alberta is one of the most important food producers in Canada and water managers and stakeholders are willing to expand agricultural activities in this region. Therefore, in this level of assessment the joint effect of changing streamflow, temperature, precipitation and irrigation area on the water resource system is evaluated. For this purpose, it is assumed that streamflow, precipitation and irrigation

area can decrease (-25%) or increase (+25%) in historical time series. Also another scenario is defined under which these variables will not change. For temperature three scenarios for decrease (-2 °C), no change and decrease (+2 °C) in historical time series are defined as well. These scenarios are coupled and fed in top selected IE and the vulnerability of the system under defined scenarios of change will be evaluated.

Chapter 6. Results

6.1 Individual emulators for each variable

As described in Chapter 5, for each variable 77 alternative hypotheses are developed. 7 emulators are MLR-based (according to 7 scenarios of predictor selection) and other 70 emulators are ANN-based (according to 7 scenarios of predictor selection × 10 scenarios for number of neurons ranging from 1 to 10). For emulators developed using ANN approach, corresponding to minimum best BIC, optimal number of neuron for each variable is found. This leads to selected 7 ANN-based individual emulators. As a result, for each variable, 14 alternative hypotheses for emulators based on the configuration hierarchy outlined in chapter 5 has been set up. Here, the focus is on presenting the optimum neuron number for each variable developed using ANN approach. Figures 13 to 20 show the optimum neuron number for each variable during the calibration period.

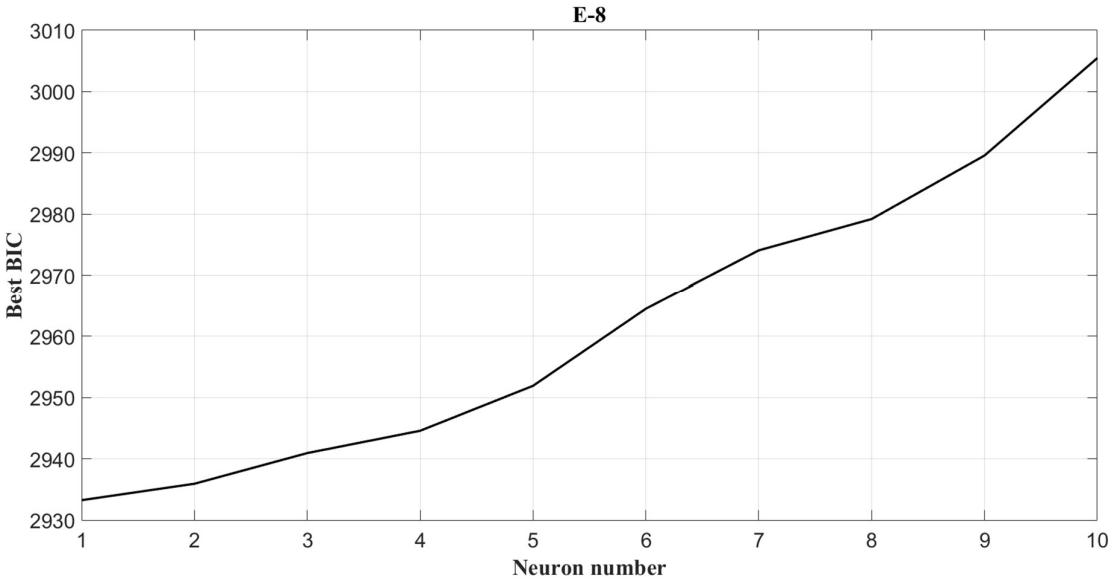

Fig 13. Optimum neuron number for individual emulator of lake evaporation for the perfect *priory* scenario in predictor selection during the calibration period.

As shown in Figure 13, in the case that lake evaporation emulators developed with *perfect* priory knowledge regarding the independent variables, the emulator with only one neuron shows the highest accuracy and least complexity. Results of the optimum neuron numbers for the emulators developed in the two other defined scenarios of predictor selection are demonstrated in Figure 14.

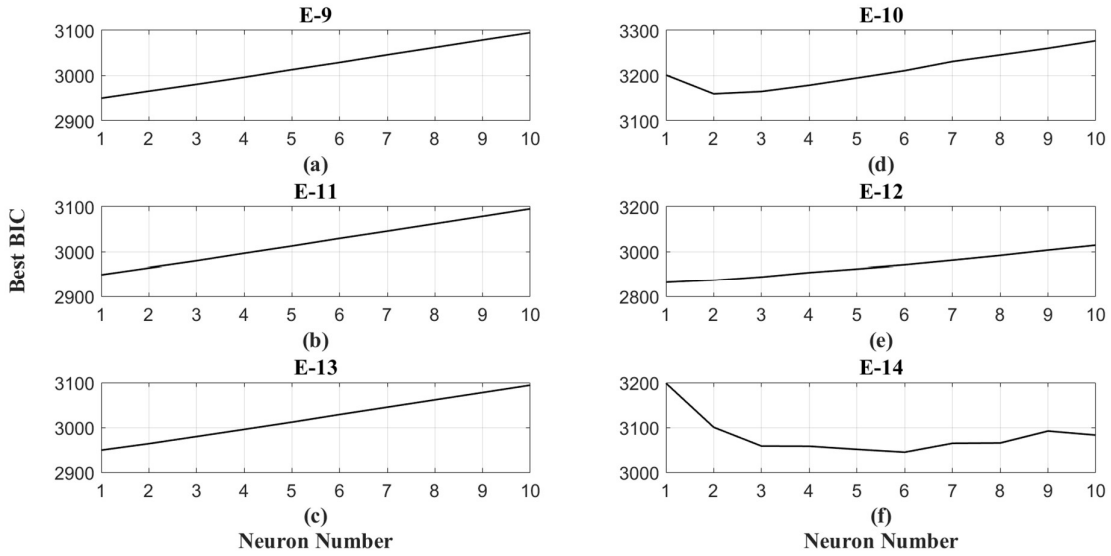

Fig 14. Optimum neuron numbers for individual emulators of lake evaporation during the calibration period when (1) predictors are known but their relevant time signatures are unknown (E-9, E-11 and E-13) and (2) predictors and their relevant time signatures are unknown (E-10, E-12 and E-14).

Panels (a), (b) and (c) in Figure 14 present lake evaporation individual emulators which have been developed in the second scenario of predictor selection. In this scenario, the predictors are unknown and have been chosen from a pool of variables. Based on emulator configuration hierarchy, these models are called E-9, E-11 and E-13. In the right side of the figure, Panels (d), (e) and (f) belong to the individual emulators that their predictors as well as their relevant time signature are unknown. These emulators are named as E-10, E-12 and E-14. As presented in the figure, the optimum neuron number for the emulators with known predictors and unknown time signatures is one. Whereas for the other three individual emulators, the optimum neuron number is two, one and six for E-10, E-12 and E-14, respectively. Figure 15 shows the optimum neuron number of individual emulator for water withdrawal when a perfect knowledge about the necessary input variables and their associated time signatures is available. Based on emulator configuration hierarchy, WD-8 is the model of water withdrawal with known proxies. In this figure, x-axis presents the number of neurons and y-axis shows best *BIC* values corresponding to each neuron number.

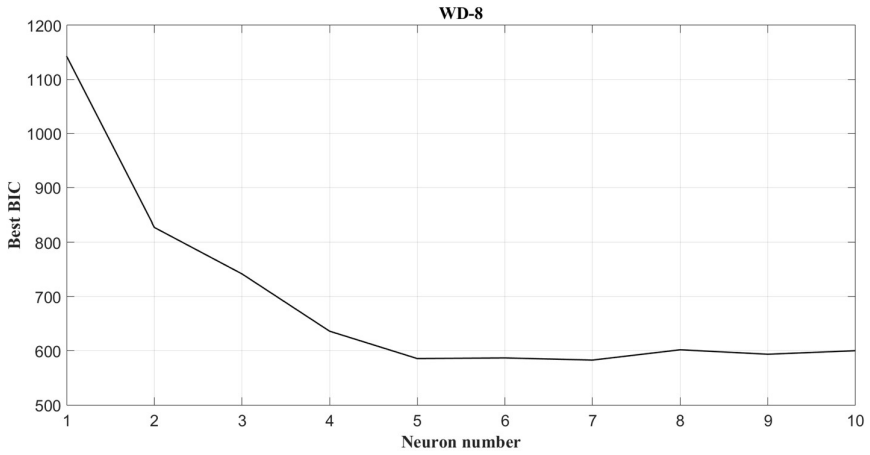

Fig 15. Optimum neuron number for individual emulator of water withdrawal for the perfect *priory* scenario in predictor selection during the calibration period.

Based on Figure 15, when the required predictors with their relevant time signatures are known, optimum neuron number for developed individual emulator of water withdrawal is seven. The optimum number of neurons for developed individual emulators of water withdrawal for the other two scenarios of predictor selection is demonstrated in Figure 16.

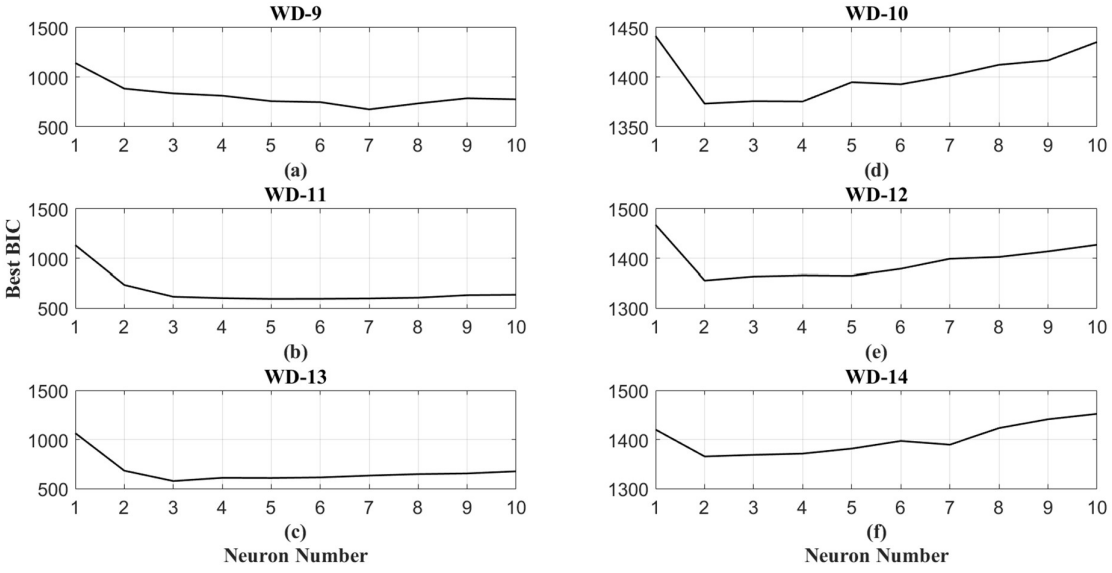

Fig 16. Optimum neuron numbers for individual emulators of water withdrawal during the calibration period when (1) predictors are known but their relevant time signatures are unknown (WD-9, WD-11 and WD-13) and (2) predictors and their relevant time signatures are unknown (WD-10, WD-12 and WD-14).

Figure 16 shows the individual emulators for water withdrawal developed with known predictors but unknown time signatures in panels (a), (b) and (c) corresponding to emulators WD-9, WD-11 and WD-13. Moreover, panels (d), (e) and (f) demonstrate individual emulators of water withdrawal with unknown predictors and time signatures corresponding to models WD-10, WD-12 and WD-14. Based on this figure, optimum neuron number for models WD-9, WD-11 and WD-13 are seven, five and three, respectively. Also all the individual models developed with the third predictor selection scenario show that their optimum neuron number is two. The optimum neuron number for irrigation demand emulator is demonstrated in Figure 17.

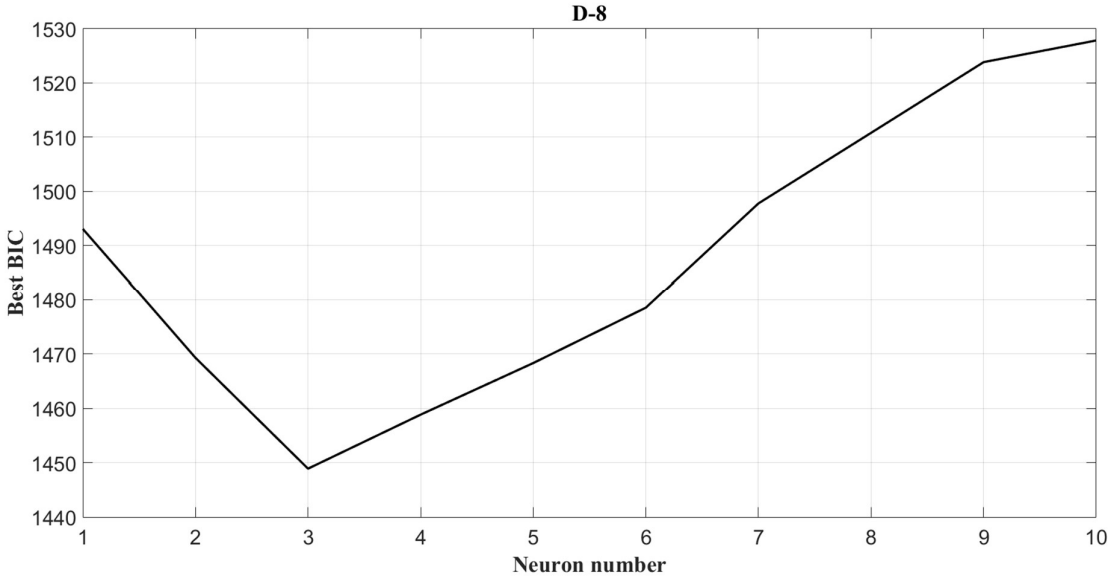

Fig 17. Optimum neuron number for individual emulator of irrigation demand for the perfect *priory* scenario in predictor selection during the calibration period.

As shown in the figure, individual emulator of irrigation demand that have been developed using the perfect priori knowledge regarding the predictors has three neurons. Figure 18 illustrates the optimum number of neurons for the irrigation demand emulators in the second and third scenarios of predictor selection.

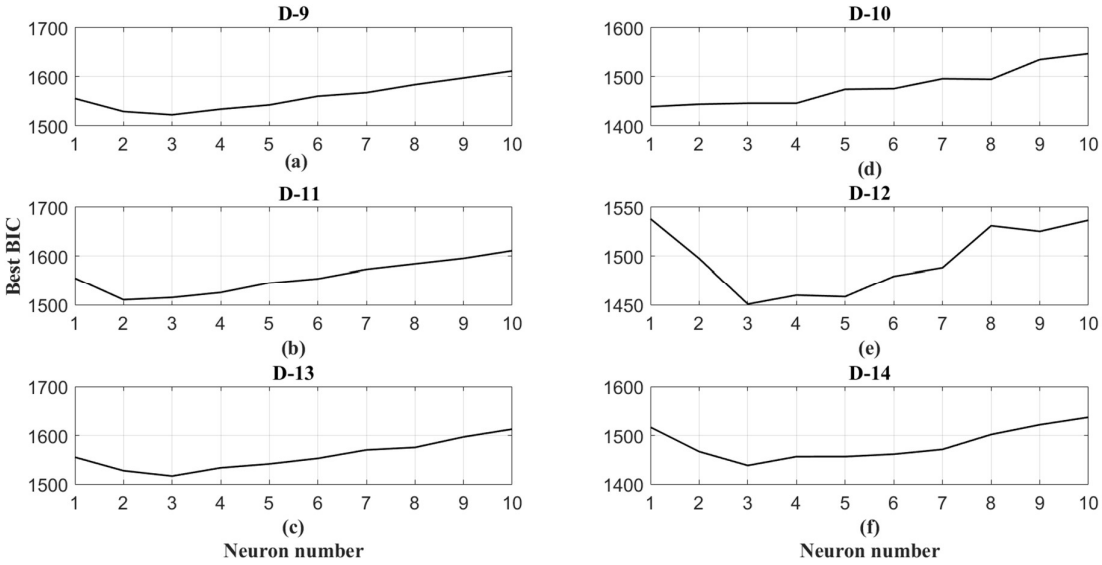

Fig 18. Optimum neuron numbers for individual emulators of irrigation demand during the calibration period when (1) predictors are known but their relevant time signatures are unknown (D-9, D-11 and D-13) and (2) predictors and their relevant time signatures are unknown (D-10, D-12 and D-14).

Panel (a), (b) and (c) are related to the individual emulators of irrigation demand with known predictors but unknown time signatures (D-9, D-11 and D-13). Moreover, Panels (d), (e) and (f) belong to the individual emulators of irrigation demand with unknown predictors and their related time signatures (D-10, D-12 and D-14). The optimum number of neurons for models with only known predictors are three, two and three, as shown in Panels (a) to (c) and for models with the third scenario of predictor selection are one, three and three, indicated in Panels (d) to (f). The optimum number of neurons for the individual emulator of reservoir release with perfect *priori* knowledge of the model's predictors is shown in Figure 19. According to emulator configuration hierarchy, R-8 is the model of reservoir release with known proxies. In this figure, x-axis presents different number of neurons which have been considered in this study, and y-axis shows best *BIC* values corresponding to each neuron number. Since we considered 1 to 10 neurons to develop emulators for the four variables (i.e. lake evaporation, water withdrawal, irrigation demand and reservoir release) the range of x-axis varies between 1 to 10.

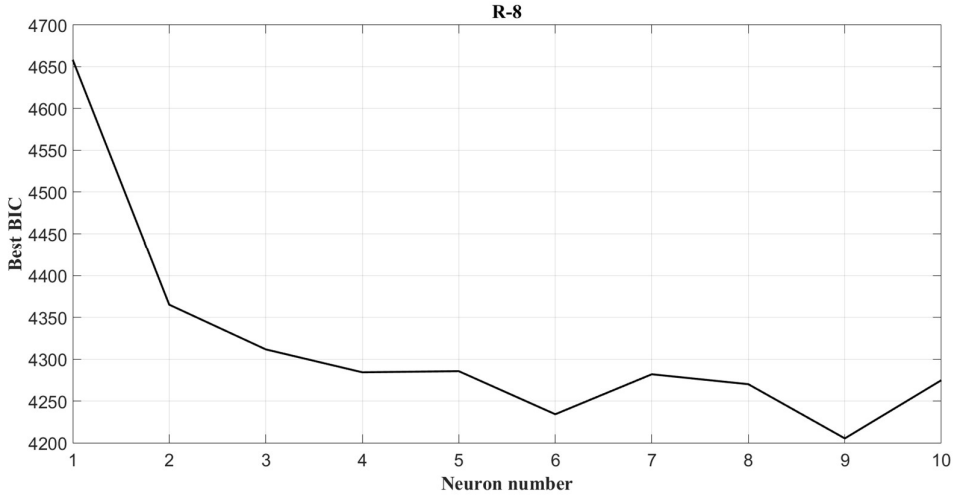

Fig 19. Optimum neuron number for individual emulator of reservoir release for the perfect *priory* scenario in predictor selection during the calibration period.

Based on Figure 19, when a complete knowledge regarding predictors and their relevant time signature is available, an individual emulator with 9 neurons can optimally describe reservoir release. Figure 20, demonstrate optimum number of neurons for the emulators that their predictors and/or their time signature are unknown.

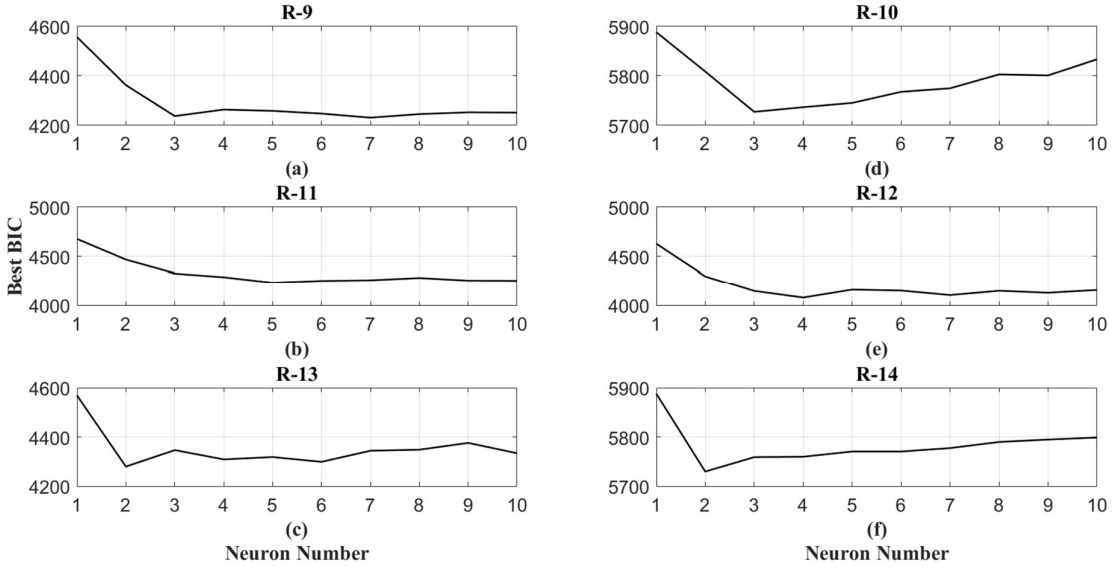

Fig 20. Optimum neuron numbers for individual emulators of reservoir release during the calibration period when (1) predictors are known but their relevant time signatures are unknown (R-9, R-11 and R-13) and (2) predictors and their relevant time signatures are unknown (R-10, R-12 and R-14).

Figure 20 shows the individual emulators of reservoir release when their predictors are known but there is no knowledge about their time signatures. These emulators are presented in Panels (a), (b) and (c) which correspond to models R-9, R-11 and R-13. In the right side of the figure, Panels (e), (f) and (g), present individual emulators that their predictors and the relevant time signatures are unknown. These models are R-10, R-12 and R-14, based on the emulator configuration hierarchy. For the first group of emulators, optimum number of neurons corresponding to models R-9, R-11 and R-13 are three, five and two and individual emulators in the second group are optimised with three, four and two neurons for emulators R-10, R-12 and R-14, respectively.

Having developed 14 alternative hypotheses for emulators, the behaviour of models in representing the four variables based on which the models have been developed is assessed. This assessment is run during the test data period. Based on this study, it would be possible to investigate the accuracy and uncertainty of emulators to track the WRMM simulations. The expected annual WRMM lake evaporation and model estimations for the emulators developed using MLR and ANN techniques during test period are shown in Figure 21.

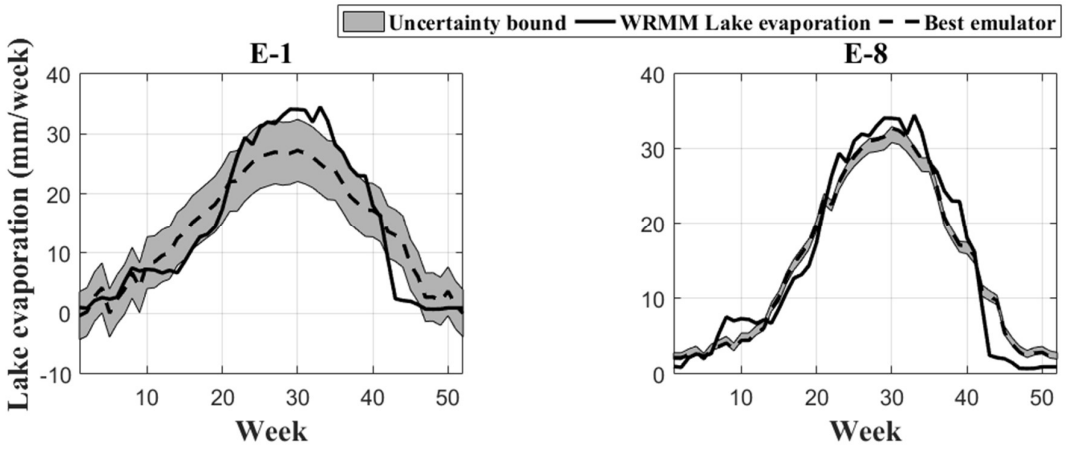

Fig 21. Expected annual WRMM lake evaporation simulations (solid line) and best-fit emulators' estimation (dashed line) and corresponding predictive uncertainty bound (the grey envelope) during the test period for the emulator developed using: (a) MLR and (b) ANN techniques when perfect *priori* knowledge about predictors is available.

Left panel in Figure 21 belongs to the individual emulator of lake evaporation developed using MLR technique. For this emulator, perfect knowledge regarding the model's predictors is available (E-1). Right panel presents the emulator which have been developed using ANN technique. For this emulator also predictors and their time signatures are fully known (E-8). In these panels, the solid lines belong to WRMM lake evaporation simulation during the test period, dashed lines represent best emulator estimations and the gray envelops demonstrate the uncertainty of models. Results show that both emulators overestimate WRMM lake evaporation during spring and fall and underestimate WRMM lake evaporation during summer. Moreover, comparing two panels, it is clear that the emulator developed with ANN technique is less uncertain in comparison with the MLR-based emulator. Figure 22 presents weekly time series of WRMM lake evaporation simulations, best-fit emulator's estimation and corresponding uncertainty bound for emulators E-1 and E-8.

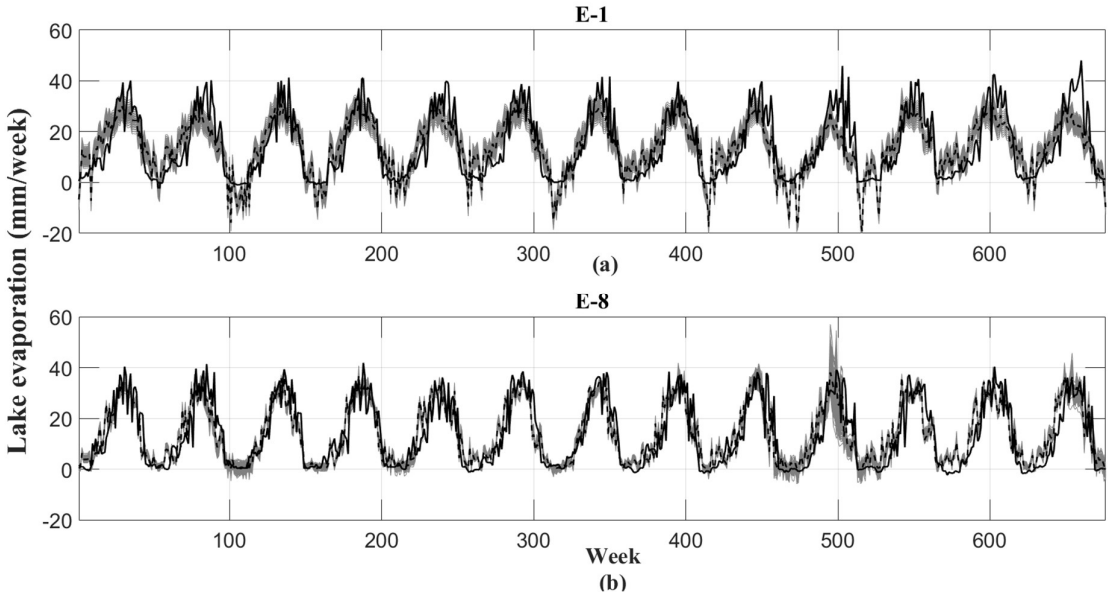

Fig 22. Weekly time series of WRMM lake evaporation simulations (solid lines) and best-fit emulators' estimations (dashed lines) and corresponding predictive uncertainty bound (the grey envelopes) during the test period for the emulator developed using: (a) MLR and (b) ANN approaches when perfect *priori* knowledge about predictors is available.

The description of lines and features in the figure is the same as what mentioned above. Panels (a) and (b) belong to emulators E-1 and E-8, respectively. Based on this figure, model E-8 shows less uncertainty. In particular, model E-1 demonstrates high uncertainty in extreme low values which dominantly occurs throughout the period. Figure 23 shows the expected annual

estimations of emulators developed based on partially known or unknown predictors with MLR and ANN techniques during the test period.

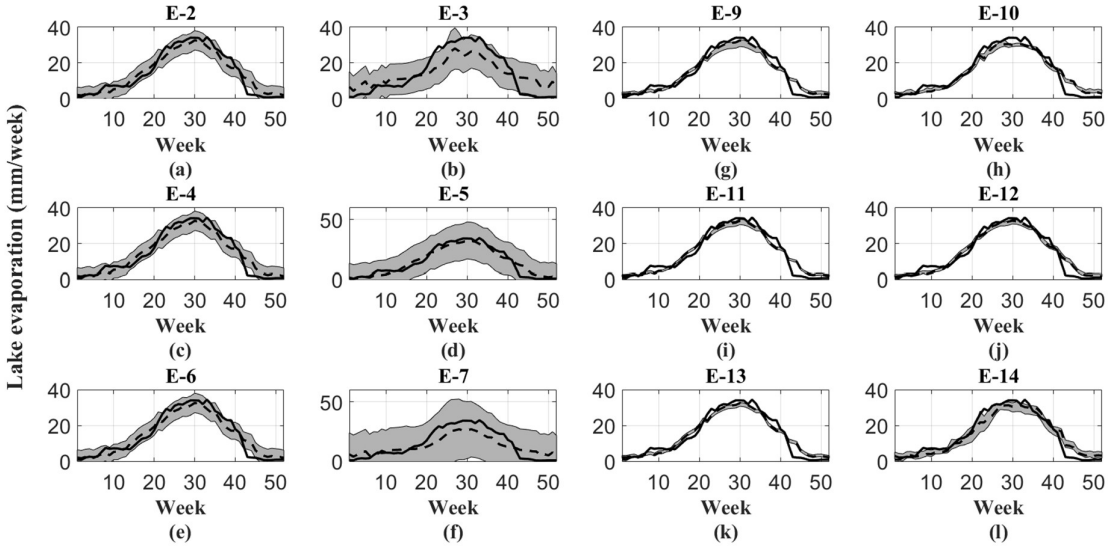

Fig 23. Expected annual WRMM lake evaporation simulations (solid lines) and best-fit emulators' estimations (dashed lines) and corresponding predictive uncertainty bound (the grey envelopes) during the test period for the emulator developed using MLR and ANN techniques when predictors are partially known or unknown.

Panels (a) to (f) belong to emulators of lake evaporation developed using MLR technique. Emulators shown in Panels (g) to (l) are developed by applying ANN technique. As presented in Panels (a) to (f), models E-2, E-4 and E-6 are less uncertain in comparison with models E-3, E-5 and E-7. For the first three emulators although the predictors were unknown and were chosen from a pool of potential variables but their relevant time signatures were known. However, for the three latter emulators, both predictors and their time signatures were unknown. In the other side, Panels (g) to (l) show that except E-14 that performs higher uncertainty bound, all the other five emulators are almost equally uncertain. In addition, the models developed with ANN technique are less uncertain in comparison with models developed using MLR technique. Moreover, all the models shown in Figure 23 overestimate WRMM lake evaporation in spring and fall and underestimate WRMM lake evaporation during summer. Figure 24 presents the weekly time series of WRMM lake evaporation simulations, best-fit emulator's estimation and corresponding uncertainty bound for emulators developed with partially known or unknown predictors.

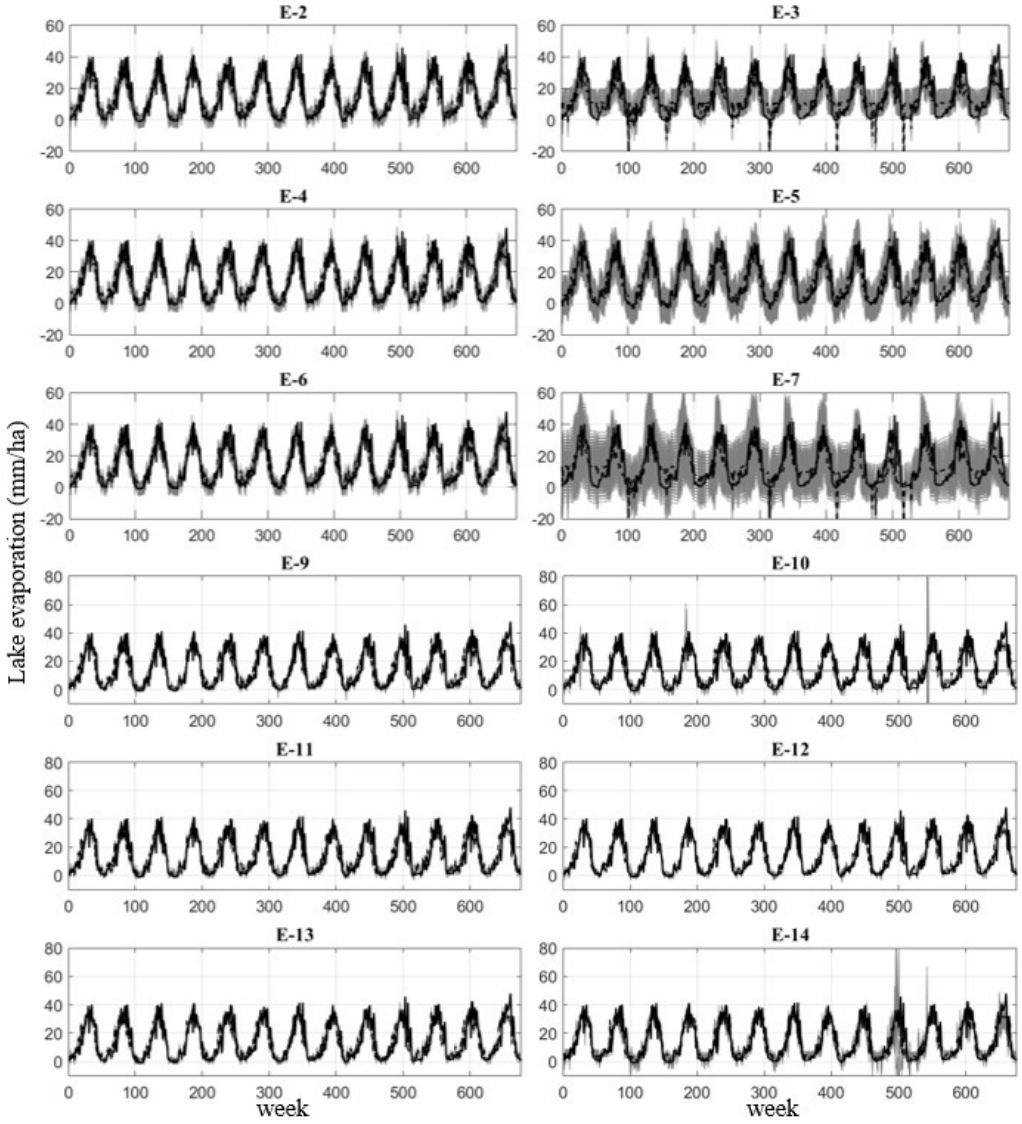

Fig 24. Weekly time series of WRMM lake evaporation simulations (solid lines) and best-fit emulators' estimations (dashed lines) and corresponding predictive uncertainty bound (the grey envelopes) during the test period for the emulator developed using MLR and ANN techniques when predictors are partially known or unknown.

As shown in the figure, models E-2, E-4 and E-6 which have been developed by applying MLR technique are presenting low uncertainty in comparison to models E-3, E-5 and E-7 which are ANN-based emulators. But the uncertainty in low extremes in these models are considerable. Models E-3, E-5 and E-7 are uncertain throughout the whole period. E-9, E-11, E-12 (MLR-based) and E-13 (ANN-based) are emulators that estimate the WRMM lake evaporation simulations acceptably. Models E-10 and E-14 are mostly uncertain in particular in extreme

low values. Two periods in model E-10 (weeks 190 and 540) and one period in model E-14 (week 500) are showing high uncertainty. Figure 25 presents expected annual water withdrawal per unit of area emulators developed with MLR and ANN techniques while the complete knowledge regarding predictors and their time signatures are available.

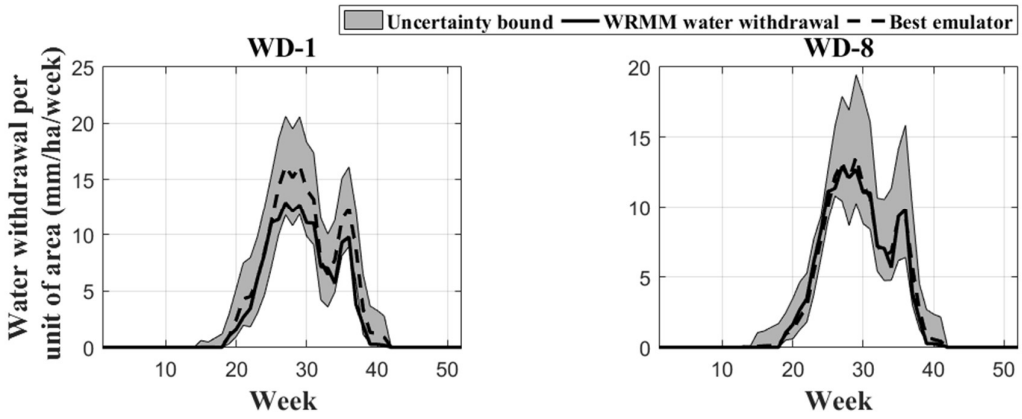

Fig 25. Expected annual WRMM water withdrawal per unit of area simulations (solid lines) and best-fit emulators' estimations (dashed lines) and corresponding predictive uncertainty bound (the grey envelopes) during the test period for the emulator developed using: (a) MLR and (b) ANN techniques when perfect *priori* knowledge about predictors is available.

The left and right panels belong to the emulators developed using MLR and ANN techniques (WD-1 and WD-8), respectively. In these models, full knowledge regarding the predictors and their relevant time signatures are available. The figure shows that the best-fit WD-1 estimation systematically overestimates the WRMM water withdrawal whereas WD-8 best simulation is more accurate. However, WD-1 is less uncertain in comparison with WD-8. Figure 26 presents weekly time series of WRMM water withdrawal per unit of area simulations, best-fit emulator's estimation and corresponding uncertainty bound for emulators WD-1 and WD-8. In this figure, x-axis shows the weeks in which the estimations have been done. Since this simulation is done in the test data period, x-axis covers 676 weeks. In this figure, y-axis shows the variation of water withdrawal throughout the period. Based on this figure, maximum water withdrawal per unit of area is 60 mm/ha/week.

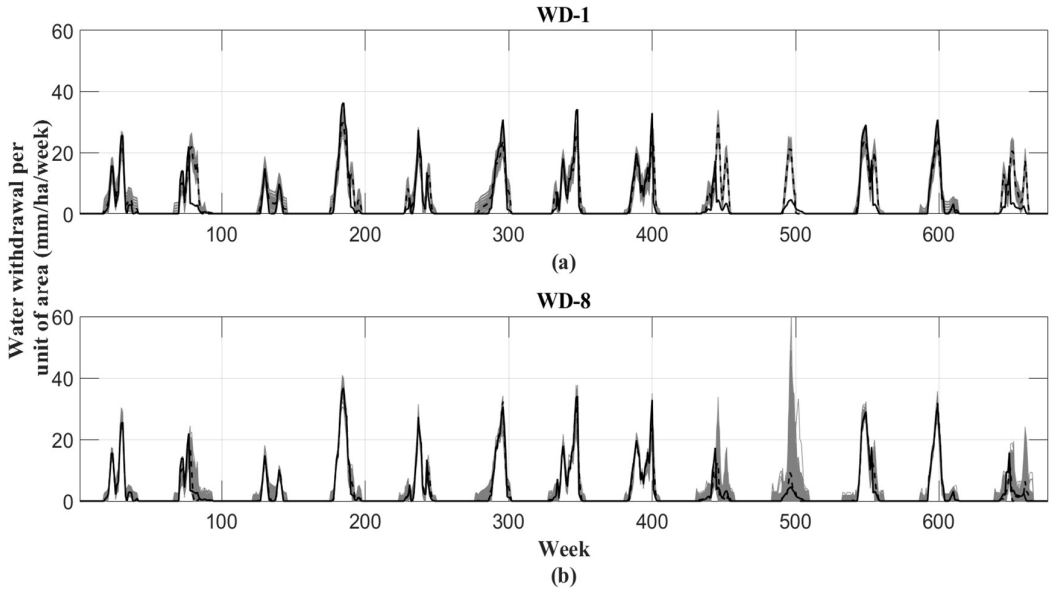

Fig 26. Weekly time series of WRMM water withdrawal per unit of area simulations (solid lines) and best-fit emulators' estimations (dashed lines) and corresponding predictive uncertainty bound (the grey envelopes) during the test period for the emulator developed using: (a) MLR and (b) ANN approaches when perfect *priori* knowledge about predictors is available.

The figure presents time series of water withdrawal per unit of area emulators' estimations (WD-1 and WD-8). In Figure 26, Panel (a) belongs to estimations of water withdrawal applying MLR technique while estimations shown in Panel (b) developed using ANN technique. In both panels, x-axis shows weeks throughout the test period and y-axis belongs to water withdrawal per unit of area. As shown in the figure, in contrast to WD-1, emulator WD-8 is more uncertain in particular around weeks 450, 500 and 650. The expected annual estimations of water withdrawal per unit of area for emulators developed with MLR and ANN techniques in the case that predictors are partially known or unknown as well as WRMM estimation during the test period are shown in Figure 27. In the figure, Panels (a) to (f) show the emulators developed using MLR technique and Panels (g) to (l) belong to emulators that ANN technique was applied to develop emulators for water withdrawal. In models WD-2, WD-4, WD-6, WD-9, WD-11 and WD-13 predictors were unknown while their time signatures were known whereas in models WD-3, WD-5, WD-7, WD-10, WD-12 and WD-14 both predictors and their relevant time signatures were unknown. As presented in the figure, models developed with ANN technique are showing less uncertainty bound in comparison with MLR-based emulators.

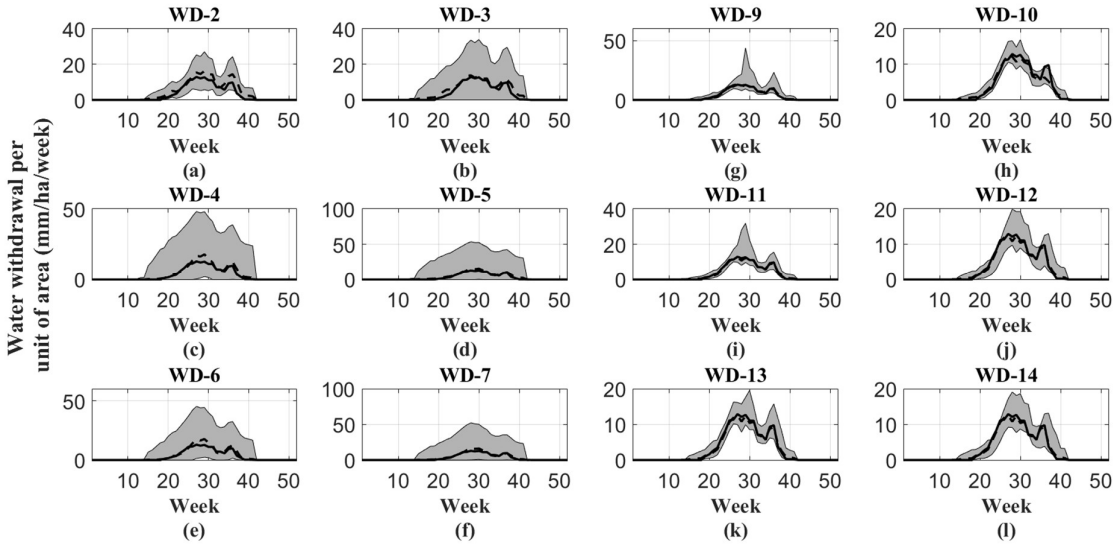

Fig 27. Expected annual WRMM water withdrawal per unit of area simulations (solid lines) and best-fit emulators' estimations (dashed lines) and corresponding predictive uncertainty bound (the grey envelopes) during the test period for the emulator developed using MLR and ANN techniques when predictors are partially known or unknown.

In addition, looking at individual emulators developed applying MLR technique, model WD-2 is performing less uncertainty. Moreover, among ANN-based emulators of water withdrawal, WD-10 is the less uncertain model. However, ANN-based water withdrawal emulator, outperform MLR-based emulator in terms of uncertainty. Figure 28 presents the weekly time series of WRMM water withdrawal per unit of area simulations, best-fit emulator's estimation and corresponding uncertainty bound for emulators developed with partially known or unknown predictors. Among emulators shown in the figure, WD-2 to WD-7 have been developed applying MLR technique while WD-9 to WD-14 are ANN-based emulators. In the first three MLR- and ANN-based emulators, the predictors were known while their relevant time signatures were unknown. In other words, proxies of the equations were partially known. On the other hand, in the latter three MLR- and ANN-based emulators, the predictors and their relevant time signatures were unknown. In the case that predictors are not fully known, they have been selected by the previously mentioned input variable selection scheme. Among models developed with MLR technique (i.e. WD-2 to WD-7), emulator WD-2 is showing less uncertainty. Also, the other ANN based emulators (i.e. WD-9 to WD-14) are presenting less uncertainty in comparison with MLR-based emulators in a majority of weeks except three periods around weeks 190, 450 and 500.

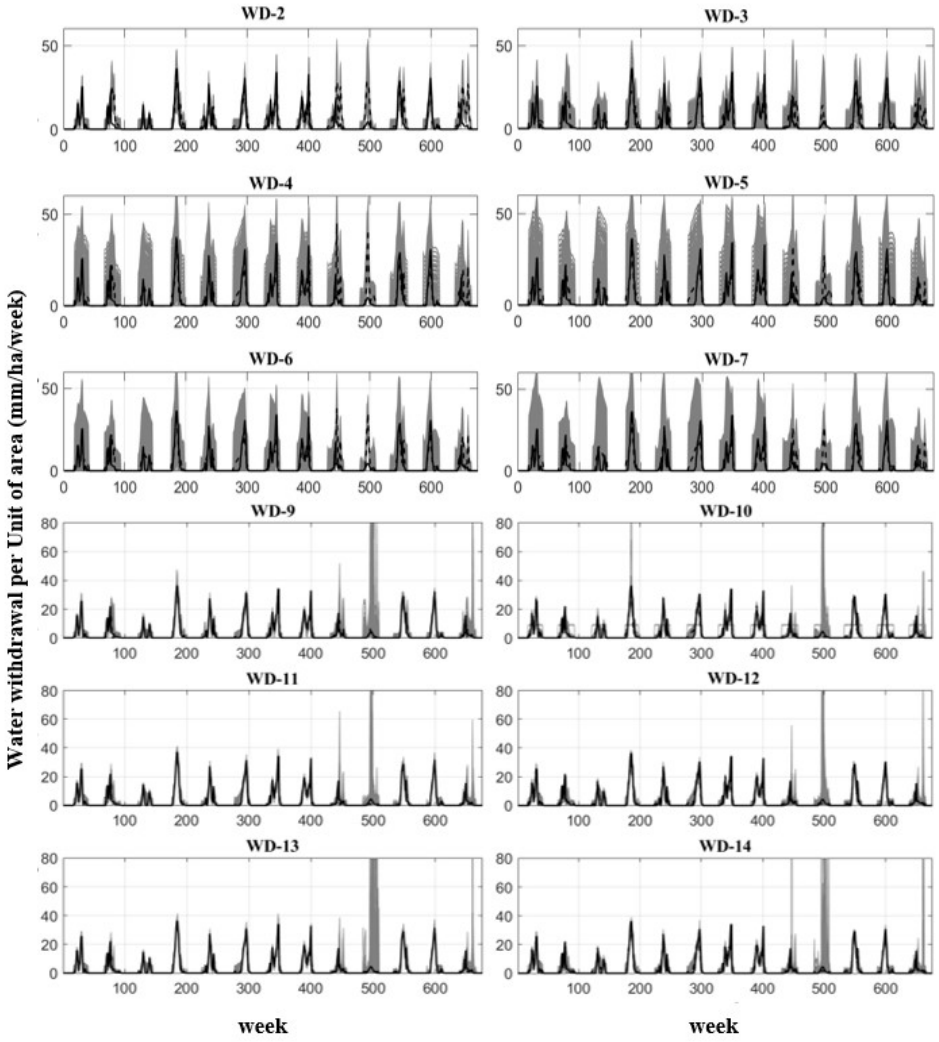

Fig 28. Weekly time series of WRMM water withdrawal per unit of area simulations (solid lines) and best-fit emulators' estimations (dashed lines) and corresponding predictive uncertainty bound (the grey envelopes) during the test period for the emulator developed using MLR and ANN techniques when predictors are partially known or unknown.

Comparing Figures 26 and 28, it can be concluded that emulators WD-1 and WD-8 outperform other emulators in terms of presenting lower uncertainty. Expected annual irrigation demand per unit of area emulator's estimations in the two case that emulators have been developed by MLR and ANN techniques are presented in Figure 29. In addition, in the two panels WRMM estimations and best emulators' estimations have been shown. In this figure, x-axis shows 52 weeks throughout a year and y-axis shows irrigation demand per unit of area in mm/ha/week.

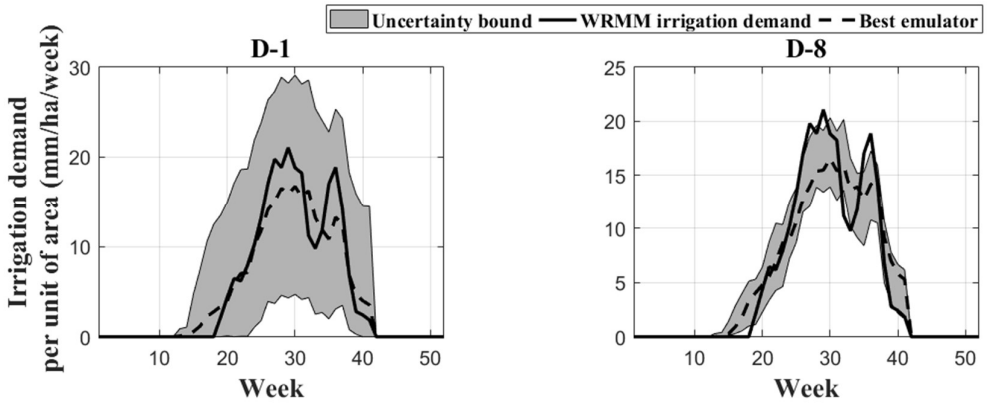

Fig 29. Expected annual WRMM irrigation demand per unit of area simulations (solid lines) and best-fit emulators' estimations (dashed lines) and corresponding predictive uncertainty bound (the grey envelopes) during the test period for the emulator developed using: (a) MLR and (b) ANN techniques when perfect *priori* knowledge about predictors is available.

Model D-1 and D-8 developed using MLR and ANN techniques, respectively. As shown in the figure, model D-8 is less uncertain in comparison with model D-1. Figure 30 shows weekly time series of WRMM irrigation demand per unit of area simulations, best-fit emulator's estimation and corresponding uncertainty bound for emulators D-1 and D-8.

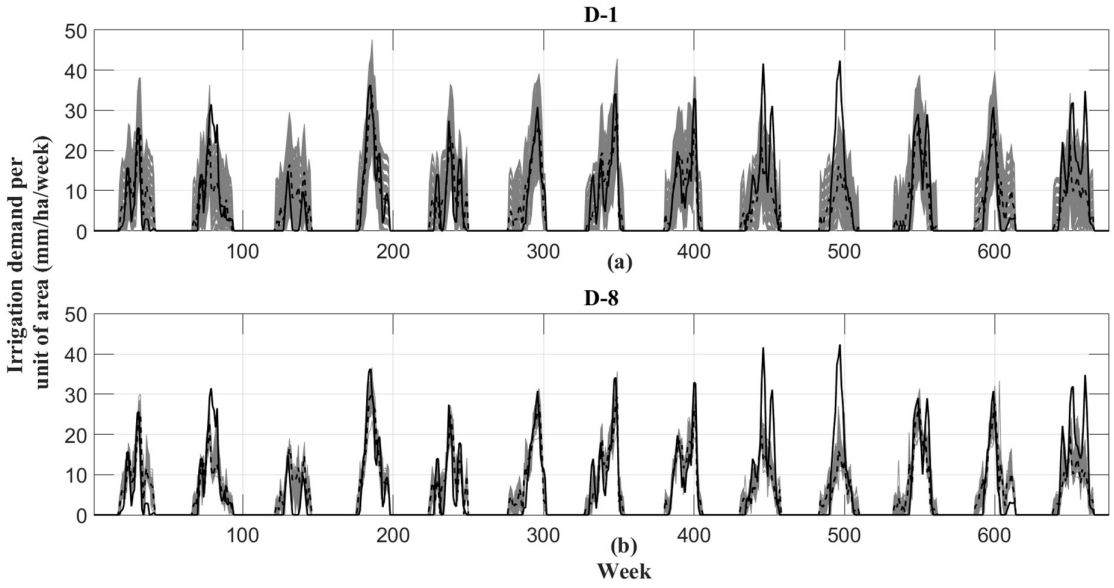

Fig 30. Weekly time series of WRMM irrigation demand per unit of area simulations (solid lines) and best-fit emulators' estimations (dashed lines) and corresponding predictive uncertainty bound (the grey envelopes) during the test period for the emulator developed using: (a) MLR and (b) ANN approaches when perfect *priori* knowledge about predictors is available.

Figure 30 presents irrigation demand per unit of area emulators' estimations (D-1 and D-8). As shown in the figure, D-8 shows better estimations of WRMM irrigation demand simulations in comparison with D-1. The expected annual estimations of irrigation demand per unit of area emulators developed with MLR and ANN techniques as well as WRMM estimation during the test period are shown in Figure 31.

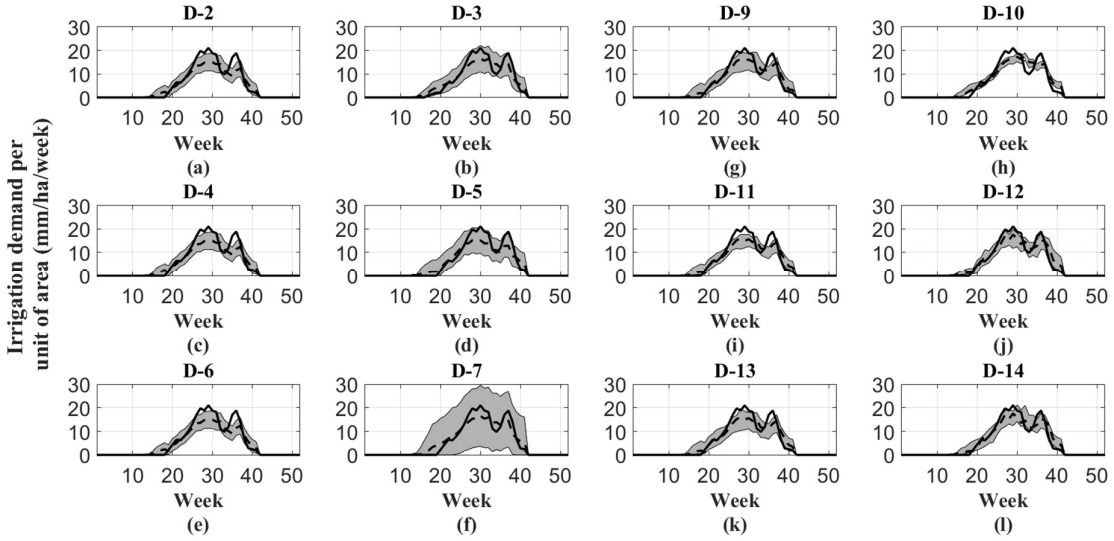

Fig 31. Expected annual WRMM irrigation demand per unit of area simulations (solid lines) and best-fit emulators' estimations (dashed lines) and corresponding predictive uncertainty bound (the grey envelopes) during the test period for the emulator developed using MLR and ANN techniques when predictors are partially known or unknown.

Panels (a) to (f) belong to emulators developed MLR technique and for emulators shown in panels (g) to (l) are ANN-based emulators. In models D-2, D-4 and D-6 as well as D-9, D-11 and D-13 predictors were known but their time signatures are unknown. Whereas in other models, both predictors and time signatures were unknown. Panels (a) to (f) show that the first three models (i.e. D-2, D-4 and D-6) that are developed with the second scenario of predictor selection are less uncertain in comparison with the three other models. However, for the emulators developed implementing ANN technique, except D-10 that shows less uncertainty, the other models are almost equally uncertain. But the last six models show less uncertainty in comparison with the first six emulators. Figure 32 shows the weekly time series of WRMM irrigation demand per unit of area simulations, best-fit emulator's estimation and corresponding uncertainty bound for emulators developed with partially known or unknown predictors.

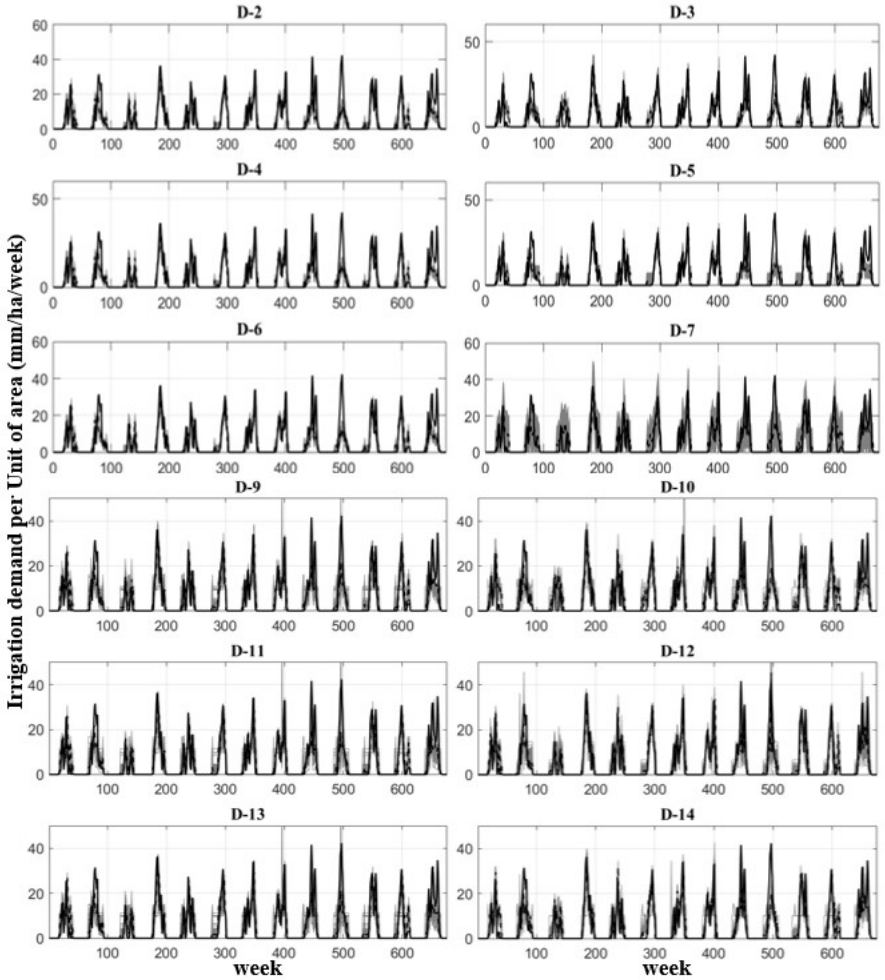

Fig 32. Weekly time series of WRMM irrigation demand per unit of area simulations (solid lines) and best-fit emulators' estimations (dashed lines) and corresponding predictive uncertainty bound (the grey envelopes) during the test period for the emulator developed using MLR and ANN techniques when predictors are partially known or unknown.

Models D-2 to D-7 are MLR-based emulators while D-9 to D-14 are ANN-based emulators. In the three first models, predictors were partially known whereas in the latter three models' proxies were fully unknown and found by applying an input variable selection scheme. Based on this figure, among models developed with MLR technique, emulator D-7 shows higher uncertainty. Also, the other six ANN-based emulators are presenting almost the same uncertainty in in comparison with D-2, D-3, D-4, D-5 and D-6 emulators. The expected annual reservoir release estimation of WRMM and the emulators developed with respect to fully knowledge about their predictors are presented in Figure 33.

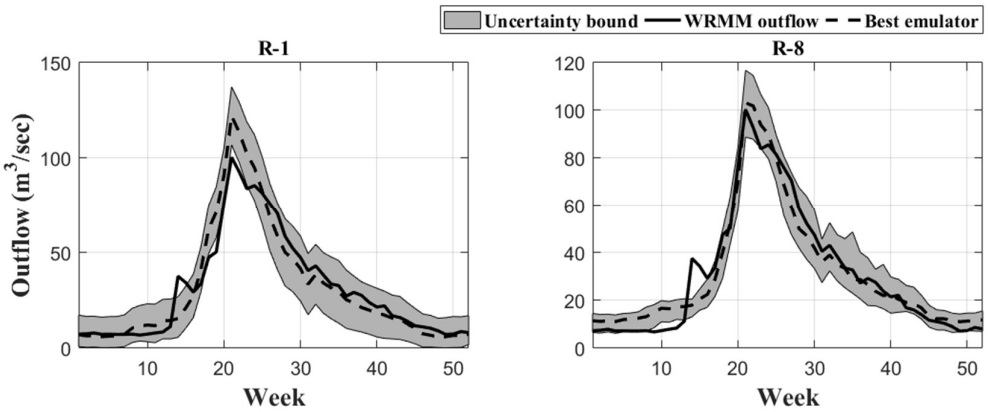

Fig 33. Expected annual WRMM reservoir release simulations (solid lines) and best-fit emulators' estimations (dashed lines) and corresponding predictive uncertainty bound (the grey envelopes) during the test period for the emulator developed using: (a) MLR and (b) ANN techniques when perfect *priori* knowledge about predictors is available.

Left panel belongs to emulator developed with MLR technique while in the right panel, the emulator was developed with ANN technique. Based on this figure, emulator R-8 estimates WRMM reservoir release with higher accuracy and less uncertainty in comparison with model R-1. Figure 34 presents weekly time series of WRMM reservoir release simulations, best-fit emulator's estimation and corresponding uncertainty bound for emulators R-1 and R-8.

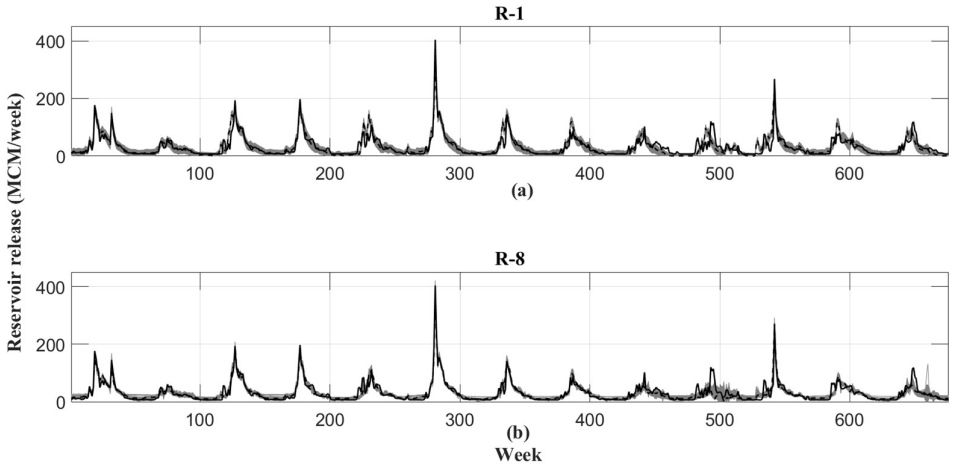

Fig 34. Weekly time series of WRMM reservoir release simulations (solid lines) and best-fit emulators' estimations (dashed lines) and corresponding predictive uncertainty bound (the grey envelopes) during the test period for the emulator developed using: (a) MLR and (b) ANN approaches when perfect *priori* knowledge about predictors is available.

Figure 34 shows reservoir release emulators' estimations (R-1 and R-8). R-1 and R-8 are developed applying MLR and ANN techniques, respectively. As presented in the figure, R-8 demonstrates better estimations with less uncertainty of WRMM reservoir release simulations with less uncertainty in comparison with R-1. Figure 35 shows the expected annual reservoir release for the emulators developed using MLR and ANN techniques and the predictors of the models were partially known or fully unknown.

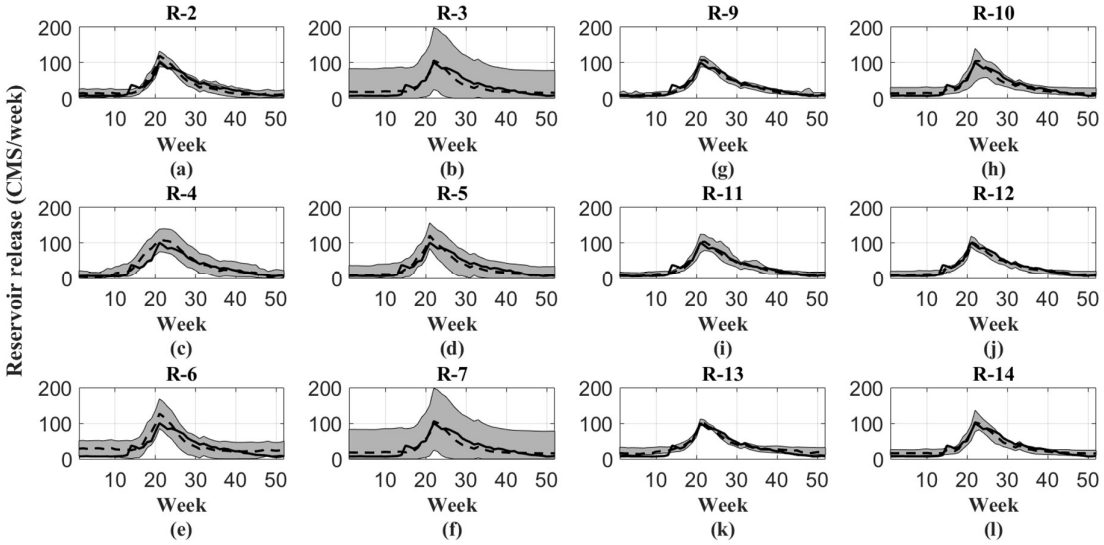

Fig 35. Expected annual WRMM reservoir release simulations (solid lines) and best-fit emulators' estimations (dashed lines) and corresponding predictive uncertainty bound (the grey envelopes) during the test period for the emulator developed using MLR and ANN techniques when predictors are partially known or unknown.

In this figure also Panels (a) to (f) and (g) to (l) are developed with MLR and ANN techniques, respectively. In the models R-2, R-4, R-6, R-9, R-11 and R-13 predictors were known but their time signatures were unknown. Whereas in the other models (R-3, R-5, R-7, R-10, R-12 and R-14) not only predictors were unknown but there was no available knowledge regarding their time signatures. Between MLR-based emulator, model R-2 shows the minimum uncertainty. Moreover, models R-9 to R-14 are showing almost the same uncertainty bound. In addition, the uncertainty of these models are less in comparison with the other six MLR-baseed emulators. Figure 36 shows the weekly time series of WRMM reservoir release simulations, best-fit emulator's estimation and corresponding uncertainty bound for emulators developed with partially known or unknown predictors.

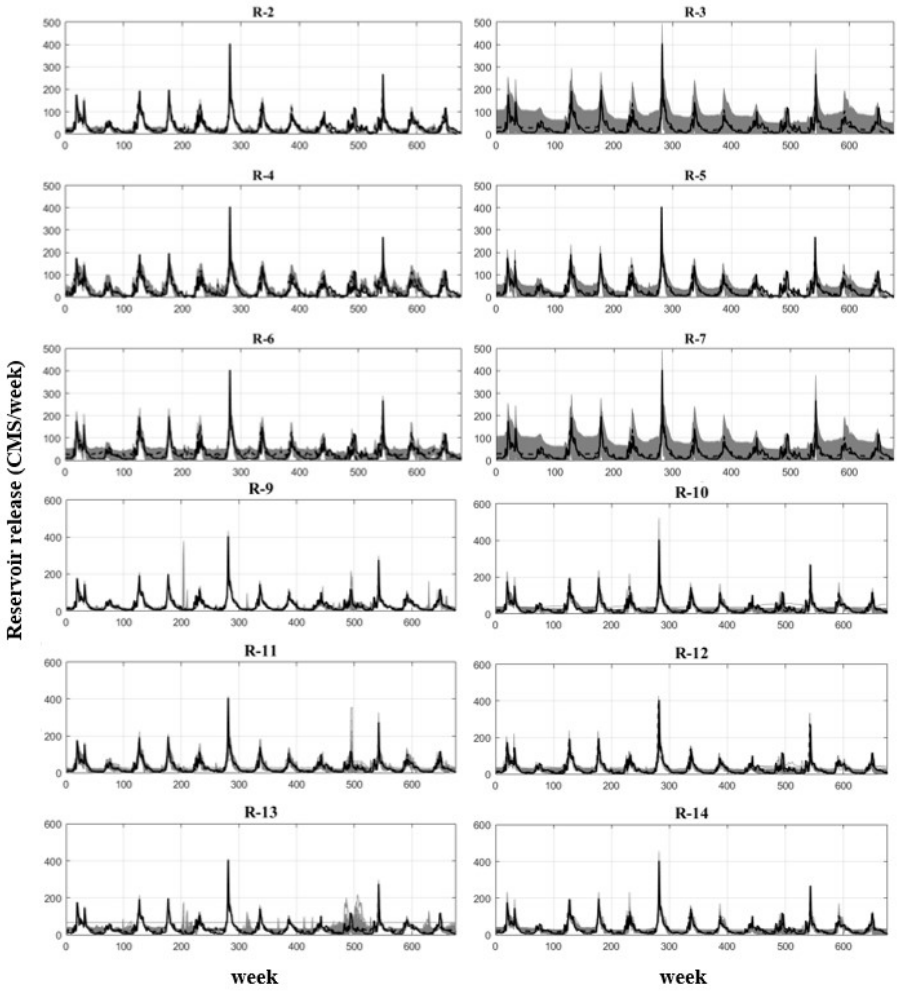

Fig 36. Weekly time series of WRMM reservoir release simulations (solid lines) and best-fit emulators' estimations (dashed lines) and corresponding predictive uncertainty bound (the grey envelopes) during the test period for the emulator developed using MLR and ANN techniques when predictors are partially known or unknown.

Based on this Figure 36, among models developed with MLR technique, emulator R-2 and R-4 are showing less uncertainty bound. Also, in ANN based emulators, R-9, R-11, R-12 and R-14 are presenting less uncertainty in comparison with other emulators. Having developed individual emulators for the four variables, it is possible to falsify these emulators in order to choose best emulators that are able to represent the dynamic of variables that based on them emulator have been developed. With this approach, the aim is finding emulators that address higher accuracy and less uncertainty. For this purpose, different emulators are compared based on their optimality (*BIC* of the best fit) and uncertainty (95% confidence interval for *BIC*)

during the testing phase. Here, *BIC* is chosen to compare different emulators because this goodness-of-fit index addresses both accuracy and complexity together (see – equation 17). Based on this criterion, the mean square error term defined in the equation addresses accuracy while more complex models are penalized. To tackle complexity, *BIC* prevents overfitting by introducing a penalty term for the number of parameters in the model. Deviation from target values or increased number of parameters result in increased *BIC* index. The results of comparing developed emulators for the four variables are shown in Figure 37. In this figure, panels (a), (b), (c) and (d) are related to emulator developed for reservoir evaporation, local irrigation withdrawal, local irrigation demand and reservoir release. Based on Panel (a), ANN-based emulators are predominantly presenting less uncertainty in comparison with MLR-based emulators. Moreover, except models E-1, E-3 and E-7 all other emulators are able to track WRMM lake evaporation estimations with the same range of optimality. Moreover, MLR-based emulators are covering larger range of both uncertainty and optimality. In addition, Panel (b) demonstrates that the emulators developed applying MLR technique are performing closely in terms of optimality. Also the range of uncertainty covered with these emulators is less in comparison with ANN-based emulators. In contrast, ANN-based emulators are dispersedly distributed in the panel. This implies that ANN-based emulators are covering a larger range of optimality and accuracy. Panel (c) provides information about irrigation demand emulators. Based on this panel, all ANN-based models are showing better optimality in comparison with other developed emulators. Also except D-1 and D-7 all other models are almost equally uncertain. Based on this panel, the range of uncertainty of MLR-based emulators is larger whereas these emulators cover a smaller range of optimality. For reservoir release emulators (Panel-D), MLR-based emulators are presenting less range of optimality but they cover larger range of uncertainty. Majority of ANN-based emulators are able to track WRMM estimations with better optimality and uncertainty.

Considering reservoir evaporation, E-12 represent the configuration with the highest optimality as well as the least trade-off between the optimality and uncertainty. E-9 and E-11 are rather undistinguishable and provide the emulators with the least uncertainty. For irrigation withdrawal, the ANN emulator identified through perfect *priori* (i.e. WD-8) represent the modeling option with the highest optimality and the least accuracy/uncertainty trade-off; the MLR-based emulator with known inputs (WD-1), however, represents the option with the least uncertainty. Regarding irrigation demand, D-12, D-10 and D-14 are the hypotheses with

highest optimality, least uncertainty and the least trade-off between optimality and uncertainty. For reservoir release, these hypotheses would be R-11, R-2 and R-9 respectively.

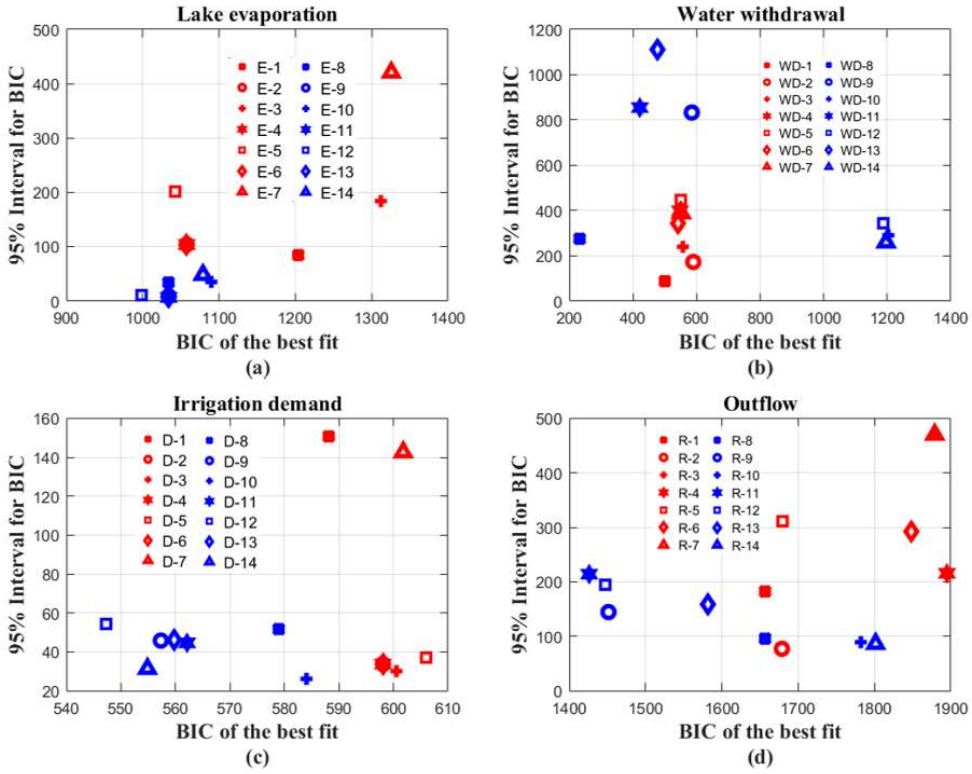

Fig. 37. Performance of alternative hypotheses for emulation models in representing (a) reservoir evaporation, (b) local irrigation withdrawal, (c) local irrigation demand, and (d) reservoir release.

In addition to the chosen emulators, the best emulators identified through perfect *priori* has also been selected. For all variables, ANN-based configurations outperform MLR options based on the *BIC* measure during the testing phase. In total, the 14 non-falsified configurations (i.e. four for reservoir evaporation, two for irrigation withdrawal, four for irrigation demand and four of reservoir release) are considered, with which the integrated emulators are built. Table 2 and 3 summarize the configurations of these non-falsified emulators and their associated goodness-of-fit measures during calibration and testing periods.

Table 2. The ID, input variables and structure of non-falsified emulators identified for the four variables of lake evaporation (*E*), locall water withdrawal (*WD*), local water demand (*D*) and release (*R*) at the Oldman Reservoir.

Variable	Model	Predictors	# of hidden neurons
E (mm/week)	E-8	$[S_{t-1}, T_t]$	1
	E-9	$[T_t^2, T_t, T_t^{-1}]$	1
	E-11	$[T_t^2, T_t, T_t^{-1}]$	1
	E-12	$[T_t, T_{t-1}^3, T_t^2, T_{t-1}]$	1
WD (mm/ha/week)	WD-1	$[D_t, S_{t-1}]$	N/A
	WD-8	$[D_t, S_{t-1}]$	7
D (mm/ha/week)	D-8	$[P_{t-1}, WD_{t-1}, T_t]$	3
	D-10	$[exp(WD_{t-2}), WD_{t-1}^2, T_{t-1}^2, P_{t-2}^{-1}]$	1
	D-12	$[WD_{t-2}^3, log(WD_{t-2}), exp(T_{t-1}), exp(WD_{t-1})\ ]$	3
	D-14	$[exp(WD_{t-2}), WD_{t-1}^2, T_{t-1},\ P_{t-2}^{-1}]$	3
R (CMS/week)	R-2	$[D_t^{0.5}, I_t^{-1}, I_t, S_{t-1}^3]$	N/A
	R-8	$[S_{t-1}, I_t, E_t, P_t, D_t]$	9
	R-9	$[D_t^{0.5}, I_t^{-1}, I_t, S_{t-1}^3]$	3
	R-11	$[D_t^{0.5}, exp(I_t), S_{t-1}^3, log(I_t)]$	5

As presented in Table 2, all the non-falsified emulators of lake evaporation are developed by ANN technique. Among these emulators, only E-8 is the model in which the predictors are selected based on perfect *priori* knowledge. In the other three emulators predictors are partially known or unknown. However, these three emulators are only dependant on different functions of temperature (i.e. $T_{t-1}^3, T_{t-1}T_t, T_t^{-1}, T_t^2$). This implies that ANN can adequately estimate any variable even when proxies are not physically meaningful. In addition, for ANN-based irrigation demand emulators in which predictors and their relevant time signatures are unknown (i.e. D-10, D-12 and D-14) same issue happens. Water withdrawal or precipitation occurred in two previous time-step are among the selected predictors of these models. However, these information is not physically meaningful. Because the resolution of data used in this study is weekly and water withdrawal or precipitation that occurred back in two weeks does not affect the amount of irrigation water demand in the current week. Since both water withdrawal emulators are the ones in which perfect *priori* knowledge about their proxies is available, the predictors of these models are physically meaningful. For reservoir release emulators also, except R-8 in which proxies are fully known, in other emulators predictors were partially known (R-2, R-9 and R-11). However, the selected predictors are physically meaningful.

Table 3. Goodness-of-fit measurement for the selected emulation models for lake evaporation, water withdrawal, irrigation demand and release at the Oldman Reservoir, during calibration and testing periods.

Variable	Model	Period	RMSE	R^2	NSE	LRMSE	REP
E (mm/week)	E-8	Calibration	5.51	0.82	0.82	1.33	0.12
		Testing	5.79	0.80	0.80	0.93	0.13
	E-9	Calibration	5.51	0.82	0.82	1.28	0.12
		Testing	5.79	0.80	0.80	0.96	0.15
	E-11	Calibration	5.51	0.82	0.82	1.28	0.13
		Testing	5.79	0.80	0.80	0.92	0.14
	E-12	Calibration	5.24	0.84	0.84	1.34	0.10
		Testing	5.45	0.82	0.82	0.90	0.14
WD (mm/ha/week)	W-1	Calibration	4.71	0.79	0.78	1.82	0.15
		Testing	5.44	0.63	0.59	1.73	0.05
	W-8	Calibration	2.01	0.96	0.96	1.60	0.01
		Testing	2.20	0.93	0.93	1.35	0.06
D (mm/ha/week)	D-8	Calibration	5.98	0.67	0.67	2.08	0.14
		Testing	7.25	0.54	0.53	2.39	0.24
	D-10	Calibration	6.16	0.65	0.65	1.99	0.12
		Testing	7.38	0.51	0.51	2.30	0.24
	D-12	Calibration	5.52	0.72	0.72	2.06	0.06
		Testing	6.50	0.63	0.62	2.31	0.11
	D-14	Calibration	5.38	0.73	0.73	2.01	0.03
		Testing	6.67	0.60	0.60	2.20	0.14
R (CMS/week)	R-2	Calibration	18.25	0.90	0.90	0.26	0.08
		Testing	17.02	0.78	0.77	0.33	0.08
	R-8	Calibration	11.84	0.96	0.96	0.18	0.02
		Testing	13.83	0.85	0.85	0.21	0.11
	R-9	Calibration	11.56	0.96	0.96	0.16	0.01
		Testing	11.79	0.89	0.89	0.18	0.07
	R-11	Calibration	11.44	0.96	0.96	0.16	0.00
		Testing	11.29	0.90	0.90	0.17	0.04

6.2 Integrated emulators

The non-falsified individual emulators are able to represent the dynamics of the four variables (i.e. lake evaporation, water withdrawal, irrigation demand and reservoir release) with highest accuracy and less uncertainty. However, here the aim is understanding the local dynamics of the water resource system at the Oldman Reservoir, considering the underlying interplays with hydro-climatological conditions and human decision on the irrigation area. The protocol applied to develop individual emulators will enable them to see the interactions between these variables and hydro-climatological conditions and/or irrigation area. But they are not able to represent the local dynamics of within the water system. For this purpose, the non-falsified emulators are coupled to develop integrated emulators through which the dynamics of the system with accounting for the climate condition and human intervention in irrigation area can be assessed (see – Figure 38 for IEs description).

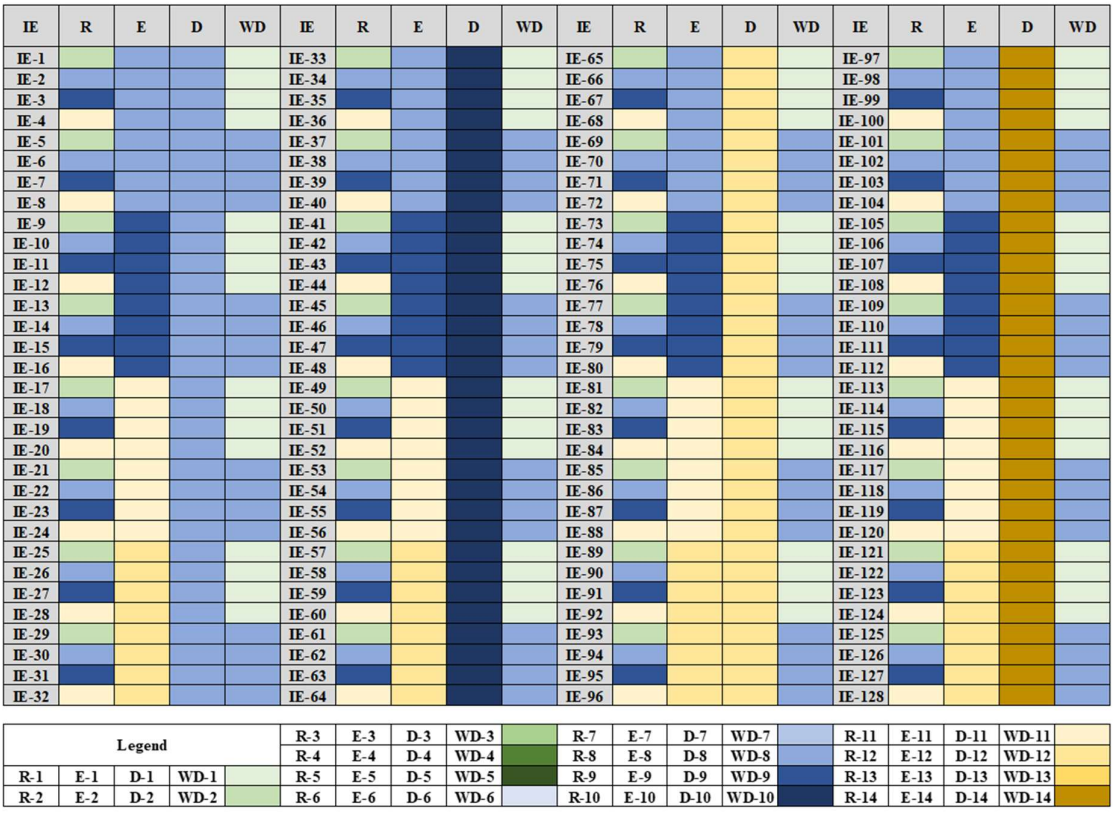

Fig 38. The description of 128 IEs obtained by coupling of four non-falsified individual emulators for lake evaporation, two non-falsified individual emulators for water withdrawal, four non-falsified individual emulators for irrigation demand and four non-falsified individual emulators for release.

Considering the 14 non-falsified emulators, there can be 128 configurations for IEs, obtained through mix-and-match (i.e. $4 \times 2 \times 4 \times 4 = 128$). These IEs can be used for detailed description of the water allocation at the Oldman Reservoir – see Figure 10(e) for an IE example, obtained by linking emulators with known input variables.

In order to easily compare the goodness-of-fit measures of the 128 emulators in tracking WRMM storage estimations they ranked and plotted. Figure 39 compares the goodness-of-fit measures of the IEs in tracking the weekly WRMM simulations of the storage in the Oldman Reservoir in the semi-coupled mode during the testing period.

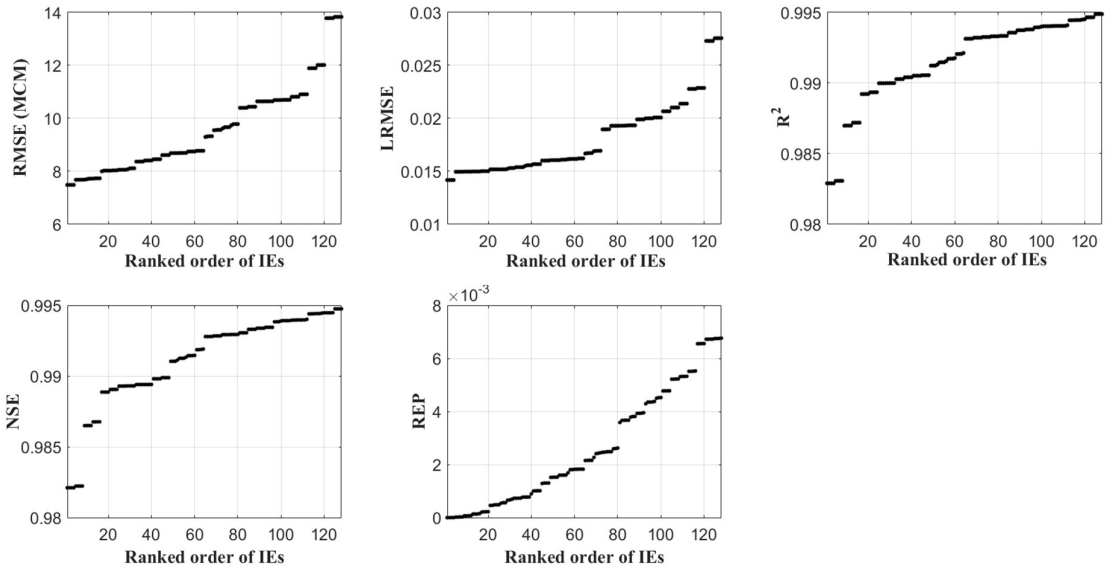

Fig 39. Performance measures of the 128 IEs in representing reservoir storage in semi-coupled simulation mode during the testing phase.

This analysis can reveal how error propagation between individual emulators can contribute into formation of error in estimation of the storage at the same time-step. Considering the results of this analysis, it is obvious that apart from *RMSE*, the difference between IEs in the semi-coupled mode is quite marginal. The differences between IEs with respect to *RMSE* is also marginal when it is put in the context of massive water storage in the Oldman Reservoir, which is at least around 100 MCM at any given week during testing period – see Figure 44 (a) for the weekly WRMM simulation of the Oldman Reservoir during this time episode.

Differences between IEs however are revealed in the fully-coupled simulation mode, performed during the validation phase. In the fully-coupled simulation, the storage values are updated at every time-step and therefore the error can propagate from one time-step to the next. To discriminate between the IEs in the fully-coupled mode, the *IPE* index during the validation period is calculated. Results are demonstrated in Figure 40 in which panel (a) presents the sorted *IPE* index for the 128 IEs and panel (b) focuses on the top seven IEs that have marginal differences with respect to the *IPE* index. These IEs include IE-26, IE-6, IE-18, IE-22, IE-10, IE-14 and IE-2. The description of the top seven IEs is presented in Table 4.

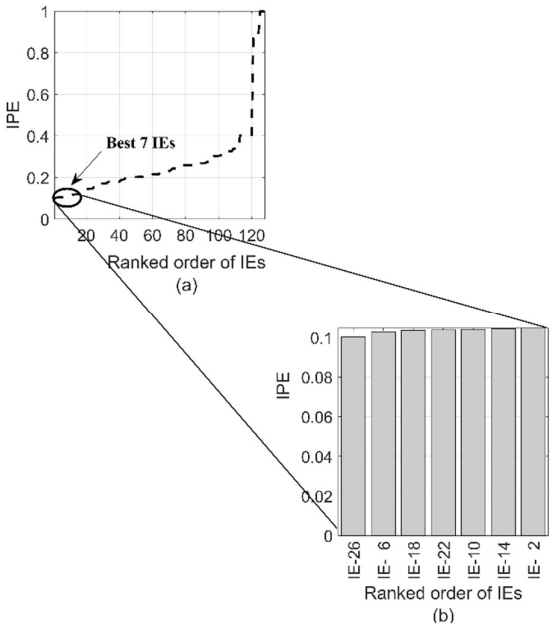

Fig. 40. Calculated *IPE* index for the performance of 128 the IEs in the fully-coupled simulation mode during the validation phase.

Table 4. The description of seven best IEs for describing the detailed dynamics at the Oldman Reservoir.

ID	Emulator for the lake evaporation	Emulator for the local water withdrawal	Emulator for the local water demand	Emulator for the reservoir release
IE-26	E-12	WD-1	D-8	R-8
IE-6	E-8	WD-8	D-8	R-8
IE-18	E-11	WD-1	D-8	R-8
IE-22	E-11	WD-8	D-8	R-8
IE-10	E-9	WD-1	D-8	R-8
IE-14	E-9	WD-8	D-8	R-8
IE-2	E-8	WD-1	D-8	R-8

It is worthwhile to emphasize that all these seven IEs are identified by linking emulators that are identified through perfect *priori* for irrigation withdrawal (WD-1 and WD-8), local irrigation demand (D-8) and reservoir release (R-8). This highlights the fact that emulators, in which input variables are selected based on some physical justifications are more robust in fully-coupled simulations and therefore they can be more suitable for continuous simulations. To have a more rigorous understanding of the performance of the seven IEs described in Table 4, the goodness-of-fit measures in representing the lake evaporation, local water withdrawal, local water demand, reservoir release and storage in semi-coupled and fully-coupled modes during testing, validation and the whole data periods are compared. Figures 41, 42 and 43 depict these results. In these figures the goodness-of-fit measures of all the four variables as well as reservoir storage that had been estimated by the top seven non-falsified IEs in the three mentioned periods (test- Figure 41, validation- Figure 42 and whole data period- Figure 43) are compared. From left to right, columns belong to lake evaporation, water withdrawal, irrigation demand, reservoir release and storage, respectively. In each subplot, the top seven non-falsified emulators (i.e. IE-26, IE-6, IE-18, IE-22, IE-10, IE-14, and IE-2) are presented in x-axis. Also in the five rows, *RMSE*, R^2, *NSE, LRMSE* and *REP* of IEs are compared.

As can be seen, the seven IEs perform similarly for all considered variable with respect to $RMSE$, R^2, NSE and $LRMSE$ in representing the dynamic of lake evaporation, water withdrawal, irrigation demand, reservoir release and storage. For instance, in all seven IEs, nash sutcliffe efficiency (NSE) for lake evaporation, water withdrawal, irrigation demand, reservoir release and storage in the test period is almost 0.8, 0.39, 0.5, 0.98 and 0.8, respectively. However, IEs can be discriminated based on their *REP*, particularly for water withdrawal and water demand in which IEs can be clearly clustered into two groups (IE-6, IE-22, IE-14 and IE-26, IE-18, IE-10, IE-2). As the emulator of water demand in all IEs is the same (D-8), the difference between IEs in representing the water demand is due to the errors introduced through coupling with different water withdrawal models. Systematically, it can been seen models IE-6, IE-22 and IE-14 that are identified using the WD-8 show improved *REP* measures. Also the selected individual emulators of water withdrawal, irrigation demand and reservoir release are ANN-based emulators. Accordingly, the three selected IEs (IE-6, IE-22, and IE-14) are used in order for further impact assessments studies.

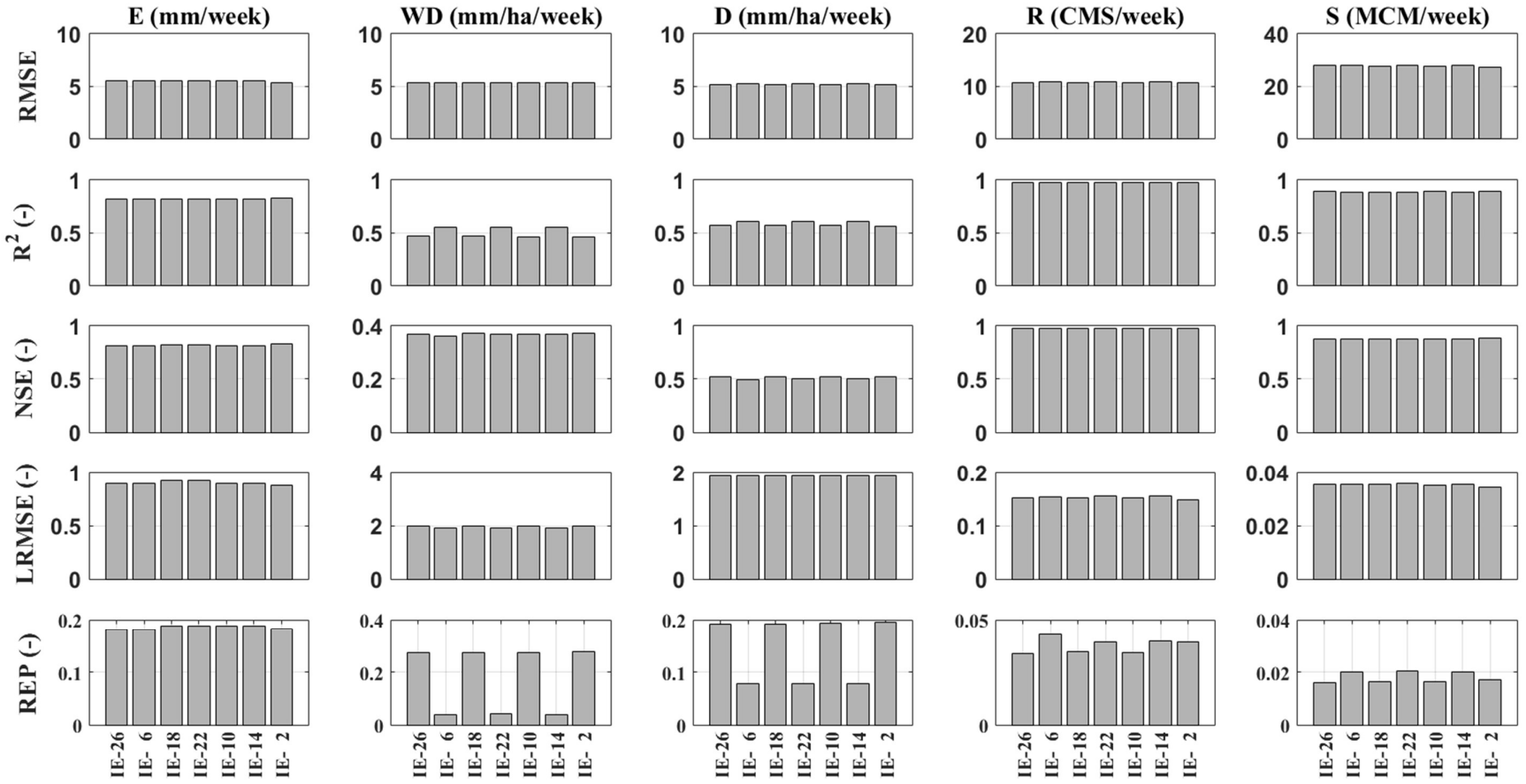

Fig 41. Comparison between $RMSE, R^2, NSE, LRMSE\ and\ REP$ measures of (from top to bottom respectively) of IE-26, IE-6, IE-18, IE-22, IE-10, IE-14 and IE-2 in representing lake evaporation, water withdrawal, irrigation demand, reservoir release and storage (from left to right respectively) during the testing period.

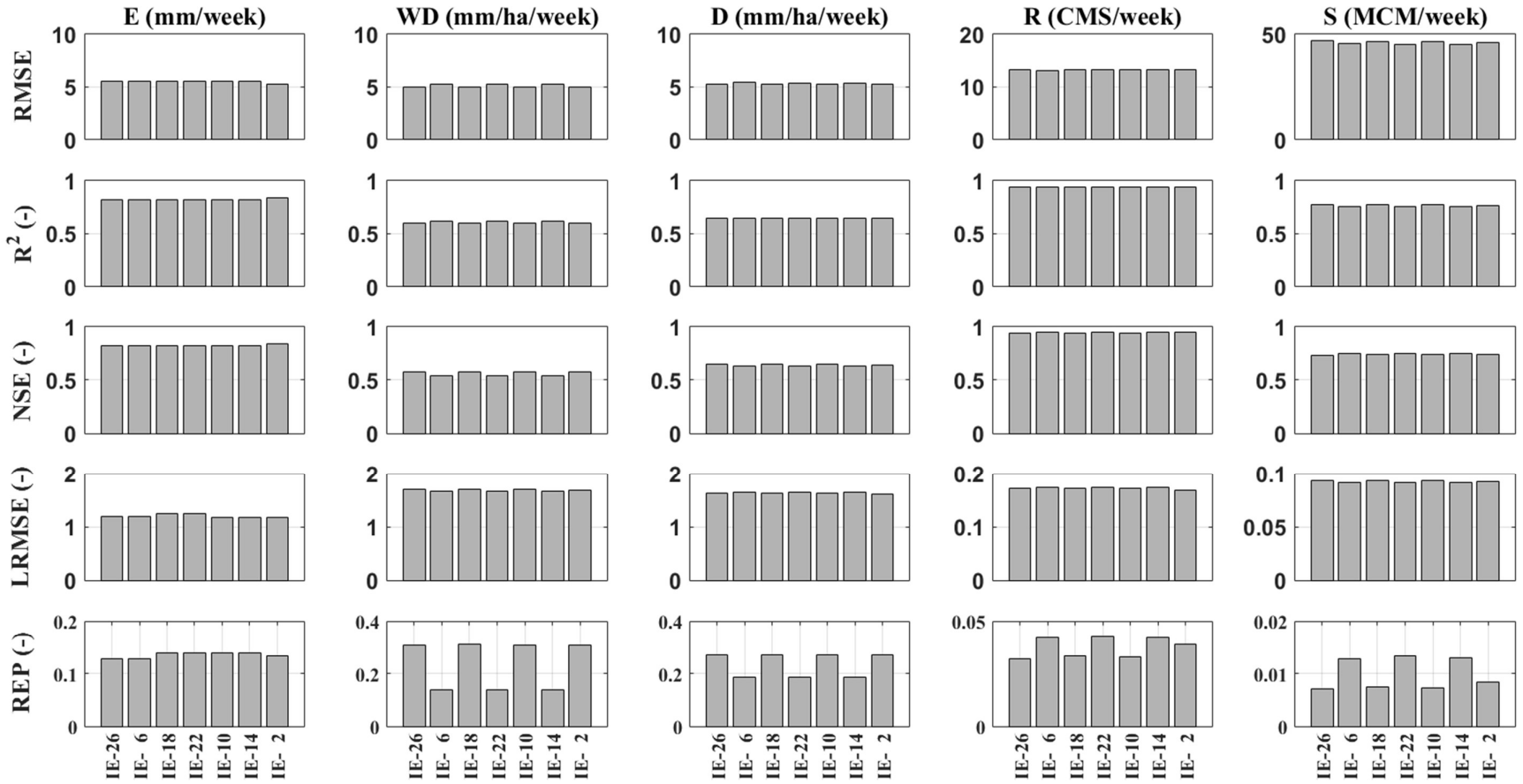

Fig 42. Comparison between *RMSE, R^2, NSE, LRMSE* and *REP* measures of (from top to bottom respectively) of IE-26, IE-6, IE-18, IE-22, IE-10, IE-14 and IE-2 in representing lake evaporation, water withdrawal, irrigation demand, reservoir release and storage (from left to right respectively) during the validation period.

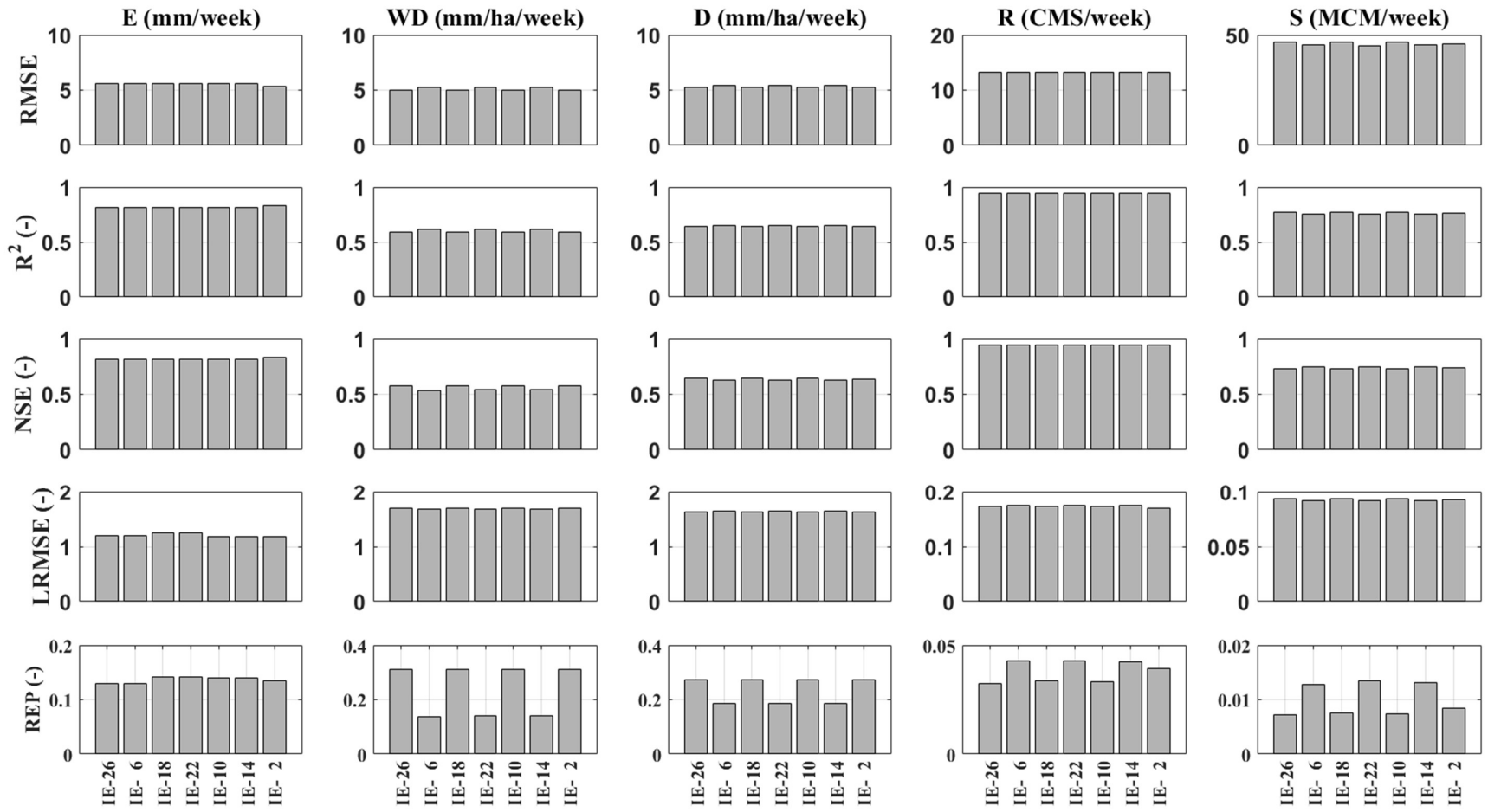

Fig 43. Comparison between *RMSE, R^2, NSE, LRMSE* and *REP* measures of (from top to bottom respectively) of IE-26, IE-6, IE-18, IE-22, IE-10, IE-14 and IE-2 in representing lake evaporation, water withdrawal, irrigation demand, reservoir release and storage (from left to right respectively) during the whole data period.

Figure 44 and 45 compare the weekly time series as well as the expected annual fluctuations of the reservoir storage simulated at the Oldman Reservoir using the WRMM (solid line) and the three non-falsified IEs in semi- and fully-coupled modes during the testing, validation and the whole data periods. Considering the semi-coupled mode, non-falsified IEs provide very similar simulations that match the WRMM results almost perfectly – see panels (a) and (b) in Figure 44. Considering the fully-coupled simulations made during the validation and the whole data periods, the difference between IEs become more obvious and the departure between results obtained by IEs and WRMM increases. For continuous weekly simulations, non-falsified IEs can adequately capture the reservoir dynamics during high storage periods, although the performance of IEs declines during periods with low storage (see Panel (c) in Figure 44 and Panel (a) in Figure 45). Considering the expected annual storage, non-falsified IEs underestimate WRMM simulations during winter and spring and overestimate the WRMM results during the fall season (see Panel (d) in Figure 44 and Panel (b) in Figure 45).

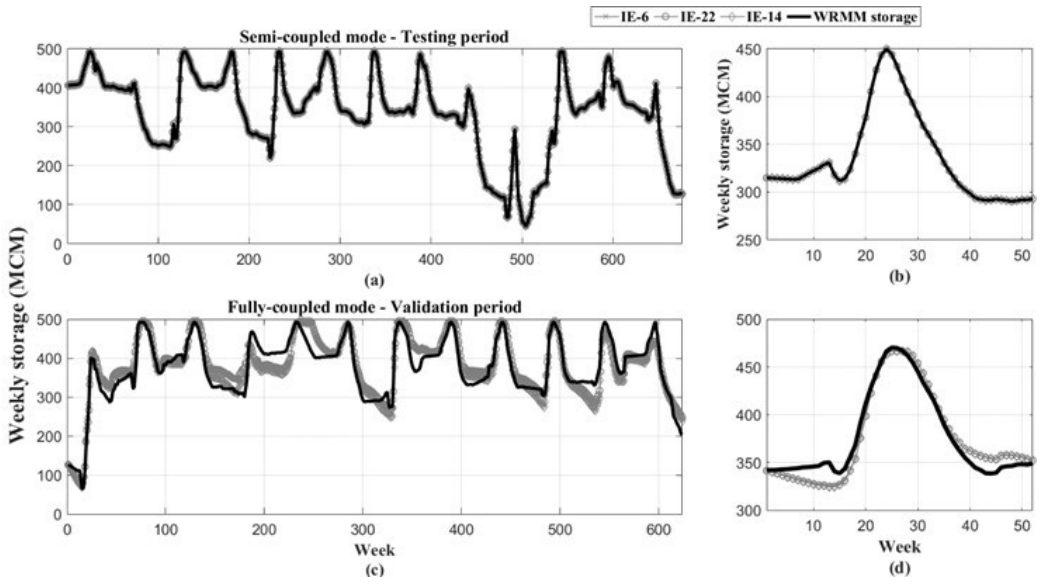

Fig. 44. Weekly time series of WRMM storage and the three non-falsified IEs in semi- and fully-coupled modes during testing and validation periods along with corresponding expected annual storage of WRMM and non-falsified IEs.

In Figure 44, Panels (a) and (c) belong to time series of reservoir storage in test and validation periods. Also Panels (b) and (d) show the expected annual storage in the two mentioned periods. In all panels, four lines are presented of which three belong to the top non-falsified emulators and one is reservoir storage.

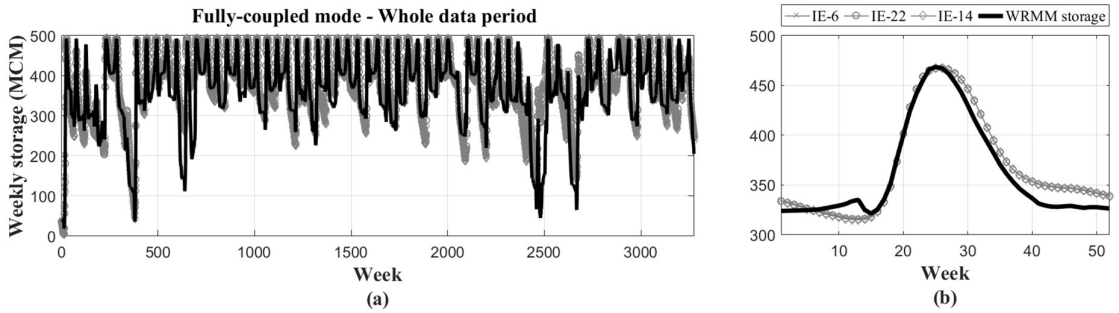

Fig. 45. Weekly time series and expected annual storage of WRMM and seven selected Integrated Emulators in fully-coupled mode in the whole data period.

In panel (a), x-axis shows the whole data period (63 × 52 = 3276 weeks) and y-axis belongs too weekly storage in MCM. Also in Panel (b), x-axis presents 52 weeks in a whole year. In Panel (a) the time seris of reservoir storage is presented in which three belong to top three non-falsified integrated emulators and one is WRMM reservoir storage. Panel (b) demonstrates the expected annula storage. Based on Panel (b), WRMM estimation is understimated in winter wheras in summer and fall stimations by IEs are overstimating WRMM reservoir storage.

Chapter 7. Application of integrated emulators for impact assessment

So far, individual emulators developed, tested and falsified and top emulators that adequately represent dynamics of WRMM variables were selected. Then, they coupled to create integrated emulators through which dynamics of the system, considering the underlying interplays with hydro-climatological conditions and human decision on the irrigation area can be assessed. The inclusion of hydro-climatological conditions in emulators is mainly due to the fact that climate variability and change is predominantly taking place in this region. Consequently, this has effects on streamflow, lake evaporation and irrigation water demand. In addition, agriculture is a primary activity in the Oldman River basin and both policy makers and stakeholders are interested in increasing the area of irrigation districts in this region. Decreasing water availability and increasing water demand with a severe completion for water in this region are resulting in vulnerability of this water resource system. To understand the sensitivity of the water resource system at the Oldman Reservoir to changing streamflow, climate, and irrigation area the non-falsified IEs are used. It should be noted that the sensitivity analysis made by developed IEs is more informative locally than the one performed by the WRMM as, (i) the dynamics of reservoir evaporation are directly linked to the climate and storage state, and (ii) the dynamics of water withdrawal and water demand are coupled and linked to climate condition and antecedent soil moisture conditions, manifested through water withdrawal at the previous time-step.

Here, the vulnerability assessment study is performed in three different levels:

(a) In the first level of impact assessment, the response of the system to changes in inflow characteristics, namely annual flow volume and peak is analysed. In this regard, different scenarios of changing annual flow volume and peak are defined. For each scenario different realizations for streamflow are stochastically reconstructed and the effect of changing streamflow characteristics on the performance of the system is evaluated.

(b) In the second level of impact assessment study, different scenarios of temperature are obtained from NASA-NEX downscaled global climate projections. Seven scenarios of warming are defined and various realizations for each scenario of warming will be found. Having different scenarios for changing streamflow and temperature, it will be possible to assess the response of the system to the joint scenarios of these variables.

(c) Finally in a more broad view, in the third level of assessment, the sensitivity of the system to changing streamflow, climate including both precipitation and temperature as well as irrigation area is assessed. Therefore, for inflow to reservoir, precipitation and irrigation area three scenarios of zero or ±25% and for temperature also three scenarios of zero or ±2°C change in the historical time series are considered to provide a holistic understanding of the system response to changes in both natural and anthropogenic conditions. These can make various scenarios of change under which the sensitivity of the system can be assessed.

To assess the system sensitivity to changing conditions, a set of performance indicators is considered. These indicators include (1) the expected number of weeks in a typical year in which the reservoir storage goes below 25% of its capacity, (2) the expected local water supply deficit during a typical year, (3) the expected number of weekly spill events during one typical year, and (4) the expected median release from reservoir during a typical year. These performance indicators, together, provide a holistic view on the performance of the Oldman reservoir, both locally and regionally. In fact, low storage and annual water supply deficit are indicators describing the performance of the system locally. In addition, number of spill events and median outflow are describing the regional behaviour of the system. This is due to the fact that (1) Lethbridge is located downstream of the reservoir and is prone to excessive flow that evacuates from reservoir and (2) reservoir outflow describes how regional irrigation networks are supplied due to manifestation of their water demand in this indicator.

Having defined scenarios of change in streamflow, climate, and human management practices, it is possible to assess the behaviour of the system under each or joint scenarios of change. Here, in order to assess the behaviour of the system under changing condition, each performance indicator is found based on different realizations of streamflow and temperature or other drivers of change on the water system and then is averaged for a long-term period (30 year). In fact the impact assessment study is done based on the long-term behaviour of the Oldman Reservoir. Assessment of the system's behaviour under changing scenarios is performed in the vulnerability assessment study. Here, in order to perform this analysis, the conventional methods which are regularly used are implemented. In particular, two bottom-up, top-down and joint bottom-up top-down impact assessment methods are applied in this study, as introduced in Chapter 4. In addition, one heuristic approach which can be considered as a bottom-up approach is defined and proposed. All three vulnerability studies will show the

impact of changing condition on the Oldman Reservoir. The definition, implementation and the data support of these methods of assessment are presented in the next sub-sections.

7.1 Assessment Framework

Here, in order for impact assessment study, both bottom-up and top-down approaches are adopted. In the first level of impact assessment, the bottom-up approach is used to evaluate the effect of changing streamflow on the system's behaviour. In this respect, characteristics of streamflow, namely timing of the annual peak flow and annual flow volume are considered and streamflow regime is stochastically reconstructed and fed into the top non-falsified emulator to evaluate the behaviour of the system under changing streamflow. Moreover, in the second scenario of impact assessment, a top-down approach is used to generate various scenarios of temperature. In this assessment study, different scenarios of warming climate are considered and the joint impact of changing streamflow and temperature on the behaviour of the system is evaluated. To apply this study a joint bottom-up/top-down approach is used. In the third impact assessment study, implementing a heuristic approach, different scenarios for inflow to the reservoir, temperature and precipitation and changing the irrigation area of local irrigation districts are considered and the behaviour of the system under defined changing condition is analysed. Next section describes the methods employed for flow reconstruction and developing scenarios of warming temperature.

7.1.1 Streamflow reconstruction for bottom-up impact assessment

In order to assess the effect of changing water availability on the defined performance indicators, two indicators of flow regime, namely annual flow volume and timing of the annual peak, are considered. These characteristics are subject to change due to observed changes in streamflow characteristics of the Oldman River headwaters. Then for the bottom-up impact assessment of changing streamflow regime, Ensemble generation scheme, introduced by Nazemi et al. (2013), is applied to stochastically reconstruct weekly realizations for possible water availability. These realizations are produced under pre-defined historical annual volume and timing of the annual peak. In this level of assessment climate variables are not incorporated in the reconstruction procedure.

The selected range for timing of the annual peak and annual flow volume includes -5 to +8 weeks and -25% to +25%, respectively. These ranges are examined because they have been considered in the previous research studies. Considering one week and 5% increment in annual timing of the peak and annual flow volume, 14 × 11 = 154, possible streamflow regime conditions are produced. For each of the 154 scenarios, 100 realizations for streamflow are reconstructed. Moreover each realization is generated for a 30 year (1961 to 1990) period of weekly data. For 154 possible regime conditions and 100 realization of streamflow for 30 year weekly data, 154 × 100 × 30 = 462,000 years of simulations for each performance indicator (low storage duration, water supply deficit, number of spill events and median reservoir release) are developed. Then for each streamflow realization, the considered performance indicators are found annually and averaged for the whole period to come up with an expected measure during a typical operational year. For this impact assessment study, the top non-falsified IE, i.e. IE-6 is selected as the best emulator of WRMM.

In addition, among 154 different scenarios of changing annual flow volume and timing of the annual peak, three specific flow regime conditions, i.e., (-4, -25%), (0, 0), and (4, +25%) are getting more focused. These three conditions are representations of dry, historical and wet regime conditions, respectively – see Figure 46. Based on different realizations of streamflow in the three selected regime conditions, the probabilistic profiles (risk profiles) for the defined performance indicators can be developed. These representations are used for quantifying the risk in the system performance due to changing water availability.

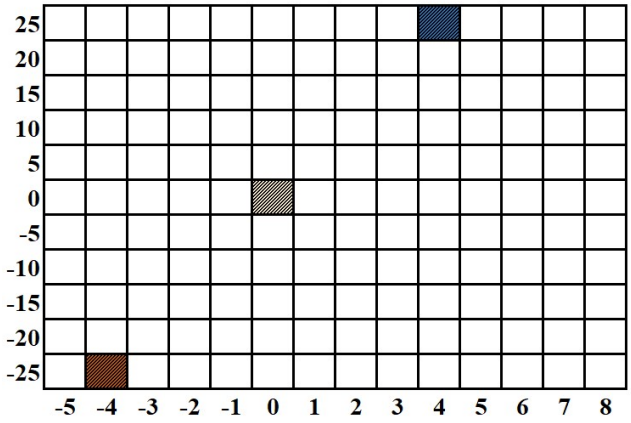

Fig. 46. Defiened three regime conditions for dry (-4, -25%), historical (0, 0) and wet (+4, +25%) regime conditions.

7.1.2 Temperature scenarios for joint bottom-up/top-down impact assessment

Due to climate change and variability, temperature in the study area in increasing. This has significant effects on water availability and demand. In order to assess the impact of warming climate on the Oldman River system, using a top-down approach different scenarios of changing temperature are developed. For this purpose, temperature data is derived from National Aeronautics and Space Administration (NASA). NASA has downscaled historical and future daily temperature simulations for the period of 1950 to 2099 of 21 IPCC-CMIP5 models. The spatial resolution of this data is 25 × 25 Kilometers globally. Since the resolution of the NASA data is compatible with the study area, this data is directly used without downscaling in this study.

To use the obtained daily data for the scenario assessment, first the temporal resolution of temperature time series is changed to weekly scale. Then different scenarios of warming are defined in a way that the long term expected annual temperature is equal to the historical temperature, or it increases in increments of +0.5 °C, up to the long term expected annual temperature plus 3 °C. For this purpose, a 30 year period window is defined and moved throughout the whole period of data. Then expected annual temperature for each 30 year period is found and clustered to seven defined groups. Finally, from each group 100 realizations of temperature are randomly selected.

Based on the fact that both streamflow and temperature are changing in the study area, in this vulnerability assessment study, the joint impact of changing streamflow and temperature are considered. In order to assess the joint impact of changing streamflow and temperature on the system's behaviour, joint bottom-up and top-down approaches introduced previously is applied. The protocol of reconstructing the streamflow is the same as what have been explained in the previous sub-section. As shown in Figure 46, 154 scenarios for timing of the annual peak flow and annual flow volume are defined. For each scenario, 100 realizations for streamflow have been developed as defined in the previous sub-section. In addition, as discussed here, for each of the 7 scenarios of changing temperature (i.e. from zero to +3 °C), 100 weekly realization of weekly temperature are developed. All the realizations of streamflow and temperature are generated representing 30 year of weekly data. In the case of coupling all the mentioned scenarios for streamflow and temperature, 154 × 100 × 7 × 100 × 30 = 323,400,000 years of simulation would be developed. For this huge amount of calculation there was not

adequate hardware available to run all the simulations within the period that this study was being done. For this reason we only focused on the three regime conditions i.e. dry, historical and wet that have been introduced in the previous sub-section. By this approach, 3 × 100 × 7 × 100 × 30 = 6,300,000 years of simulations for each performance indicator are developed.

7.1.3 Scenarios of inflow, climate and irrigation area for bottom-up impact assessment

For the third level of vulnerability assessment study, a bottom-up approach is applied. For this purpose, three predefined states, representing increase, no-change and decrease in streamflow, climate and irrigation area are considered. For inflow, precipitation and irrigation area, the scenarios for increase and decrease are identified as ±25% change in the historical time series. For temperature, the scenarios of change have been considered as ±2°C change in historical temperature series during this period. Combining these ad-hoc scenarios of change, there would be 81 (3^4) joint settings for independent variables, with which the sensitivity of the system at the Oldman Reservoir can be assessed.

7.1.4 Data support for top-down impact assessment

Here, in order to implement top-down impact assessment study, temperature data is derived from National Aeronautics and Space Administration (NASA). NASA has downscaled historical and future daily temperature simulations for the period of 1950 to 2099 of 21 IPCC-CMIP5 models. The spatial resolution of this data is 25 × 25 Kilometers globally. Since the resolution of the NASA data is compatible with the study area, this data is directly used without downscaling in this study. The multi-model downscaled data product is available in NASA's Earth Exchange Global Daily Downscaled Projections. Table 5 presents the list of climate models used in order to extract temperature data for the impact assessment study.

Table 5. Description of the 21 IPCC-CMIP5 climate models.

Model's name	Institution	Latitude resolution (°)	Longitude resolution (°)
ACCESS1-0	CSIRO (Commonwealth Scientific and Industrial Research Organisation, Australia), and BOM (Bureau of Meteorology, Australia)	1.2500	1.8750

CSIRO-MK3-6-0	Commonwealth Scientific and Industrial Research Organisation in collaboration with the Queensland Climate Change Centre of Excellence	1.8653	1.8750
MIROC-ESM	Japan Agency for Marine-Earth Science and Technology, Atmosphere and Ocean Research Institute (The University of Tokyo), and National Institute for Environmental Studies	2.7906	2.8125
BCC-CSM1-1	Beijing Climate Center, China Meteorological Administration	2.7906	2.8125
GFDL-CM3	NOAA's Geophysical Fluid Dynamics Laboratory	2.0000	2.5000
MIROC-ESM-CHEM	Japan Agency for Marine-Earth Science and Technology, Atmosphere and Ocean Research Institute (The University of Tokyo), and National Institute for Environmental Studies	2.7906	2.8125
BNU-ESM	College of Global Change and Earth System Science, Beijing Normal University	2.7906	2.8125
GFDL-ESM2G	NOAA's Geophysical Fluid Dynamics Laboratory	2.0225	2.0000
MIROC5	Japan Agency for Marine-Earth Science and Technology, Atmosphere and Ocean Research Institute (The University of Tokyo), and National Institute for Environmental Studies	1.4008	1.4063
CanESM2	Canadian Centre for Climate Modelling and Analysis	2.7906	2.8125
GFDL-ESM2M	NOAA's Geophysical Fluid Dynamics Laboratory	2.0225	2.5000
MPI-ESM-LR	Max Planck Institute for Meteorology (MPI-M)	1.8653	1.8750
CCSM4	National Center for Atmospheric Research	0.9424	1.2500
INMCM4	Institute for Numerical Mathematics, Moscow, Russia	1.5000	2.0000
MPI-ESM-MR	Max Planck Institute for Meteorology (MPI-M)	1.8653	1.8750
CESM1-BGC	National Science Foundation, Department of Energy, National Center for Atmospheric Research	0.9424	1.2500
IPSL-CM5A-LR	Institut Pierre-Simon Laplace	1.8947	3.7500
MRI-CGCM3	Meteorological Research Institute	1.1215	1.1250
CNRM-CM5	Centre National de Recherches Météorologiques/Centre Européen de Recherche et Formation Avancées en Calcul Scientifique	1.4008	1.4063

IPSL-CM5A-MR	Institut Pierre-Simon Laplace	1.2676	2.5000
NorESM1-M	Norwegian Climate Centre	1.8947	2.5000

7.2 Impact assessment of changing water availability

In the first impact assessment study, different scenarios of streamflow are stochastically reconstructed and fed into the top non-falsified integrated emulator i.e. IE-6. This assessment is applied for 14 scenarios for changing annual timing of the peak and 11 scenarios for change in annual flow volume, as shown in Figure 46. Then, the effect of changing streamflow on the four defined performance indicators is assessed. As introduced previously, these indicators are expected number of low storage duration, expected annual water deficit, expected number of spill events and expected median outflow. Figure 47 presents the response surfaces for the four defined performance criteria.

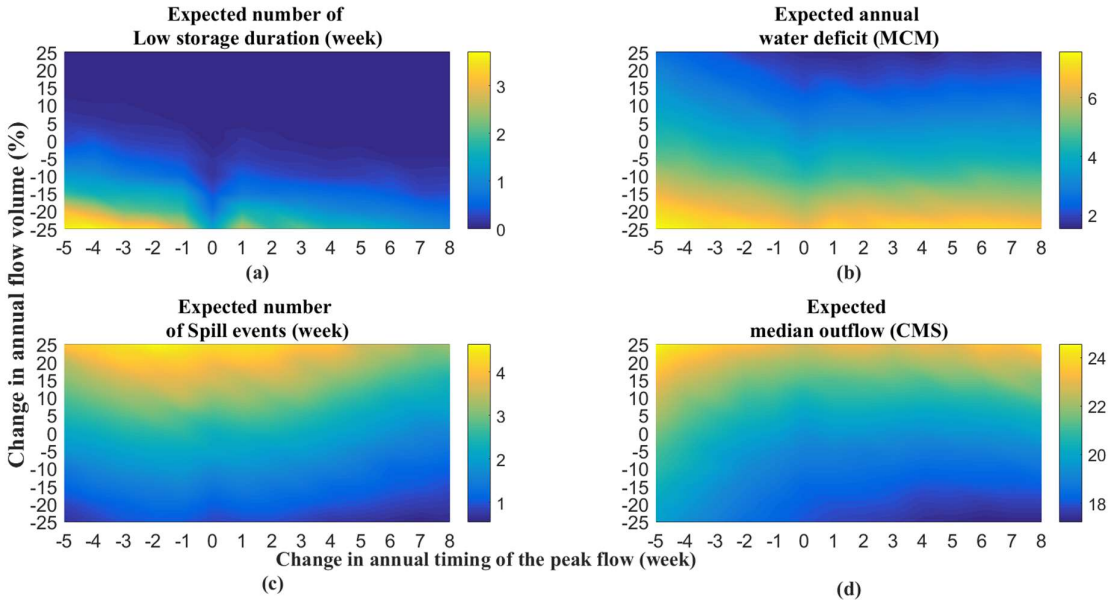

Fig. 47. Response surface for performance indicators under changing water availability. In this figure, Panel (a) to (d) belong to expected number of low storage duration, expected annual water deficit, expected number of spill events and expected median outflow, respectively.

Panel (a) presents the expected annual number of low storage duration. This panel shows a strong dependency between this indicator and the annual flow volume. When the flow volume rises up to +25%, the low storage does not take place, even if the annual peak ranges from -5 to +8 weeks. When the annual volume decreases by -25%, then the duration of low storage is dependent on the timing of the annual peak. In this case when the timing of the annual peak

changes from -5 to +8 weeks, the low storage duration ranges from almost 3 to 1 week per year. In addition, when the annual peak does not change, the low storage duration is almost zero for all scenarios of annual flow volume. From this assessment it can be concluded that in dry conditions the duration in which the reservoir storage is below 25% of its capacity increases.

Panel (b) shows the effect of water availability on the water supply deficit. Based on this figure, this indicator is significantly sensitive to annual flow volume. By changing the annual flow volume from -25% to +25%, the annual water supply deficit varies from 7 to 2 MCM in a typical operational year. In other words, by increasing flow volume, the annual water supply deficit decreases. Moreover, for each scenario of annual flow volume ranging from -25% to +25%, water supply deficit is minimum when the timing of the annual peak flow doesn't change (i.e. timing of the annual peak is equal to zero). It implies that if peak flow happens in advance or is delayed, it is not matched with the peak irrigation water demand resulting is increased water supply deficit.

Panel (c) shows the impact of water availability on expected number of spill events. Based on this figure, with increasing annual volume to +25%, the expected annual number of spill events increases to over 4 weeks. This indicator is more sensitive to annual volume rather than timing of the annual peak. But there is a slight sensitivity when the two marginal values for timing of the peak is considered. In brief, when the annual peak moves toward -5 and +8 week, the expected number of spill events gradually decreases. Whereas when the annual peak is not changed (i.e. equals to zero), the spill events indicator is of the maximum number of occurrences. In other words, when the annual peak is delayed or advanced, the number of annual spill events declines. Based on this assessment, in wet regime conditions due to increased number of spill events, measures should be taken in order to handle excessive flows evacuated from reservoir that can result in damages for the both human and properties located downstream of the dam.

Panel (d) demonstrates the dependency between median reservoir release and the annual flow volume and timing of the peak. Based on this figure, when the annual flow volume increases, the median reservoir release is significantly increased as well. It implies that local irrigation demand can be satisfied and higher amount of water is released to allocate regional water demand since downstream irrigation demand has been incorporated in the outflow.

Consequently water supply deficit related to both local and regional irrigation districts declines with increased flow volume. In addition, by altering the timing of the annual peak, the median release is subjected to change. When timing of the annual peak moves toward -5 and +8, the median outflow rises. It can be interpreted that by changing the annual timing of the peak, the peak flow and peak irrigation water demand are not synchronized and excessive water that have not been used in the local irrigation network releases to downstream. Based on this study, the minimum median release takes place when the annual flow volume decreases to -25% and the annual peak advances toward +8 weeks. In this case the median release decreases to almost 18 CMS. In addition, the maximum outflow happens when the annual flow volume goes up to +25% and the annual peak is delayed for -5 weeks. In this case the maximum Q50 is 24 CMS. The result of this assessment shows that in dry regime condition median outflow is decreased while in the wet regime condition this indicator rises.

These vulnerability maps only show the expected of performance indicators over 100 realizations in each cell for one statistical measure. As a result, the risk in the system performance due to random variability in each cell is not addressed. At this point, by considering different realizations for streamflow in the three defined regime conditions (i.e. dry, historical and wet regimes), the Empirical Cumulative Distribution Function (ECDF) of the four performance indicators (i.e. expected number of low storage duration, expected annual water deficit, expected number of spill events and expected median outflow) can be found. With this approach these information can provide a notion of risk due to natural variability in the system performance. To obtain risk profiles, each performance indicator is found during a typical operational year and averaged for the whole 30 year of the period. Since 100 realizations for streamflow are available, for each performance indicator 100 values are obtained. Having the ensemble of all values it would be possible to find ECDF for each performance indicator and in each regime condition. Figure 48 shows the risk profiles of the performance indicators under selected specific flow conditions. In Panel (a), x-axis shows the number of weeks in which low storage takes place in a typical year. The y-axis in this panel, and the other three panels, also corresponds to the density of the occurrence of each indicator. This panel shows that in historical and wet conditions, the duration of low storage is zero, while in dry condition, up to 3 weeks of low storage is expected with highest probability. In addition, the maximum number of weeks in which the reservoir experiences low storage takes place in dry regime condition with 10 weeks in an operational year. The panel also shows that wet regime condition

provides the highest variation in comparison to historical and dry regimes, indicating that wetter regime leads to larger uncertainty in duration of low storage.

Panel (b) presents the probabilistic risk profile of expected annual water deficit. In this figure, x-axis corresponds to the annual volume of water deficit in MCM. Based on this panel it can be concluded that in dry condition the water supply deficit happens with the highest probability with the maximum of 7.5 MCM. When changing toward wet condition, this indicator decreases to 3.5 and 2 MCM in historical and wet regime conditions. In addition, maximum annual water supply deficit in the dry, historical and wet regimes are 11.5, 6 and 3 MCM, respectively. Based on this panel, the minimum annual water supply deficit for the dry, historical and wet regimes are 3.5, 1 and 0 MCM. Amongst the three regimes, dry regime condition shows the highest variation in comparison to historical and wet regimes, stipulating that dryer regime leads to larger uncertainty in annual water supply deficit.

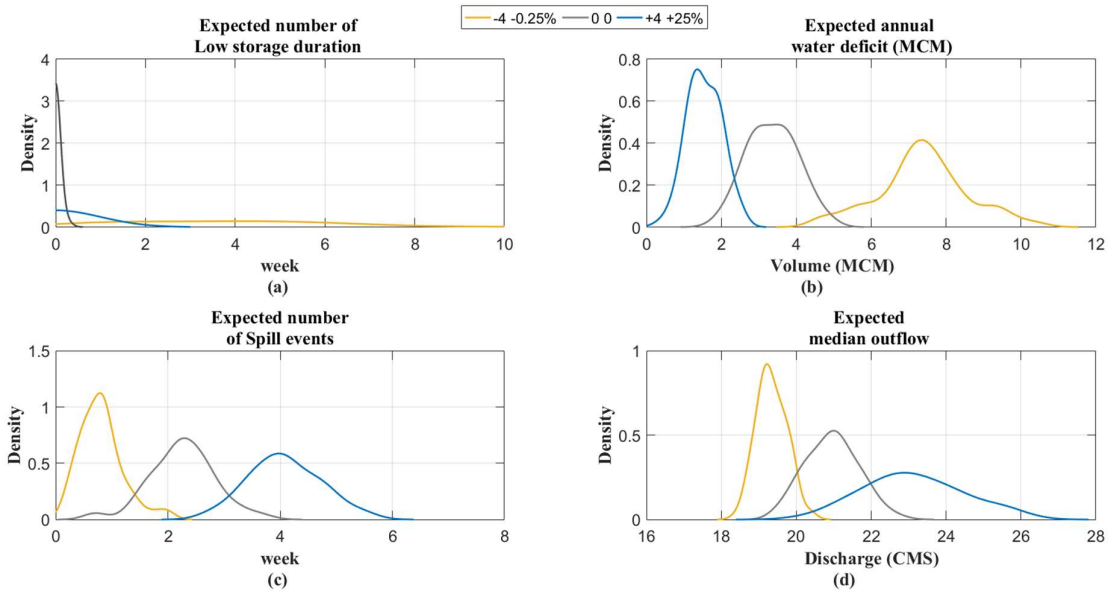

Fig. 48. Probabilistic risk profiles for the defined performance indicators under selected specific flow conditions. Panel (a) to (d) belong to expected number of low storage duration, expected annual water deficit, expected number of spill events and expected median outflow, respectively.

Panel (c) shows the risk profiles of expected number of spill events for the three specific regime conditions. In this figure, x-axis corresponds to number of weeks in which spill events occur. The figure indicates the gradual change of this indicator when the condition varies from dry to

wet. In brief, towards wet condition, the expected number of spill events increases. Based on this panel, number of weeks in which spill events occur with the highest probability in dry, historical and wet regimes are 0.7, 2.2 and 4, respectively. Based on extremes in this panel, the minimum number of spill events in dry and historical regimes is 0 while the minimum in wet regime would be 2 weeks. Focusing on the maximum extreme, 2.2, 4.2 and 6.3 weeks are expected as highest number of spill events during an operational year for dry, historical and wet regimes, respectively. Based on this panel, wet regime condition shows the highest variation in comparison to historical and dry regimes, showing that in wet regime larger uncertainty in annual number of spill events is expected.

Finally, Panel (d) analyses the median reservoir release, and the figure shows that in dry condition the median release with the highest probability is less than 20 CMS and gradually increases when the condition shifts to historical and wet to 21 and 23 CMS, respectively. In addition, looking at minimum extremes indicates that in dry, historical and wet regimes, the minimum annual reservoir outflows are almost 18 MCM. Also maximum extremes for this indicator in the dry, historical and wet regimes are 21.7, 23.8 and 27.9 CMS, annually. Moreover, wet regime condition shows more variation in comparison to the other two conditions.

Based on findings in this section, in dry condition low storage occurs more in comparison to the other two regimes. This can affect recreational activities around the Oldman Reservoir which can have social consequences in this region. At the same time in this condition, water supply deficit in local irrigation area increases. By decreased median outflow, it can be induced that regional irrigation districts will be faced with water scarcity as well. Since the region is one of the main food producers in Canada, measures should be taken by water managers to come up with solutions and adaptation strategies to compensate probable losses. In contrast, in wet condition the probability occurrence of low storage and local water supply deficit decreases. Consequently, by increased median outflow it can be concluded that regional water supply deficit decreases. But in this condition, number of spill events increases and since Lethbridge is located downstream of the reservoir, individuals and their properties are prone to extensive losses. In this case, water managers should be aware and equipped with protocols and strategies to minimize the effects of flooding in this region.

7.3 Joint impact assessment of changing streamflow and temperature

As discussed before, due to climate variability and change, not only the incoming inflow to the Oldman River basin is declining but the weather is getting warmer. This puts the water system under a significant pressure due to limited water availability and increased water demand resulting from changing climate. In brief, these stressors make the water system vulnerable. In order to assess the effect of changing streamflow and temperature on the system, joint bottom-up and top-down methods is applied. First, implementing a bottom-up approach, streamflow which originates from Rocky Mountains is stochastically reconstructed. Defining the three conditions, namely dry, historical and wet, 100 realizations for streamflow corresponding to each condition reconstructed. Then applying a top-down approach scenarios of changing temperature obtained from NASA climate models. In this regard, seven scenario for warming temperature defined. These scenarios correspond to realizations in which the long term expected temperature is equal to the historical temperature, or it increases in increments of +0.5 °C, up to the long term expected annual temperature plus 3 °C. For each scenario, 100 realizations for temperature in dry, historical and wet regime conditions found. Finally, different scenarios of streamflow and temperature are fed into the top non-falsified emulator (i.e. IE-6) and the behaviour of the system is evaluated. Here, the response of the system to changing scenarios is evaluated through four performance indicators which are expected number of low storage duration, expected annual water deficit, expected number of spill events and expected median outflow. Figure 49 shows the probabilistic risk profiles for the expected number of low storage duration in the three regime conditions. In these panels the performance indicators are shown when only streamflow is changing or the both streamflow and temperature are subject to change. For changing temperature, as mentioned before, seven warming scenarios are defined.

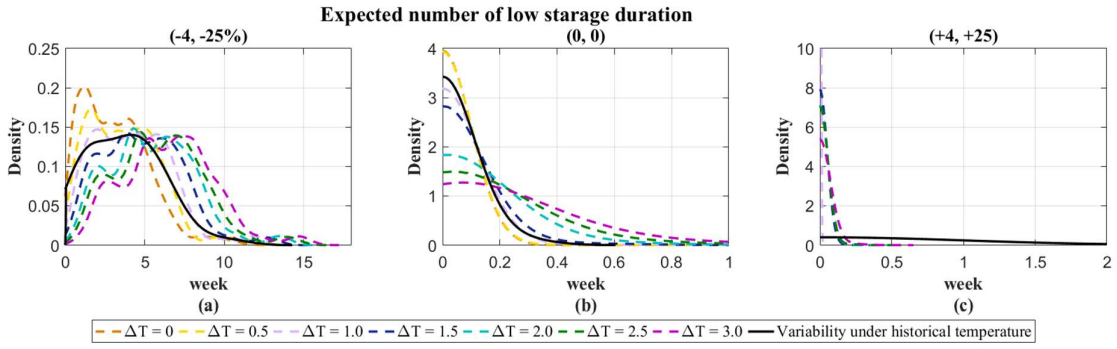

Fig. 49. Probabilistic risk profiles for expected number of low storage duration under the joint scenarios of change of stremflow and temperature in three specific flow regime conditions. Panels (a) to (c) belong to expected number of low storage duration in dry (-4, 25%), historical (0, 0) and wet (+4, 25%) regime conditions, respectively.

In Figure 49, x-axis presents the number of weeks in which low storage happens and y-axis shows the density of expected number of low storage duration. Black solid lines are the probability distribution functions of expected low storage duration, which had been developed with different scenarios of streamflow in the three regime conditions. To find expected low storage duration only under different scenarios of streamflow, 100 reconstructed realizations of streamflow are fed to the selected IE and temperature is kept as historical values. Then low storage duration for each operational year is found and averaged for the whole period. Having 100 values for this indicator, it would be possible to find the probability distribution function. Colored-dashed lines are probability distribution functions of this indicator under the joint scenario of changing streamflow and temperature. Again under joint scenario of changing streamflow (100 realizations) and temperature (100 realizations) and for 7 scenario of warming, annual low storage duration was found and averaged for all the period. Having 10,000 values for this indicator for each scenario of warming the probability distribution functions developed and added to the figure. Panel (a) in Figure 49 demonstrates that in the case of warming scenarios in dry regime condition, the expected number of low storage duration increases. This performance criteria can go up from 3.1 to 6.5 weeks, with the highest density when the temperature increases. In addition, in dry regime condition, warmer weather increases the maximum number of low storage duration to 17 weeks during an operational year. Also the variability of the probability distribution functions for scenarios of changing streamflow and joint scenarios of changing streamflow and temperature are almost the same.

Panel (b) shows this indicator in the historical regime condition. Based on this panel, with the maximum probability, expected annual low storage duration in this regime is zero. Moreover the maximum extreme value of expected low storage duration in this condition increases to 1 week per year with the highest probability for the all scenarios of warming. Also the variation of all the probability distribution functions are almost the same in the joint scenarios of changing streamflow and temperature. But the variability of the probability distribution function related to changing scenarios of streamflow is less. This implies that under the joint changing streamflow and temperature, the uncertainty in this indicator is increased.

Panel (c) shows that in wet regime condition the expected annual low storage duration is equal to zero, and warming condition does not affect this performance criteria. The maximum low storage duration decreases to 0.6 week per year for all the joint scenarios of streamflow and temperature. Also the variability in this indicator are almost the same in the all assessed scenarios. But the variation of expected low storage duration decreases when regime condition changes from dry to historical and wet. It can be noted that in wetter climate the uncertainty regarding this indicator is declined.

As discussed previously, declining headwaters streamflow incoming to the system, increasing temperature and developing socio-economic activities in this region puts an unprecedented pressure on water resources in the study area. Agriculture is the major activity in this region as the main food producer. This brings about the need to assess how agriculture activities are affected under different scenarios of change. Figure 50 presents the joint impact of streamflow and temperature on expected annual water deficit.

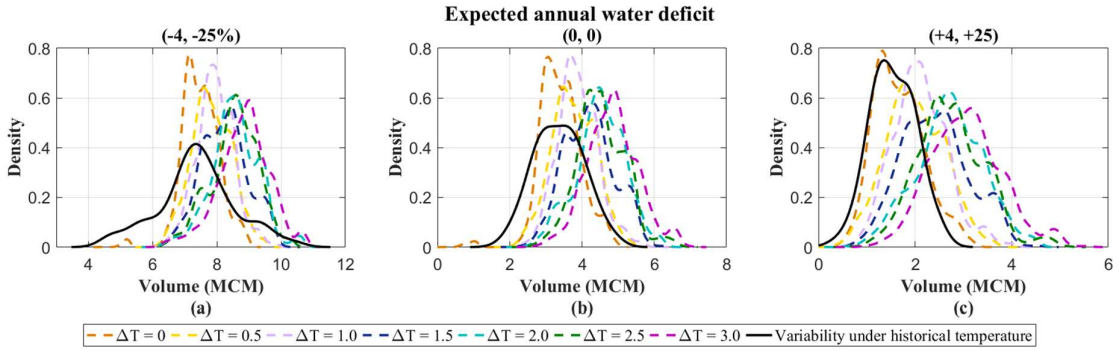

Fig. 50. Probabilistic risk profiles for expected annual water deficit under the joint scenarios of change of stremflow and temperature in three specific flow regime conditions. Panels (a) to (c) belong to expected annual water deficit in dry (-4, 25%), historical (0, 0) and wet (+4, 25%) regime conditions, respectively.

In Figure 50, x-axis shows the volume of water deficit in MCM, and y-axis presents the density of expected annual water deficit. The black solid lines are the probability distribution functions of this indicator under different scenarios of streamflow in the three regime conditions. The water supply deficit under changing streamflow has been found for each operational year and

averaged for the whole period. Then for 100 realization of streamflow the probability distribution function obtained and added to this figure. Colored-dashed lines represent this indicator under the joint impact of streamflow and temperature. Annual water supply deficit under the joint changing scenarios of streamflow (100 realizations) and temperature (100 realizations) for each warming scenario (7 scenarios) was found and averaged for the whole period. Then the probability distribution functions found and presented in the figure. The figure shows that when the temperature gets warmer the expected annual water deficit increases in all three regime conditions in comparison with the scenario that only streamflow is changed. In the dry regime condition (Panel- a) the maximum change of this indicator with the highest density when the temperature varies from historical values to historical values plus 3 °C is 1.3 MCM, and the expected annual water deficit changes from 7.5 MCM to 8.8 MCM. Corresponding to joint scenario of changing streamflow and temperature under $\Delta T = 0$ °C, the annual water supply deficit under changing streamflow is 7.5 MCM with the highest probability. In this regime condition, minimum and maximums extremes are increased with increasing temperature but the variability of probability distribution functions for the joint scenarios of changing streamflow and temperature in 7 scenarios of warming are the same. In contrast, the variability of this indicator when only scenarios of changing streamflow is considered is larger. This indicated that in warmer climate the uncertainty in water supply deficit is smaller.

In historical regime condition, this performance criteria varies from 3.4 to 4.8 MCM with the highest probability (1.4 MCM increase, as shown in Panel- b). In addition, extreme maximum of water supply deficit increases when the temperature gets warmer in all the scenarios of change. Maximum water deficit when the historical temperature is raised to +3 °C is almost 8 MCM. Moreover, the variability of this indicator is almost the same when either scenarios of changing streamflow or the joint scenarios of changing streamflow and temperature are considered.

In wet regime condition (Panel- c), this indicator changes from 1.6 MCM (identical to water supply deficit under changing streamflow only) to 3.0 MCM, corresponding to a 1.4 MCM increase with the highest probability. With increasing temperature extreme maximum water supply deficit rises to 6 MCM annually. Moreover, the variability of this indicator is larger

when the temperature is getting warmer. This shows higher uncertainty in this indicator in warmer climate.

As mentioned before Lethbridge is located downstream of the Oldman Reservoir and is prone to excessive flows that evacuate from the reservoir. In the case of flood events a great amount of loss can be expected in this region. This shows the importance of vulnerability assessment of the system under flood events. Figure 51 presents the joint impact of streamflow and temperature on expected number of spill events.

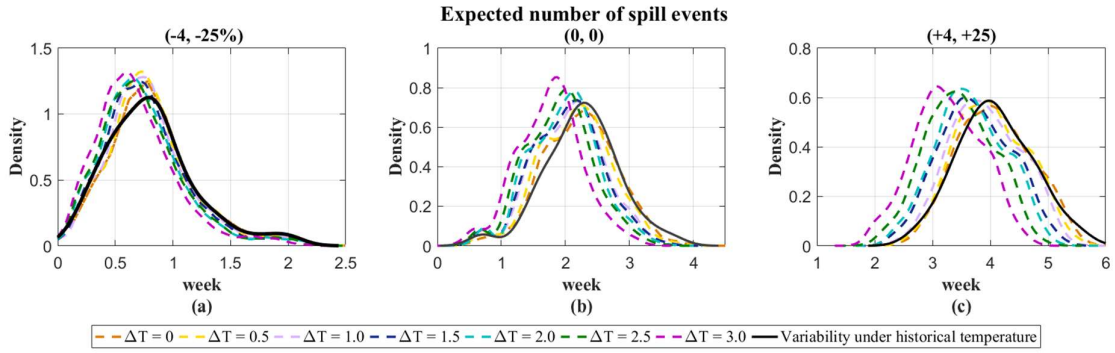

Fig. 51. Probabilistic risk profiles for expected number of spill events under the joint scenarios of change for stremflow and temperature in three specific flow regime conditions. Panels (a) to (c) belong to expected number of spill events in dry (-4, -25%), historical (0, 0) and wet (+4, +25%) regime conditions, respectively.

Figure 51 shows the probability distribution functions of expect number of spill events under changing streamflow with historical temperature (black solid lines) and seven defined scenarios of changing streamflow and temperature (colored-dashed lines). Similar to previous analysis, under changing streamflow, annual number of spill events have been found and averaged for the whole data period. Having 100 values of this indicator corresponding to 100 realizations of streamflow the probability distribution function was developed (Black solid line). Same procedure was taken to add PDFs under joint scenarios of changing streamflow and temperature. For 100 scenarios of streamflow and 100 scenarios for temperature, the performance indicator was found under 7 scenarios of warming. Having 10,000 values for each scenario of warming, PDFs developed and added to the panel. Panel (a), (b), and (c) belong to the dry, historical and wet conditions, respectively. The panels represent that warming

scenarios can decrease the expected number of spill events and this change is more significant in the wet regime condition. In the dry regime condition, the expected annual number of spill events under changing streamflow and joint scenario of changing streamflow and temperature when $\Delta T = 0$, is 0.85 week with the highest probability. With warming climate, this indicator declines to 0.65 weeks (0.2 week change). Based on this panel, extremes and variation of all PDFs are almost the same. In historical regime condition, expected number of spill events for changing streamflow and joint changing streamflow and temperature is 2.2 weeks per year with the highest probability. Warmer climate decreases this indicator to 1.9 weeks (0.3 week change). Based on this study, extremes and variability are almost the same for all PDFs presented in the panel. In wet regime condition, expected annual number of spill events in the case of changing streamflow and the scenario of changing streamflow and temperature for no change in expected temperature is 4 weeks. When ΔT goes up to +3 °C this indicator declines to 3 weeks corresponding to 1 week decrease. In addition, extreme minimum for the 3 °C warming decreases to 0.3 week and extreme maximum for the same scenario moves to 5.2 weeks. In all the scenarios PDFs have the same variability. Looking at the panels again, it can be found that by moving from dry to historical and wet regimes, the most change in the expected number of spill events happens in Panel (c) with 1 week decrease in this performance indicator. This shows that in wet regime condition, the system is more uncertain in spill events in comparison with historical and dry regime conditions.

The Oldman Reservoir not only allocates water to the local irrigation districts but it provides regional irrigation districts with their water demand. The regional water demand is manifested in the Oldman Reservoir outflow. By considering the changes in streamflow and temperature that have been and are currently taking place in this region, assessing the behaviour of reservoir under changing condition is important. The effect of changing both streamflow and temperature on the reservoir median release is demonstrated in Figure 52.

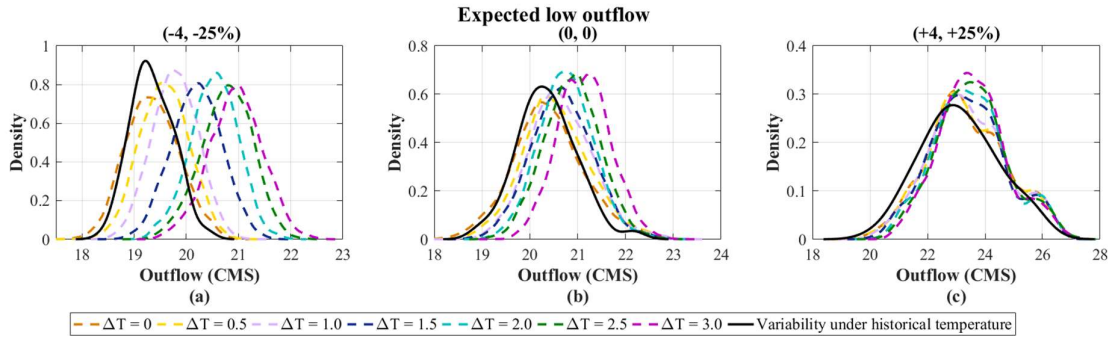

Fig. 52. Probabilistic risk profiles for reservoir's median release under the joint scenarios of change of stremflow and temperature in three specific flow regime conditions. Panels (a) to (c) belong to expected low outflow in dry (-4, -25%), historical (0, 0) and wet (+4, +25%) regime conditions, respectively.

In Figure 52, x-axis shows the reservoir release in CMS and y-axis is the density of this indicator. Black solid lines are the probability distribution functions of median release, which had been found through different scenarios of streamflow in the three regime conditions. The median reservoir release found for each operational year for each streamflow realization and averaged for the whole period. Having 100 realizations for streamflow, this indicator had 100 values with which the corresponding PDF developed. Colored-dashed lines show the probability distribution functions of median release under the joint impact of changing streamflow and temperature in the mentioned regime conditions. Reservoir median release found for 100 realizations of streamflow and 100 realizations for temperature under 7 scenarios of warming climate. This results in 10,000 values for median reservoir release for each warming scenario. With these values PDFs under climate warming scenarios found and added to the figures. As shown in Figure 52, with warming temperatures, the expected median reservoir release increases in the three panels. The maximum increase happens in dry regime condition, whereas the minimum change takes place in the wet regime condition. Based on Panel (a), median reservoir release for changing streamflow scenario and the joint changing streamflow and temperature under $\Delta T = 0$ °C, is 19.3 CMS with the highest probability. In the scenario in which $\Delta T = 3$ °C, this indicator increases to 20.9 CMS corresponding to 1.6 CMS change. In this regime condition, extreme minimums and maximums also rise with warming scenarios. In the warmest scenario, extreme minimum increases to 19 CMS and extreme maximum goes up to 23 CMS. The variability of PDFs under changing streamflow and joint streamflow and temperature are almost the same.

In historical regime condition, expected median reservoir release increases in warmer climate. The PDF corresponding to reservoir release under changing streamflow and joint changing streamflow and temperature is 20.2 CMS with the highest probability. When temperature goes up, this indicator rises to 21.1 CMS (0.9 CMS change). In the warmest scenario, extreme minimum and maximum are corresponding to 19 and 24 CMS, respectively. Moreover, the variability of PDFs in this figure are almost the same.

In wet regime condition (Panel- c), same as the two other regimes, the median reservoir release increases with rising temperature. With the highest probability, this indicator in the scenario of changing streamflow and joint changing streamflow and temperature is 22.9 CMS and increases to 23.6 CMS in the warmest temperature scenario with the highest probability (0.7 CMS change). Extreme minimum and maximum as well as variability of PDFs are almost the same. Comparing the changes happens in the values of the median reservoir release with highest probability indicates that by altering the regime condition from dry to historical and wet, the magnitude of change decreases. This demonstrates that in wet regime condition the system's outflow is less uncertain.

In order to identify the effect of warming climate on the four performance indicators, each indicator that had been found under the joint changing scenarios of streamflow (100 realizations) and temperature (100 realizations) in 7 scenarios of warming averaged and presented in Figure 53. With this approach it is possible to assess the behaviour of the system (which is defined with the four performance criteria) under warming climate.

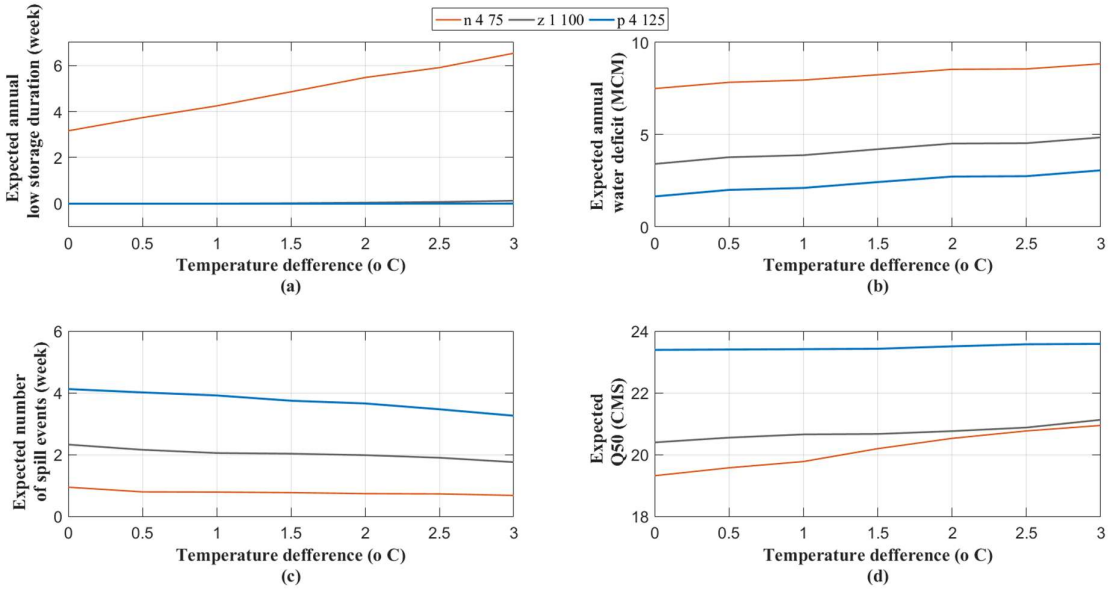

Fig. 53. Joint impact assessment of changing streamflow and temperature on the four defined performance criteria in the three specific flow regime conditions. Panel (a) to (d) show the effect of changing temperature on expected annual low storage duration, expected annual water deficit, expected number of spill events and expected median reservoir release.

In Panel (a) and all other panels, x-axis shows the temperature increments from 0 to +3 °C, which demonstrate different scenarios of warming conditions. In addition, three lines with different color saturations in all panels are representing wet, historical, and dry regime conditions, from highest to lowest saturation, respectively. In this panel, y-axis presents the expected annual low storage duration. As shown in this panel, expected annual low storage duration in historical and wet conditions is not sensitive to climate warming. However, in dry regime condition this performance criteria increases when temperature goes up. Based on this panel, although there is no variability in historical and wet regime conditions but change in this index is significant in dry regime condition. In dry regime, 1 °C rise in temperature results in 1.6 weeks increase in expected low storage duration. This implies that in dry regime condition, this indicator is more uncertain in comparison with the other two regime conditions. Therefore, in dry regime condition measures should be taken by water managers in order to face this extreme event condition.

Panel (b) also shows the joint impact of changing streamflow and temperature on the expected annual water deficit. Based on the figure, this criteria increases when temperature goes up in all the considered scenarios. The rates of increase are almost the same which indicates the same

variability in all three regime conditions. When temperature gets warmer for 1 °C, the expected water supply deficit increases 0.5 MCM during a growing season. This shows that the system is of the same uncertainty in water supply deficit in dry, historical and wet regimes. Moreover, in wet regime condition, the expected annual water supply deficit is minimum in comparison to the historical and dry regime conditions, respectively. In addition, the increase in this performance indicator, from wet to historical and from historical to dry regime condition, are not the same. It can be concluded that, in this case, the system is more sensitive when a dry condition happens. Since the system is more vulnerable in providing irrigation water demand with adequate water quantity, actions should be taken to minimize the risk in the system.

As shown in Panel (c), when temperature is getting warmer the expected number of spill events decreases. This index is more sensitive to temperature in wet regime condition, with the higher line gradient, in comparison to the other two regime conditions. With 1 °C increase in temperature, expected number of spill events decreases 0.3 week per year in wet regime condition. Whereas in historical regime condition 1 °C rise in temperature makes 0.07 week decline in this indicator. However, in dry regime condition, the sensitivity of number of spill events to temperature is marginal and with 1 °C increased temperature only 0.03 week change in this indicator is expected. This shows that in wetter climate, number of spill events is more uncertain in comparison to the other two regimes. Moreover, the decrease in this performance indicator, from dry to historical and from historical to wet regime condition, are not the same. It can be concluded that, in this case, the system is more sensitive when a wet regime condition takes place.

Panel (d) also shows the sensitivity of the median reservoir release to the changing conditions. At the first glance, the panel presents that when the regime condition changes from dry to wet, Q50 significantly increases. In addition, with increasing temperature this indicator rises as well. As discussed previously, the reservoir release is a representative of the water that is allocated to regional irrigation networks. Increasing reservoir release under warming condition demonstrates that when the system is under pressure, higher amount of water is evacuated from the reservoir in order to provide regional agriculture sectors with their water demand. This is in accordance with the main model. In the original model (WRMM), regional irrigation networks have higher priority in comparison to local irrigation district. The gradient of the lines in historical and wet regimes shows that this indicator is not highly dependent on warming condition. In other words, with 1 °C increase in temperature, median reservoir outflow rises

quite limited in wet and 0.3 CMS in historical regime conditions. Whereas in dry regime condition, expected median release increases 0.5 CMS with 1 °C increased temperature. This shows that the variability in dry condition is greater in comparison with the other two regimes and the behaviour of the system under dry regime condition in more uncertain. It is of a great interest that in dry and historical regime conditions, when the climate is warmer by +2 °C or more, expected Q50 in dry regime condition approaches the values of this indicator in the historical regime condition. It can be concluded that in both dry and historical regime conditions, when temperature rises to expected long term historical plus 2 °C or more, the expected median release will be almost the same.

Based on the presented panels, low storage in historical and wet conditions is not occurred while in wet regime it increases in warmer weather. Also local and regional (Q50) water supply deficit increase in the three regimes when temperature rises. But the rate of increase in local water supply deficit is more in comparison with regional water supply deficit. It implies that when there is a pressure on this water system, the priority is to maintain reservoir storage. It can be due to preventing sediment spreading or the importance of recreational activities in this region. Regional irrigation networks also have the second priority due to our findings. In warmer climate, when the system is under pressure, Q50 rises whereas local irrigation networks are facing increasing water deficit. Based on our findings, it can be concluded that in this water system, reservoir storage, regional and local irrigation networks have the highest to lowest priority.

7.4 Impact assessment of changing inflow, climate and irrigation area

In order to accomplish the third level of vulnerability assessment, a heuristic approach is applied. Due to changing climate, as discussed in previous sections, incoming inflow to the system is subject to change. In addition, the climate is getting warmer and the magnitude and variability of temperature and precipitation are changing. Moreover, considering developing socio-economic activities in this region water demand has an increasing trend and requests for water is heightened. In this level of impact assessment study, the vulnerability of the system under changing streamflow, climate including temperature and precipitation and the effect of human intervention in changing irrigation area is evaluated. In this scope, three predefined states, representing increase, no-change and decrease in streamflow, climate and irrigation area are considered. For inflow, precipitation and irrigation area, the scenarios for increase and

decrease are identified as ±25% change in the historical time series. With this approach different realizations for these variables are developed. For temperature, the scenarios of change have been considered as ±2°C change in historical temperature series during this period. The combination of all the considered scenarios of change, will produce 81 joint settings for each variables. Input time series corresponding to these joint scenarios are fed to the top selected non-falsified IE to simulate the local behaviour of water resource system at the Oldman reservoir. Then the effect of defined scenarios of change on the expected number of low storage duration in a typical year, the expected local water deficit during a typical year, the expected number of weekly spill events during one typical year, and the expected median release from reservoir during a typical year is analysed. Figure 54 shows the sensitivity of above performance measures to the considered joint scenarios of change based on the top non-falsified IE (i.e. IE-6), which stands as the most accurate non-falsified IE based on the analysis made in Chapter 6. In each panel, the joint scenarios for inflow, temperature, precipitation and irrigation area along with the corresponding sensitivity in the performance indicator are shown from left to right, respectively. The color bar shows the magnitude of considered indicators, sorted from the lowest to the highest values. White, gray and black colors show decrease, no-change and increase in magnitude of independent variables.

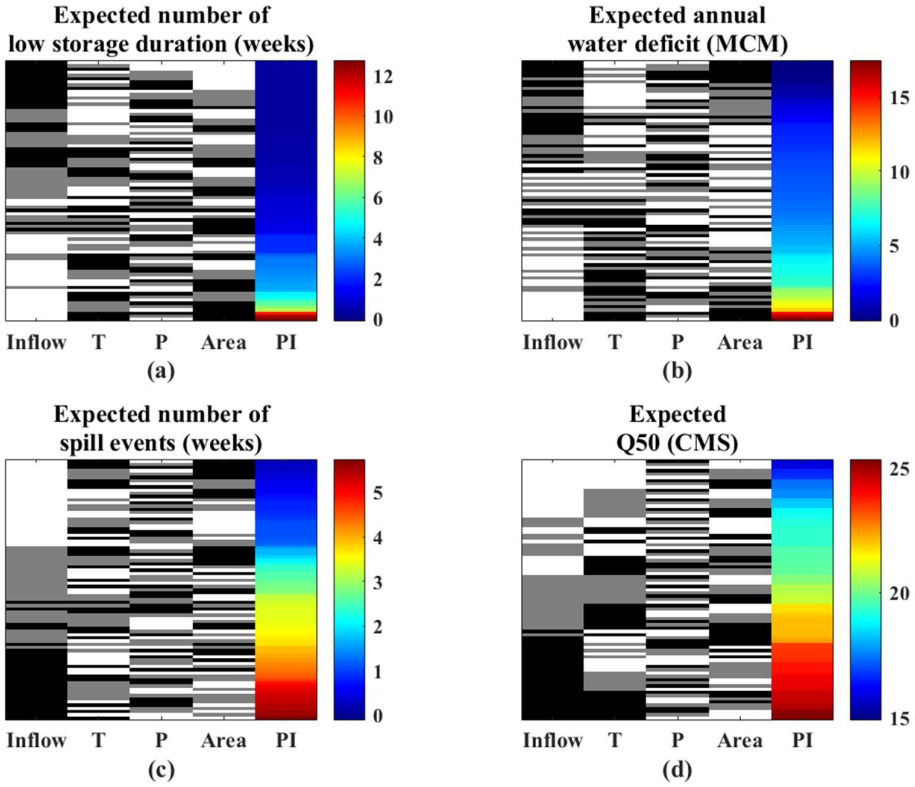

Fig. 54. The effect of changing Inflow, temperature (T), precipitation (P) and irrigation area (Area) on (a) the number of low storage duration, (b) annual water deficit, (c) number of spill events and (d) median release. Color bar shows the value of performance indicator (PI) under scenarios of change. Black, grey and white bars show increase, no change or decrease in independent variables.

Based on Figure 54, decreased inflow particularly when it combines with increased irrigation area and warming temperature can severely change the number of weeks with low reservoir storage. Considering the local irrigation deficit, inflow and temperature are the key triggering factors for alteration in this indicator. Considering spill events, it can be argued that inflow is the most influencing variable on increasing the expected number of event in a typical year and 25% increase in inflow can change the spill event from two to five weeks in a typical year. This finding is in accordance with the study run in the first level of impact assessment. Inflow is also the main triggering factor for changes in the median reservoir release in a typical operational year, although changes in the local temperature can perturb the effect of the changing factors on the annual median release, due to alteration in the reservoir evaporation.

It should be noted that changing the integrated emulator, with which the performance of the system is assessed, can alter the results of the sensitivity analysis. To showcase the uncertainty in the impact assessment as a result of altering the emulator, the sensitivity analysis with other two non-falsified emulators has been repeated, i.e. IE-22 and IE-14, and the changes in the estimated performance indicators under the same joint scenarios of change has been inspected and ordered according to Figure 55 for each performance indicator. It should be noted that these IE-22 and IE-14 differ from IE-6 only in terms of the emulator used for lake evaporation: E-8 in IE-6 is substituted by E-11 and E-9 in IE-22 and IE-14, respectively. Figure 55 summarizes the findings. In panels, x-axis belong to models IE-22 and IE-14. These panels show how much change in performance indicators takes effect when the emulator of lake evaporation is change. In all panels, colorbars show the magnitude of change in the four performance indicators. No change is corresponding to white color white positive and negative changes are shown with red and blue colors. Larger distance from zero (white) gets more saturation in red or blue. Considering low storage periods, altering the emulators related to reservoir evaporation can cause up to 20% change in the estimated performance indictor depending to the changing condition considered. In this case, altering the emulator for lake evaporation mainly results in overestimating the changes witnessed by IE-6, which is more highlighted when E-8 is substituted by E-9. Similarly, the identified deficit in local irrigation supply is sensitive to the choice of emulator used for representing reservoir evaporation. In particular, substituting E-8 by E-9 can result up to 10% change in the performance indicator. Considering the number of spill events in a typical year, changes in the emulators related to reservoir evaporation can cause between ±5% changes in the estimated value. Considering the expected median of annual reservoir release, the changes in the identified sensitivity due to changes in the IEs are rather marginal and stay between 0 to 1% under the considered scenarios of change. From the figure it can be concluded that the major change is in the expected low storage duration indicator and the minor change is in median reservoir release. This indicates that IEs with marginal differences during the historical conditions can provide rather different estimates under changing conditions – see Bormann et al. (2011). This can highlight the role of impact model in portraying the sensitivity of water resource systems to changing conditions, indicating added uncertainty as a result of the choice of the model with which the vulnerability is assessed.

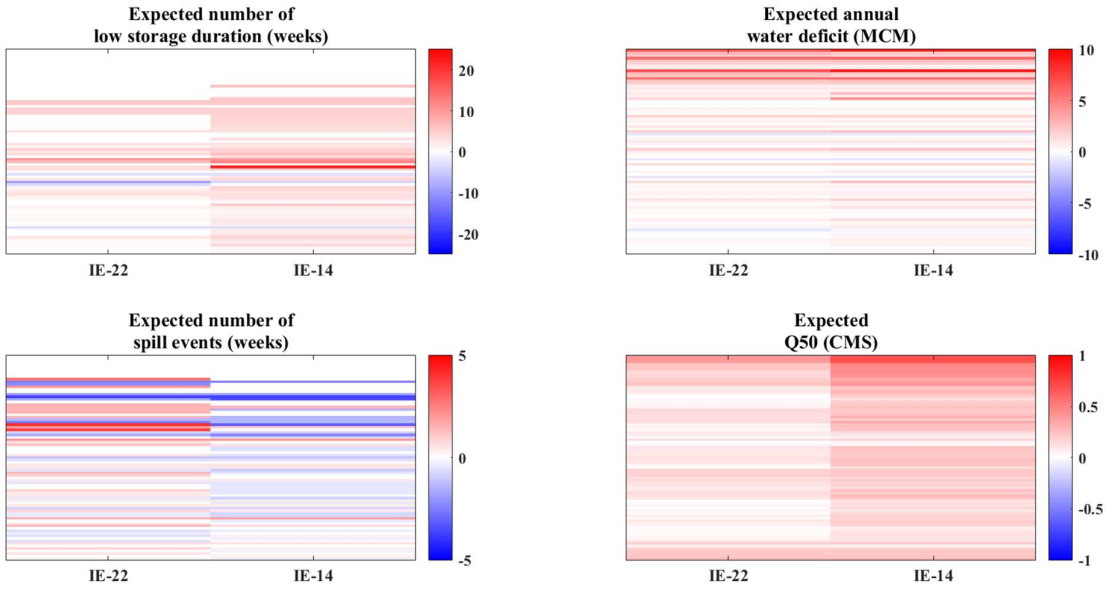

Fig. 55. Relative change in the performance indicators obtained by IE-22 and IE-14, compared to IE-6 for expected number of low storage duration, expected annual water deficit, expected number of spill events, and expected median flow during a typical year.

In order to quantify the level of confidence of top non-falsified models, IE-22 and IE-14, in representing the behaviour of Oldman Reservoir, the probability distribution functions for to the four performance criteria are found and presented in Figure 56. In this Figure, Panels (a) to (d) belong to expected low storage duration, expected annual water deficit, expected number of spill events and expected Q50, respectively. Also x-axis shows the percent of change in estimation of performance indicators with respect to model IE-6 and y-axis shows the density. The performance of the two models are presented by red (IE-22) and blue (IE-14) colors. Based on Panel (a), in estimation of low storage duration, model IE-22 shows -10 to +10 percent of change whereas model IE-14 ranges between -9 to +25 percent. Moreover, as presented in Panel (b), for the expected annual deficit, IE-22 performs a range of change from -1.5 to +7 percent while IE-14 has a greater range from -1.5 to +9 percent. Panel (c) belongs to expected number of spill events in which IE-22 and IE-14 show a range of ±4 percent and -4 to +2 percent of change with respect to model IE-6, respectively. The last panel also shows the performance of the two models in estimation of Q50. Based on this panel, the percent of change in representing this indicator by the models are marginal and similar.

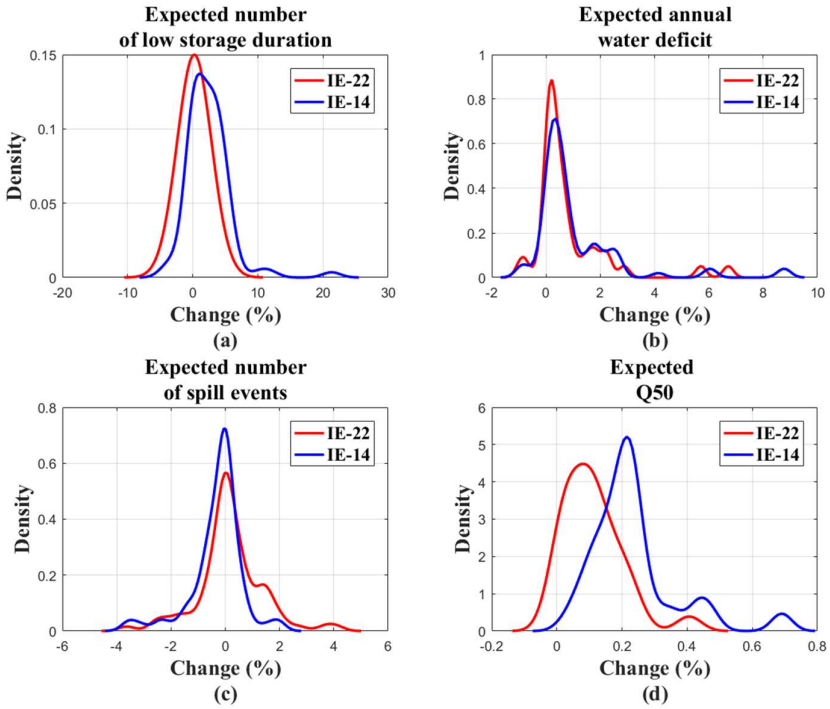

Fig. 56. Probability distribution functions related to models IE-22 and IE-14 in representing the change in the four performance criteria with respect to model IE-6. Panels (a) to (d) belong to low storage duration, expected annual water deficit, expected number of spill events and expected Q50, respectively.

Chapter 8. Summary and conclusions

The increasing pressure on freshwater resources necessitates developing improved tools with which potential vulnerabilities in water resource systems can be diagnosed and quantified. Despite major breakthroughs in integrated water resource management models, existing IWRMs do not reveal required details within all components of the system in consideration. To overcome the limitations in existing IWRMs in terms of representing details, here, using an emulation approach is suggested with which a new set of functional relationship can be added to the original model to improve process representations only where and when needed. The functionality of this approach in understanding the detailed dynamics of water resource systems developed around the Oldman River in southern Alberta, Canada which is tested in this study. An existing IWRM, i.e. WRMM, developed by Alberta Environment (2002a) as a benchmark model is considered for which the emulators are developed. To represent a detailed representation of the system dynamics at the Oldman Reservoir, MLR- and ANN-based emulators for (1) lake evaporation, (2) irrigation water withdrawal, (3) irrigation water demand and (4) the reservoir release are developed considering different scenarios for input selection. In the first scenario, it was assumed that a complete knowledge regarding predictors and their time signatures is available. This knowledge was taken from literature and was proven with available data related to the case study. In the second scenario, predictors were chosen from a pool of potential variables in which time signatures were known. In this scenario various nonlinear transformations of these variables were considered. In the third scenario, time signatures of predictors were also unknown and potential variables with time lags were included in the pool of potential predictors. An input variable selection scheme was applied to find most relevant predictors in second and third scenarios. To apply the input variable selection scheme three measures of dependence i.e. Kendall's tau, Pearson's correlation coefficient and Spearman's rho were considered.

For each variable, 77 emulators, (7 with MLR and 70 with ANN technique) were developed and their performance was evaluated based on various goodness-of-fit measures against WRMM simulations. Then some of the emulators were falsified based on their relative performance with respect to accuracy, uncertainty as well as the trade-off between accuracy and uncertainty. The non-falsified emulators were coupled to form 128 IEs, with which the detailed dynamics at the Oldman Reservoir can be described. These IEs were rigorously intercompared in semi- and fully-coupled simulation modes in testing and validation periods.

The performance of the integrated emulators was assessed and top non-falsified integrated emulators were chosen.

Considering emulation models developed, the results showed that ANN-based emulators generally outperform simpler emulators developed using MLR. Moreover, it was found that ANN is a powerful tool that can estimate variables even with not physically meaningful predictors. As an example, although based on the considered configuration, lake evaporation is dependent on both temperature and reservoir storage but some lake evaporation emulators are only dependent on different functions of temperature. These emulators are amongst the models that perform highest accuracy or less uncertainty. In addition, although emulators developed assuming partial knowledge of the input variables were able to simulate the considered variables in individual and semi-coupled mode, they were outperformed by emulators configured based on the perfect *priori*. This can highlight the importance of the expert knowledge in forming efficient emulators.

Accordingly, the top selected non-falsified emulators were used to explore the sensitivity of the water resource system at the Oldman Reservoir to (1) changing streamflow, (2) streamflow and temperature and (3) streamflow, climate and irrigation area. To evaluate the reservoir sensitivity to changing conditions, a set of performance indicators defined. These include (1) the expected number of weeks in an operational year in which the reservoir storage goes below 25% of its capacity, (2) the expected local water deficit during a typical year, (3) the expected number of weekly spill events during one typical year, and (4) the expected annual median reservoir release. Expected low storage duration and water supply deficit indicate local behaviour of the reservoir whereas expected number of spill events and median reservoir release are representations of regional behaviour of the system as the reservoir release supplies water for the Lethbridge northern irrigation district. In order to evaluate the vulnerability of the system under the three defined changing scenarios, bottom-up, joint bottom-up/top-down, and a heuristic techniques of impact assessment applied. For the first impact assessment study, two indicators of flow regime, namely annual flow volume and timing of the annual peak, were considered. 11 scenarios of change for annual flow volume (ranging from 0.75% to 1.25%) and 14 scenarios of change for the annual peak (ranging from -5 to +8 weeks) resulted in 154 scenarios for changing streamflow. Then for each scenario applying ensemble generation scheme, 100 realizations for this variable were found. These scenarios fed into the top non-falsified emulator (IE-6) and the behaviour of the system under changing scenarios assessed.

By defining three regime conditions corresponding to dry (-4, -25%), historical (0, 0) and wet (+4, +25%), findings show that in the historical and wet regime conditions, low storage duration is not changed whereas in dry condition up to 3 weeks of low storage is expected. Also in wet condition, expected annual water deficit with higher variability is less in comparison with the other two regimes. In addition, expected number of spill events and its variability are subject to increase from dry to historical and wet regime conditions. This shows that this indicator is more uncertain in wetter conditions. Moreover, median reservoir release and its variability are subject to increase from dry to historical and wet regime conditions. This study not only evaluates the behaviour of the system under different scenarios but shows the variability in the performance indicators. The variability of performance indicators implies that how much the system is uncertain under defined scenarios of change. As an example, the PDF of expected number of spill events in wet regime condition with high variability intersects the PDF corresponds to historical and even dry regime conditions. This shows that although the regime condition is wet, but under certain streamflow characteristics, number of spill events can be similar to historical or even dry regime conditions. Based on the first level of impact assessment study, in dry and historical conditions, low storage does not occur in the system while local and regional irrigation networks are facing water deficit. It implies the higher priority of maintaining reservoir storage in comparison with allocating water to local and regional irrigation demand. Moreover, in wet regime condition more spill events are expected which necessitates awareness of water managers to prevent the probable consequences.

In the second level of impact assessment study, a joint bottom-up/top-down approach applied. First, temperature data obtained from NASA-NEX downscaled global climate projections. Then different scenarios of warming were defined in a way that the long term expected annual temperature is equal to the historical temperature, or increases in increments of +0.5 °C, up to the long term expected annual temperature plus 3 °C. Finally, from each group 100 realizations of temperature were randomly selected. The joint scenarios of streamflow and temperature were fed into the top non-falsified model and the sensitivity of the system under changing streamflow and temperature was assessed. With this assessment it was shown that in a warmer climate, the duration of low storage is extended, the water supply deficit will increase, the number of spill events decreases and the median reservoir release will increase. This study showed that although in warmer climate the stress on the system increases but the reservoir release which represents the regional water allocation is increased as well. This indicates that the priority of regional irrigation districts is higher rather than the local irrigation network. This

is due to the importance of the LNID over the local irrigation networks in terms of the area. (LNID area is 92,000 hectare and local irrigation network area is 6,700 hectare). In addition, although in historical and wet regime conditions local and regional irrigation districts are facing water supply deficit but the duration of low storage in these conditions is not changed. This highlights the higher priority of maintaining storage level in comparison with allocating water to local and regional irrigation districts. Higher priority of maintaining reservoir level is due to preventing sediment spreading in the region which can have significant environment consequences. Therefore, it can be concluded that in the system, highest to lowest priorities go to preventing low storage occurrence, allocating regional and local water demand. These findings are in accordance with the priority policy in the original water resource model (WRMM).

In the third level of vulnerability assessment, a heuristic approach was applied. In this study, the sensitivity of the system to streamflow, climate including temperature and precipitation and human intervention due to change in irrigation area was assessed. Three states for increase, no-change and decrease in streamflow, precipitation and irrigation area considered. The scenarios for increase and decrease were identified as ±25% change in the historical time series for streamflow, precipitation and irrigation area and ±2°C change in historical temperature series. All settings were fed to the top non-falsified model with which the sensitivity of the system at the Oldman Reservoir was assessed. It was found that inflow to reservoir and area of irrigation are the most significant drivers affecting number of low storage duration and spill events. Water deficit is sensitive to inflow, temperature and irrigation area while median release is dependent on inflow to reservoir and temperature. This holistic knowledge on local sensitivity to changing condition was not attainable using the original WRMM model.

Also it was shown that although the performance of the non-falsified IEs are identical in representing the dynamics of the Oldman Reservoir under historical data, simulations results can differ under scenarios of change. It was argued that this uncertainty, originated from the impact model with which the system sensitivity is assessed, should be recognized and handled particularly under uncertain future conditions.

Considering the promising results obtained, the application of proposed emulation approach is promoted in other case studies and/or IWRMs. Having said that, it is believed much more can be done:

(1) For developing emulators, 60% of available data was used for training emulators. It is possible to check the effect of changing this range on the performance of emulators. Also this data was taken from the beginning of the time series while it is possible to take the data randomly from anywhere throughout the whole data period and investigate any improvement in the performance of emulators. Similar to what mentioned about the data which was used for training emulation models, it is possible to consider different periods of data for testing and validating purposes or selecting these periods randomly from the whole data period.

(2) In this study, emulators were developed applying MLR and ANN approaches. However, other data-driven approaches such as Genetic Symbolic Regression (Hassanzadeh et al. 2013) can be used for building emulators.

(3) In the first level of predictor selection, we assumed that a complete knowledge regarding proxies of emulators is available. For further studies, it is possible to include other variables as predictors and check whether they can improve the performance of emulators or not.

(4) In the second and third scenarios of predictor selection scheme, only 6 different functions of potential variables considered while it is possible to apply different other functions.

(5) In the second and third scenarios of predictor selection, it was assumed that the proxies that can improve the *BIC* value for predictand residual more than 10% are considered. This limit can be decreased or increased to see the effect of including or excluding predictors in emulators' performance.

(6) In developing individual emulators we assumed that water evaporates from the lake with the same amount throughout the surface and we ignored the effect of water depth on the evaporation process. Therefore, it would be possible to include the effect of reservoir depth on the lake evaporation. In addition, we assumed that irrigation demand, water withdrawal and reservoir release are of constant values during an operational week. So it is not possible to detect changes in these variables in finer temporal resolutions. It can be possible to modify the model in a way that can address different time scales.

(7) We found the parameters of MLR-based emulators with 95% level of confidence. In the future studies this range can be changed.

(8) In order to find predictive uncertainty in MLR-based emulators, the range of each parameter was divided to four segments resulting in five different realizations for each parameter of the equations. The number of segments can be changed and by having less or

more number of parameters the predictive uncertainty regarding each emulator can be found and compared.

(9) To assess the performance of emulators *RMSE, R^2, NSE, LRMSE and REP* were used whereas it is possible to consider other error measures.

(10) In the semi-coupling mode, best emulators were selected based on the highest accuracy and least uncertainty which had been found using *BIC* measure. It was possible to take other goodness-of-fit measures such as Nash-Sutcliffe Efficiency indicator to select best emulators.

(11) In order to falsify integrated emulators, *IPE* measure was used. This indicator is a representation of *RMSE*, *LRMSE* and *REP*. It is possible to choose other error measures to define *IPE*.

(12) We only focused on the 7 top nan-falsified IEs while it was possible to consider more IEs.

(13) Emulators can be used to link the dynamics of water resource systems across a range of spatial and temporal scales and/or between water quantity and quality.

(14) The emulators developed using input and output sets of the original model (WRMM). Simulations of WRMM were based on predefined policies and priorities. Now if these policies change, the developed IEs are not able to be updated and used as emulator of WRMM. In order to tackle this issue, it is possible to define some parameters in the individual emulators in order for them to be able to take into account the policies according to the original model.

(15) In this study, only one component of the river system was emulated (Oldman Reservoir). Now if including another components is sought one way is to develop another set of emulators and going through the same procedure step by step to fine best integrated emulators. Having best IEs for the second component of the system, the next step is to coupling them with the top selected IEs of the first component and assessing the behaviour of the system under different scenarios. Developing different hypothesis for emulators, falsifying and finding best IEs and coupling them for different components of the system not only increases the complexity of the problem in hand but it needs a great amount of time to be dealt with. Another solution would be defining some parameters in the developed individual emulators based on the physical properties of reservoirs. Then by modifying the parameters it would be possible to have new IEs without the need of developing them. With this approach by one already developed IE it would be possible to assess the behaviour of the system with other components.

(16) Here, it was assumed that only one type of crop exists in the local irrigation networks. However, it is possible to consider different crop types with different water needs and by applying the top selected IE developed in study identify the vulnerability of the system under changing crop types.

(17) In the first level of impact assessment, the annual flow volume and annual peak were considered to change. Other characteristics of streamflow such as variability, rescission or the shape of the hydrograph can be included in the impact assessment study as well.

(18) In the second level of impact assessment study, the focus was only on the dry (-4, -25%), historical (0, 0) and wet (+4, +25%) regime conditions. It is possible to expand this analysis for all the 154 defined scenarios as presented in Figure 43.

(19) Also in the second level of impact assessment study, only scenarios of changing streamflow and temperature were considered. It is possible to include different scenarios of changing precipitation in the impact assessment study.

(20) In addition, the temperature data obtained from NASA-NEX global climate projections was used in this study without downscaling. The spatial resolution of this data is 25 × 25 Kilometers globally. However, it is possible to downscale this data to a finer resolution and apply it in the vulnerability assessment study.

(21) In the third level of impact assessment study, by applying a constant multiplier, values of the considered variables homogeneously decreased or increased. However, in the nature these changes are not homogeneous. Therefore, it would be possible to consider change in these variables non-homogeneously.

(22) In the third level of impact assessment, we only considered ±25% change in the historical time series of streamflow, precipitation and irrigation area, and for temperature, ±2°C in the historical time series. It is possible to consider different values for change in these variables.

References

AghaKouchak, A., D. Feldman, M. Hoerling, T. Huxman ,J. Lunds. (2015a). “Water and climate: Recognize anthropogenic drought”. *Nature News*. / 524 (7566). 409.

AghaKouchak, A., H. Norouzi, K. Madani, A. Mirchi, M. Azarderakhsh, A. Nazemi, N. Nasrollahi, A. Farahmand, A. Mehran ,E. Hasanzadehs. (2015b). “Aral Sea syndrome desiccates Lake Urmia: call for action”. *Journal of Great Lakes Research*. / 41 (1). 307-311.

Al-Najar, H. ,E. K. Ashours. (2013). “The impact of climate change and soil salinity in irrigation water demand on the Gaza Strip”. *Journal of water and climate change*. 10.2166/wcc.2013.142, / 4 (2). 118.

Alberat Environement. (2013). "2013 Flood Recovery Programs." 2013,<http://aep.alberta.ca/water/programs-and-services/2013-flood-recovery-programs/default.aspx>.

Alberta Environment (2002a). *South Saskatchewan River basin water management plan, phase one: water allocation transfers,* Calgary, Alberta, Department of Environment, Government of Alberta.

Alberta Environment (2002b). *Water for life* Alberta, Canada: Department of Environment, Government of Alberta.

Alvarez, J. F. O., J. A. de Juan Valero, J. M. T. Martín-Benito ,E. L. Matas. (2004). “MOPECO: an economic optimization model for irrigation water management”. *Irrigation Science*. 10.1007/s00271-004-0094-x, / 23 (2). 61-75.

Arnell, N. W.s. (2004). “Climate change and global water resources: SRES emissions and socio-economic scenarios”. *Global environmental change*. 10.1016/j.gloenvcha.2003.10.006, / 14 (1). 31-52.

ASCEs. (2000). “Artificial neural networks in hydrology. I: Preliminary concepts”. *Journal of Hydrologic Engineering*. doi.org/10.1061/(ASCE)1084-0699(2000)5:2(115), / 5 (2). 115-123.

Azarnivand, A. ,N. Chitsazs. (2015). “Adaptive policy responses to water shortage mitigation in the arid regions—a systematic approach based on eDPSIR, DEMATEL, and MCDA”. *Environmental monitoring and assessment*. / 187 (2). 23.

Bakker, K.s. (2012). “Water security: research challenges and opportunities”. *Science*. / 337 (6097). 914-915.

Barnett, T., R. Malone, W. Pennell, D. Stammer, B. Semtner ,W. Washingtons. (2004). “The effects of climate change on water resources in the west: introduction and overview”. *Climatic Change*. / 62 (1-3). 1-11.

Bates, B., Z. Kundzewicz ,S. Wu (2009). "Climate change and water resources in systems and sectors.". *Climate change and water.* Intergovernmental Panel on Climate Change Secretariat (IPCC), Geneva, 4**:** 53-76.

Beck, L. ,T. Bernauers. (2011). “How will combined changes in water demand and climate affect water availability in the Zambezi river basin?”. *Global Environmental Change*. 10.1016/j.gloenvcha.2011.04.001, / 21 (3). 1061-1072.

Bergstrom, J. C. ,A. Randall (2016). *Resource economics: an economic approach to natural resource and environmental policy*. Edward Elgar Publishing.

Beven, K. ,P. Smiths. (2014). “Concepts of information content and likelihood in parameter calibration for hydrological simulation models”. *Journal of Hydrologic Engineering*. 10.1061/(ASCE)HE.1943-5584.0000991, / 20 (1). A4014010.

Bishop, C. M. (1995). *Neural networks for pattern recognition*. Oxford university press, USA.

Biswas, A. K.s. (2004). “Integrated water resources management: a reassessment: a water forum contribution”. *Water international*. 10.1080/02508060408691775, / 29 (2). 248-256.

Blanning, R. W.s. (1975). “The construction and implementation of metamodels”. *simulation*. 10.1177/003754977502400606, / 24 (6). 177-184.

Bonsal, B. ,M. Regiers. (2007). “Historical comparison of the 2001/2002 drought in the Canadian Prairies”. *Climate Research*. / 33 (3). 229-242.

Bormann, H., H. M. Holländer, T. Blume, W. Buytaert, G. Chirico, J. Exbrayat, D. Gustafsson, H. Hölzel, P. Kraft ,T. Kraußes. (2011). “Comparative discharge prediction from a small artificial catchment without model calibration: Representation of initial hydrological catchment development”. *Die Bodenkultur*. / 62 (1-4). 23-29.

Brouwer, R. ,M. Hofkess. (2008). “Integrated hydro-economic modelling: Approaches, key issues and future research directions”. *Ecological Economics*. 10.1016/j.ecolecon.2008.02.009, / 66 (1). 16-22.

Brown, C., W. Werick, W. Leger ,D. Fays. (2011). “A Decision-Analytic Approach to Managing Climate Risks: Application to the Upper Great Lakes 1”. *JAWRA Journal of the American Water Resources Association*. / 47 (3). 524-534.

Brown, C. ,R. L. Wilbys. (2012). “An alternate approach to assessing climate risks”. *Eos, Transactions American Geophysical Union*. 10.1029/2012EO410001 /93 (41). 401-402.

Brownson, D. A., D. K. Kampouris ,C. E. Bankss. (2011). “An overview of graphene in energy production and storage applications”. *Journal of Power Sources*. 10.1016/j.jpowsour.2011.02.022, / 196 (11). 4873-4885.

Cai, X., D. C. McKinney ,L. S. Lasdons. (2002). “A framework for sustainability analysis in water resources management and application to the Syr Darya Basin”. *Water Resources Research*. 10.1029/2001WR000214 /38 (6).

Cai, X., M. W. Rosegrant ,C. Ringlers. (2003). “Physical and economic efficiency of water use in the river basin: Implications for efficient water management”. *Water Resources Research*. 10.1029/2001WR000748 /39 (1).

Carleton, T. A. ,S. M. Hsiangs. (2016). “Social and economic impacts of climate”. *Science*. / 353 (6304). aad9837.

Carpenter, S. R., N. F. Caraco, D. L. Correll, R. W. Howarth, A. N. Sharpley ,V. H. Smiths. (1998). “Nonpoint pollution of surface waters with phosphorus and nitrogen”. *Ecological applications*. 10.1890/1051-0761(1998)008[0559:NPOSWW]2.0.CO;2, / 8 (3). 559-568.

Castelletti, A., S. Galelli, M. Ratto, R. Soncini-Sessa ,P. C. Youngs. (2012a). “A general framework for dynamic emulation modelling in environmental problems”. *Environmental Modelling & Software*. 10.1016/j.envsoft.2012.01.002, / 34 5-18.

Castelletti, A., S. Galelli, M. Restelli ,R. Soncini-Sessa (2011). Tree-based variable selection for dimensionality reduction of large-scale control systems. *Adaptive Dynamic Programming And Reinforcement Learning (ADPRL), 2011 IEEE Symposium on*, IEEE. DOI: 10.1109/ADPRL.2011.5967387.

Castelletti, A., S. Galelli, M. Restelli ,R. Soncini-Sessas. (2012b). “Data-driven dynamic emulation modelling for the optimal management of environmental systems”. *Environmental Modelling & Software*. 10.1016/j.envsoft.2011.09.003, / 34 30-43.

Castelletti, A., F. Pianosi, R. Soncini-Sessa ,J. Antenuccis. (2010). “A multiobjective response surface approach for improved water quality planning in lakes and reservoirs”. *Water Resources Research*. 10.1029/2009WR008389, / 46 (6).

Chang, N.-B., B. J. Rivera ,M. P. Wanielistas. (2011). “Optimal design for water conservation and energy savings using green roofs in a green building under mixed uncertainties”. *Journal of Cleaner Production*. 10.1016/j.jclepro.2011.02.008, / 19 (11). 1180-1188.

Change, I. P. O. C. I.s. (2014). “Climate change”. /,

Chapin Iii, F. S., E. S. Zavaleta, V. T. Eviner, R. L. Naylor, P. M. Vitousek, H. L. Reynolds, D. U. Hooper, S. Lavorel, O. E. Sala, S. E. Hobbie, M. C. Mack ,S. Díazs. (2000). “Consequences of changing biodiversity”. *Nature*. 10.1038/35012241, / 405 234.

Chiang, Y.-M., L.-C. Chang ,F.-J. Changs. (2004). “Comparison of static-feedforward and dynamic-feedback neural networks for rainfall–runoff modeling”. *Journal of hydrology*. 10.1016/j.jhydrol.2003.12.033, / 290 (3-4). 297-311.

Climate change, I. P. O. C.s. (2007). “(Climate change 2007): The physical science basis”. *Agenda*. / 6 (07). 333.

Conway, D.s. (1996). “The impacts of climate variability and future climate change in the Nile Basin on water resources in Egypt”. *International Journal of Water Resources Development*. 10.1080/07900629650178, / 12 (3). 277-296.

Coulibaly, P., Y. B. Dibike ,F. Anctils. (2005). “Downscaling precipitation and temperature with temporal neural networks”. *Journal of Hydrometeorology*. 10.1175/JHM409.1, / 6 (4). 483-496.

Crout, N. M., D. Tarsitano ,A. T. Woods. (2009). “Is my model too complex? Evaluating model formulation using model reduction”. *Environmental Modelling & Software*. 10.1016/j.envsoft.2008.06.004, / 24 (1). 1-7.

Dawson, C. ,R. Wilbys. (2001). “Hydrological modelling using artificial neural networks”. *Progress in physical Geography*. 10.1177/030913330102500104, / 25 (1). 80-108.

Deswal, S. ,M. Pals. (2008). “Artificial neural network based modeling of evaporation losses in reservoirs”. *International Journal of Mathematical, Physical and Engineering Sciences*. / 2 (4). 177-181.

Di Pierro, F., S.-T. Khu, D. Savić ,L. Berardis. (2009). “Efficient multi-objective optimal design of water distribution networks on a budget of simulations using hybrid algorithms”. *Environmental Modelling & Software*. 10.1016/j.envsoft.2008.06.008, / 24 (2). 202-213.

Döll, P.s. (2002). “Impact of climate change and variability on irrigation requirements: a global perspective”. *Climatic change*. 10.1023/A:1016124032231, / 54 (3). 269-293.

Doney, S. C. ,S. F. Sailleys. (2013). “When an ecological regime shift is really just stochastic noise”. *Proceedings of the National Academy of Sciences*. 10.1073/pnas.1222736110, / 110 (7). 2438-2439.

Draper, A. J., M. W. Jenkins, K. W. Kirby, J. R. Lund ,R. E. Howitts. (2003). “Economic-engineering optimization for California water management”. *Journal of water resources planning and management*. 10.1061/(ASCE)0733-9496(2003)129:3(155), / 129 (3). 155-164.

Draper, N. R. ,H. Smith (2014). *Applied regression analysis*. John Wiley & Sons, New Jersey. USA.

Elliott, J., D. Deryng, C. Müller, K. Frieler, M. Konzmann, D. Gerten, M. Glotter, M. Flörke, Y. Wada ,N. Bests. (2014). “Constraints and potentials of future irrigation water availability on agricultural production under climate change”. *Proceedings of the National Academy of Sciences*. 10.1073/pnas.1222474110, / 111 (9). 3239-3244.

Elshorbagy, A., G. Corzo, S. Srinivasulu ,D. Solomatines. (2010). “Experimental investigation of the predictive capabilities of data driven modeling techniques in hydrology-Part 1: Concepts and methodology”. *Hydrology and Earth System Sciences*. 10.5194/hess-14-1931-2010, / 14 (10). 1931-1941.

Falkenmark, M.s. (2013). “Growing water scarcity in agriculture: future challenge to global water security”. *Phil. Trans. R. Soc. A*. 10.1098/rsta.2012.0410, / 371 (2002). 20120410.

Falkenmark, M., A. Berntell, A. Jägerskog, J. Lundqvist, M. Matz ,H. Tropp (2007). *On the verge of a new water scarcity: a call for good governance and human ingenuity*. Stockholm International Water Institute (SIWI), Stockholm, Sweden.

Fang, Q., L. Ma, T. Green, Q. Yu, T. Wang ,L. Ahujas. (2010). “Water resources and water use efficiency in the North China Plain: Current status and agronomic management options”. *Agricultural Water Management*. 10.1016/j.agwat.2010.01.008, / 97 (8). 1102-1116.

Faramarzi, M., K. C. Abbaspour, W. Lu, J. Fennell, A. J. Zehnder ,G. G. Gosss. (2017). “Uncertainty based assessment of dynamic freshwater scarcity in semi-arid watersheds of Alberta, Canada”. *Journal of Hydrology: Regional Studies*. 10.1016/j.ejrh.2016.11.003, / 9 48-68.

Fekete, B. M., D. Wisser, C. Kroeze, E. Mayorga, L. Bouwman, W. M. Wollheim ,C. Vörösmartys. (2010). “Millennium ecosystem assessment scenario drivers (1970–2050): climate and hydrological alterations”. *Global Biogeochemical Cycles*. 10.1029/2009GB003593 /24 (4).

Fernando, T., H. Maier ,G. Dandys. (2009). “Selection of input variables for data driven models: An average shifted histogram partial mutual information estimator approach”. *Journal of Hydrology*. 10.1016/j.jhydrol.2008.10.019, / 367 (3-4). 165-176.

Ferreyra, C., R. C. de Loe ,R. D. Kreutzwisers. (2008). “Imagined communities, contested watersheds: challenges to integrated water resources management in agricultural areas”. *Journal of rural studies*. 10.1016/j.jrurstud.2007.11.001, / 24 (3). 304-321.

Fleming, S. W. ,D. J. Sauchyns. (2013). “Availability, volatility, stability, and teleconnectivity changes in prairie water supply from Canadian Rocky Mountain sources over the last millennium”. *Water Resources Research*. 10.1029/2012WR012831 /49 (1). 64-74.

Forbes, K. A., S. W. Kienzle, C. A. Coburn, J. M. Byrne ,J. Rasmussens. (2011). “Simulating the hydrological response to predicted climate change on a watershed in southern Alberta, Canada”. *Climatic Change*. doi.org/10.1007/s10584-010-9890-x, / 105 (3-4). 555-576.

Garcia-Franco, N., E. Hobley, R. Hübner ,M. Wiesmeier (2018). "Climate-Smart Soil Management in Semiarid Regions". *Soil Management and Climate Change*. Elsevier**:** 349-368.

Gardner, M. W. ,S. Dorlings. (1998). “Artificial neural networks (the multilayer perceptron)—a review of applications in the atmospheric sciences”. *Atmospheric environment*. 10.1016/S1352-2310(97)00447-0, / 32 (14-15). 2627-2636.

Gemenne, F., J. Barnett, W. N. Adger ,G. D. Dabelkos. (2014). “Climate and security: evidence, emerging risks, and a new agenda”. 10.1007/s10584-014-1074-7, / 123 (1).

Genest, C. ,A.-C. Favres. (2007). “Everything you always wanted to know about copula modeling but were afraid to ask”. *Journal of hydrologic engineering*. 10.1061/(ASCE)1084-0699(2007)12:4(347), / 12 (4). 347-368.

George, B., H. Malano, B. Davidson, P. Hellegers, L. Bharati ,S. Massuels. (2011). “An integrated hydro-economic modelling framework to evaluate water allocation strategies II: Scenario assessment”. *Agricultural Water Management*. 10.1016/j.agwat.2010.12.005, / 98 (5). 747-758.

Giles, D. E., H. Feng ,R. T. Godwins. (2016). “Bias-corrected maximum likelihood estimation of the parameters of the generalized Pareto distribution”. *Communications in Statistics-Theory and Methods*. 10.1080/03610926.2014.887104, / 45 (8). 2465-2483.

Giordano, M. ,T. Shahs. (2014). “From IWRM back to integrated water resources management”. *International Journal of Water Resources Development*. 10.1080/07900627.2013.851521, / 30 (3). 364-376.

Gleick, P. H.s. (1998). “Water in crisis: paths to sustainable water use”. *Ecological applications*. 10.1890/1051-0761(1998)008[0571:WICPTS]2.0.CO;2, / 8 (3). 571-579.

Gober, P., C. W. Kirkwood, R. C. Balling, A. W. Ellis ,S. Deitricks. (2010). “Water planning under climatic uncertainty in Phoenix: Why we need a new paradigm”. *Annals of the Association of American Geographers*. 10.1080/00045601003595420, / 100 (2). 356-372.

Gober, P. ,H. Wheaters. (2014). “Socio-hydrology and the science–policy interface: a case study of the Saskatchewan River basin”. *Hydrology and Earth System Sciences*. 10.5194/hess-18-1413-2014, / 18 (4). 1413-1422.

Gosain, A., S. Rao ,D. Basurays. (2006). “Climate change impact assessment on hydrology of Indian river basins”. *Current science*. /, 346-353.

Graveline, N., B. Majone, R. Van Duinen ,E. Ansinks. (2014). “Hydro-economic modeling of water scarcity under global change: an application to the Gállego river basin (Spain)”. *Regional environmental change*. 10.1007/s10113-013-0472-0, / 14 (1). 119-132.

Guan, D. ,K. Hubaceks. (2008). “A new and integrated hydro-economic accounting and analytical framework for water resources: A case study for North China”. *Journal of Environmental Management*. 10.1016/j.jenvman.2007.07.010, / 88 (4). 1300-1313.

Haddeland, I., J. Heinke, H. Biemans, S. Eisner, M. Flörke, N. Hanasaki, M. Konzmann, F. Ludwig, Y. Masaki ,J. Schewes. (2014). "Global water resources affected by human interventions and climate change". *Proceedings of the National Academy of Sciences*. 10.1073/pnas.1222475110, / 111 (9). 3251-3256.

Hall, J. ,E. Borgomeos. (2013). "Risk-based principles for defining and managing water security". *Phil. Trans. R. Soc. A*. / 371 (2002). 20120407.

Hamilton, S. H., S. ElSawah, J. H. Guillaume, A. J. Jakeman ,S. A. Pierces. (2015). "Integrated assessment and modelling: overview and synthesis of salient dimensions". *Environmental Modelling & Software*. 10.1016/j.envsoft.2014.12.005, / 64 215-229.

Harou, J. J., M. Pulido-Velazquez, D. E. Rosenberg, J. Medellín-Azuara, J. R. Lund ,R. E. Howitts. (2009). "Hydro-economic models: Concepts, design, applications, and future prospects". *Journal of Hydrology*. 10.1016/j.jhydrol.2009.06.037, / 375 (3-4). 627-643.

Hassanzadeh, E., A. Elshorbagy, H. Wheater ,P. Gobers. (2014). "Managing water in complex systems: An integrated water resources model for Saskatchewan, Canada". *Environmental Modelling & Software*. 10.1016/j.envsoft.2014.03.015, / 58 12-26.

Hassanzadeh, E., A. Nazemi ,A. Elshorbagys. (2013). "Quantile-based downscaling of precipitation using genetic programming: application to IDF curves in Saskatoon". *Journal of Hydrologic Engineering*. 10.1061/(ASCE)HE.1943-5584.0000854, / 19 (5). 943-955.

He, L., B. Chapron, J. Tournadre ,R. Fablet (2014). Statistical emulation of high-resolution sar wind fields from low-resolution model predictions. *Geoscience and Remote Sensing Symposium (IGARSS), 2014 IEEE International*, Quebec City, QC, Canada, IEEE. DOI: 10.1109/IGARSS.2014.6947340.

He, L., R. Fablet, B. Chapron ,J. Tournadres. (2015). "Learning-based emulation of sea surface wind fields from numerical model outputs and SAR data". *IEEE Journal of Selected Topics in Applied Earth Observations and Remote Sensing*. 10.1109/JSTARS.2015.2496503, / 8 (10). 4742-4750.

Heinz, I., M. Pulido-Velazquez, J. Lund ,J. Andreus. (2007). "Hydro-economic modeling in river basin management: implications and applications for the European water framework directive". *Water resources management*. 10.1007/s11269-006-9101-8, / 21 (7). 1103-1125.

Herman, J. D., P. M. Reed, H. B. Zeff ,G. W. Charackliss. (2015). “How should robustness be defined for water systems planning under change?”. *Journal of Water Resources Planning and Management*. 10.1061/(ASCE)WR.1943-5452.0000509, / 141 (10). 04015012.

Herrera-Pantoja, M. ,K. Hiscocks. (2015). “Projected impacts of climate change on water availability indicators in a semi-arid region of central Mexico”. *Environmental Science & Policy*. 10.1016/j.envsci.2015.06.020, / 54 81-89.

Hipel, K., A. Miall ,D. Smith (2011). Water resources in Canada: a strategic viewpoint *Report to the Inter American National Academies of Science (IANAS)*. USA.

Hornik, K., M. Stinchcombe ,H. Whites. (1989). “Multilayer feedforward networks are universal approximators”. *Neural networks*. 10.1016/0893-6080(89)90020-8, / 2 (5). 359-366.

House, L.s. (2011). “Verifying Reification With Application to a Rainfall–Runoff Computer Simulator”. *Journal of agricultural, biological, and environmental statistics*. 10.1007/s13253-011-0075-5, / 16 (4). 513-530.

Hsiang, S., R. Kopp, A. Jina, J. Rising, M. Delgado, S. Mohan, D. Rasmussen, R. Muir-Wood, P. Wilson ,M. Oppenheimers. (2017). “Estimating economic damage from climate change in the United States”. *Science*. / 356 (6345). 1362-1369.

Hsu, K. l., H. V. Gupta ,S. Sorooshians. (1995). “Artificial neural network modeling of the rainfall-runoff process”. *Water resources research*. 10.1029/95WR01955, / 31 (10). 2517-2530.

Hurrell, J. W. ,C. Desers. (2010). “North Atlantic climate variability: the role of the North Atlantic Oscillation”. *Journal of Marine Systems*. 10.1016/j.jmarsys.2009.11.002, / 79 (3-4). 231-244.

IPCC (2007). Freshwater Resources and their management. In Climate Change 2007: Impacts,

Adaptation and Vulnerability. Contribution of Working Group II to the Fourth Assessment

Report of the Intergovernmental Panel on Climate Change, 173-210. Cambridge, UK: Cambridge University Press.

Ireson, A., A. Barr, J. Johnstone, S. Mamet, G. Van der Kamp, C. Whitfield, N. Michel, R. North, C. Westbrook ,C. DeBeers. (2015). “The changing water cycle: the Boreal Plains

ecozone of Western Canada". *Wiley Interdisciplinary Reviews: Water*. 10.1002/wat2.1098 /2(5). 505-521.

Jackson, R. B., S. R. Carpenter, C. N. Dahm, D. M. McKnight, R. J. Naiman, S. L. Postel ,S. W. Runnings. (2001). "Water in a changing world". *Ecological applications*. 10.1890/1051-0761(2001)011[1027:WIACW]2.0.CO;2, / 11 (4). 1027-1045.

Jain, A. ,A. M. Kumars. (2007). "Hybrid neural network models for hydrologic time series forecasting". *Applied Soft Computing*. 10.1016/j.asoc.2006.03.002, / 7 (2). 585-592.

Janicot, S., V. Moron ,B. Fontaines. (1996). "Sahel droughts and ENSO dynamics". *Geophysical Research Letters*. 10.1029/96GL00246 /23 (5). 515-518.

Jenkins, G. ,J. Lowes. (2003). "Handling uncertainties in the UKCIP02 scenarios of climate change". *Hadley Centre, Technical note 44, Exeter, UK*. /,

Kalbus, E., T. Kalbacher, O. Kolditz, E. Krüger, J. Seegert, G. Röstel, G. Teutsch, D. Borchardt ,P. Krebs (2012). Integrated water resources management under different hydrological, climatic and socio-economic conditions, Springer, 10.1007/s12665-011-1330-3.

Kelly, R. A., A. J. Jakeman, O. Barreteau, M. E. Borsuk, S. ElSawah, S. H. Hamilton, H. J. Henriksen, S. Kuikka, H. R. Maier ,A. E. Rizzolis. (2013). "Selecting among five common modelling approaches for integrated environmental assessment and management". *Environmental modelling & software*. 10.1016/j.envsoft.2013.05.005, / 47 159-181.

Kirk, O., T. V. Borchert ,C. C. Fuglsangs. (2002). "Industrial enzyme applications". *Current opinion in biotechnology*. 10.1016/S0958-1669(02)00328-2, / 13 (4). 345-351.

Krausmann, F., S. Gingrich, N. Eisenmenger, K.-H. Erb, H. Haberl ,M. Fischer-Kowalskis. (2009). "Growth in global materials use, GDP and population during the 20th century". *Ecological Economics*. 10.1016/j.ecolecon.2009.05.007 /68 (10). 2696-2705.

Kundzewicz, Z., V. Krysanova, R. Benestad, Ø. Hov, M. Piniewski ,I. Ottos. (2018). "Uncertainty in climate change impacts on water resources". *Environmental Science & Policy*. 10.1016/j.envsci.2017.10.008, / 79 1-8.

Kusangaya, S., M. L. Warburton, E. A. Van Garderen ,G. P. Jewitts. (2014). "Impacts of climate change on water resources in southern Africa: A review". *Physics and Chemistry of the Earth, Parts A/B/C*. 10.1016/j.pce.2013.09.014, / 67 47-54.

Lam, D., L. Leon, S. Hamilton, N. Crookshank, D. Bonin ,D. Swaynes. (2004). “Multi-model integration in a decision support system: a technical user interface approach for watershed and lake management scenarios”. *Environmental Modelling & Software*. 10.1016/S1364-8152(03)00156-7, / 19 (3). 317-324.

Lee, J.-Y. ,B. Wangs. (2014). “Future change of global monsoon in the CMIP5”. *Climate Dynamics*. doi.org/10.1007/s00382-012-1564-0, / 42 (1-2). 101-119.

Lemieux, C. J., J. Thompson, D. S. Slocombe ,R. Schusters. (2015). “Climate change collaboration among natural resource management agencies: lessons learned from two US regions”. *Journal of Environmental Planning and Management*. / 58 (4). 654-677.

Loucks, D. P., E. Van Beek, J. R. Stedinger, J. P. Dijkman ,M. T. Villars (2005). *Water resources systems planning and management: an introduction to methods, models and applications*. Paris: Unesco.

Machac, D., P. Reichert ,C. Alberts. (2016). “Emulation of dynamic simulators with application to hydrology”. *Journal of Computational Physics*. 10.1016/j.jcp.2016.02.046, / 313 352-366.

Maier, H. R. ,G. C. Dandys. (2000). “Neural networks for the prediction and forecasting of water resources variables: a review of modelling issues and applications”. *Environmental modelling & software*. 10.1016/S1364-8152(99)00007-9, / 15 (1). 101-124.

Malik, A. ,A. Kumars. (2015). “Pan evaporation simulation based on daily meteorological data using soft computing techniques and multiple linear regression”. *Water resources management*. 10.1007/s11269-015-0915-0, / 29 (6). 1859-1872.

Marques, G. F., J. R. Lund, M. R. Leu, M. Jenkins, R. Howitt, T. Harter, S. Hatchett, N. Ruud ,S. Burkes. (2006). “Economically driven simulation of regional water systems: Friant-Kern, California”. *Journal of Water Resources Planning and Management*. 10.1061/(ASCE)0733-9496(2006)132:6(468), / 132 (6). 468-479.

May, R., G. Dandy ,H. Maier (2011). "Review of input variable selection methods for artificial neural networks". *Artificial neural networks-methodological advances and biomedical applications*. InTech Rijeka, Croatia.

McDonald, R. I., P. Green, D. Balk, B. M. Fekete, C. Revenga, M. Todd ,M. Montgomerys. (2011). “Urban growth, climate change, and freshwater availability”. *Proceedings of the National Academy of Sciences*. 10.1073/pnas.1011615108, / 108 (15). 6312-6317.

McIntosh, B. S., J. C. Ascough II, M. Twery, J. Chew, A. Elmahdi, D. Haase, J. J. Harou, D. Hepting, S. Cuddy ,A. J. Jakemans. (2011). “Environmental decision support systems (EDSS) development–challenges and best practices”. *Environmental Modelling & Software*. 10.1016/j.envsoft.2011.09.009, / 26 (12). 1389-1402.

Mekonnen, B. A., A. Nazemi, K. A. Mazurek, A. Elshorbagy ,G. Putzs. (2015). “Hybrid modelling approach to prairie hydrology: fusing data-driven and process-based hydrological models”. *Hydrological sciences journal*. 10.1080/02626667.2014.935778, / 60 (9). 1473-1489.

Mekonnen, M. M. ,A. Y. Hoekstras. (2016). “Four billion people facing severe water scarcity”. *Science advances*. 10.1126/sciadv.1500323, / 2 (2). e1500323.

Merritt, W. S., Y. Alila, M. Barton, B. Taylor, S. Cohen ,D. Neilsens. (2006). “Hydrologic response to scenarios of climate change in sub watersheds of the Okanagan basin, British Columbia”. *Journal of Hydrology*. / 326 (1-4). 79-108.

Mogaji, K. A., H. San Lim ,K. Abdullahs. (2015). “Modeling of groundwater recharge using a multiple linear regression (MLR) recharge model developed from geophysical parameters: a case of groundwater resources management”. *Environmental Earth Sciences*. 10.1007/s12665-014-3476-2, / 73 (3). 1217-1230.

Moghaddasi, M., S. Morid, S. Araghinejad ,M. A. Alikhanis. (2010). “Assessment of irrigation water allocation based on optimization and equitable water reduction approaches to reduce agricultural drought losses: The 1999 drought in the Zayandeh Rud irrigation system (Iran)”. *Irrigation and drainage*. 10.1002/ird.499 /59 (4). 377-387.

Molina, J.-L., J. L. García-Aróstegui, J. Bromley ,J. Benaventes. (2011). “Integrated assessment of the European WFD implementation in extremely overexploited aquifers through participatory modelling”. *Water Resources Management*. 10.1007/s11269-011-9859-1, / 25 (13). 3343-3370.

Molina, J., J. Bromley, J. García-Aróstegui, C. Sullivan ,J. Benaventes. (2010). “Integrated water resources management of overexploited hydrogeological systems using Object-Oriented

Bayesian Networks". *Environmental Modelling & Software*. 10.1016/j.envsoft.2009.10.007, / 25 (4). 383-397.

Moursi, H., D. Kim ,J. J. Kaluarachchis. (2017). "A probabilistic assessment of agricultural water scarcity in a semi-arid and snowmelt-dominated river basin under climate change". *Agricultural Water Management*. / 193 142-152.

Nash, J. E. ,J. V. Sutcliffes. (1970). "River flow forecasting through conceptual models part I—A discussion of principles". *Journal of hydrology*. 10.1016/0022-1694(70)90255-6, / 10 (3). 282-290.

Nazemi, A. ,K. Madanis. (2017). "Urban water security: Emerging discussion and remaining challenges". *Sustainable Cities and Society*. 10.1016/j.scs.2017.09.011, /, 10.1016/j.scs.2017.09.011

Nazemi, A. ,H. S. Wheaters. (2014). "How can the uncertainty in the natural inflow regime propagate into the assessment of water resource systems?". *Advances in water resources*. 10.1016/j.advwatres.2013.11.009, / 63 131-142.

Nazemi, A. ,H. S. Wheaters. (2015a). "On inclusion of water resource management in Earth system models–Part 1: Problem definition and representation of water demand". *Hydrology and Earth System Sciences*. 10.5194/hess-19-33-2015, / 19 (1). 33-61.

Nazemi, A. ,H. S. Wheaters. (2015b). "On inclusion of water resource management in Earth system models–Part 2: Representation of water supply and allocation and opportunities for improved modeling". *Hydrology and Earth System Sciences*. 10.5194/hess-19-63-2015, / 19 (1). 63-90.

Nazemi, A., H. S. Wheater, K. P. Chun, B. Bonsal ,M. Mekonnens. (2017). "Forms and drivers of annual streamflow variability in the headwaters of Canadian Prairies during the 20th century". *Hydrological processes*. / 31 (1). 221-239.

Nazemi, A., H. S. Wheater, K. P. Chun ,A. Elshorbagys. (2013). "A stochastic reconstruction framework for analysis of water resource system vulnerability to climate-induced changes in river flow regime". *Water Resources Research*. 10.1029/2012WR012755 /49 (1). 291-305.

Nicol, L. A. ,K. Kleins. (2006). "Water market characteristics: Results from a survey of southern Alberta irrigators". *Canadian Water Resources Journal*. 10.4296/cwrj3102091, / 31 (2). 91-104.

Nikolic, V. V., S. P. Simonovic ,D. B. Milicevics. (2013). “Analytical support for integrated water resources management: a new method for addressing spatial and temporal variability”. *Water resources management*. 10.1007/s11269-012-0193-z, / 27 (2). 401-417.

Oki, T. ,S. Kanaes. (2006). “Global hydrological cycles and world water resources”. *science*. 10.1126/science.1128845, / 313 (5790). 1068-1072.

Olmstead, S. M.s. (2014). “Climate change adaptation and water resource management: a review of the literature”. *Energy Economics*. / 46 500-509.

Pahl-Wostl, C. (2003). The importance of the human dimension in integrated assessment models and processes: actor based analysis and modeling approaches. *Proceedings of the modelling and simulation society of Australia and New Zealand, MODSIM*, Citeseer.

Pahl-Wostl, C.s. (2007). “The implications of complexity for integrated resources management”. *Environmental Modelling & Software*. 10.1016/j.envsoft.2005.12.024, / 22 (5). 561-569.

Parry, M., O. Canziani, J. Palutikof, P. J. van der Linden ,C. E. Hanson (2007). *Climate change 2007: impacts, adaptation and vulnerability*. Cambridge University Press. , U.K.

Pechlivanidis, I., B. Jackson, N. McIntyre ,H. Wheaters. (2011). “Catchment scale hydrological modelling: a review of model types, calibration approaches and uncertainty analysis methods in the context of recent developments in technology and applications”. *Global NEST journal*. / 13 (3). 193-214.

Petersen-Perlman, J. D., J. C. Veilleux ,A. T. Wolfs. (2017). “International water conflict and cooperation: challenges and opportunities”. *Water International*. 10.1080/02508060.2017.1276041, / 42 (2). 105-120.

Phillips, J. R.s. (2003). “Projection-based approaches for model reduction of weakly nonlinear, time-varying systems”. *IEEE Transactions on computer-aided design of integrated circuits and systems*. 10.1109/TCAD.2002.806605, / 22 (2). 171-187.

Piani, C., G. Weedon, M. Best, S. Gomes, P. Viterbo, S. Hagemann ,J. Haerters. (2010). “Statistical bias correction of global simulated daily precipitation and temperature for the application of hydrological models”. *Journal of hydrology*. 10.1016/j.jhydrol.2010.10.024, / 395 (3-4). 199-215.

Prowse, T., S. Beltaos, J. Gardner, J. Gibson, R. Granger, R. Leconte, D. Peters, A. Pietroniro, L. Romolo ,B. Toths. (2006). “Climate change, flow regulation and land-use effects on the hydrology of the Peace-Athabasca-Slave system; Findings from the Northern Rivers Ecosystem Initiative”. *Environmental Monitoring and Assessment*. 10.1007/s10661-005-9080-x, / 113 (1-3). 167-197.

Prudhomme, C., R. Wilby, S. Crooks, A. Kay ,N. Reynards. (2010). “Scenario-neutral approach to climate change impact studies: application to flood risk”. *Journal of Hydrology*. 10.1016/j.jhydrol.2010.06.043, / 390 (3-4). 198-209.

Qin, H.-P., Q. Su ,S.-T. Khus. (2011). “An integrated model for water management in a rapidly urbanizing catchment”. *Environmental Modelling & Software*. 10.1016/j.envsoft.2011.07.003, / 26 (12). 1502-1514.

Ratto, M., A. Castelletti ,A. Paganos. (2012). “Emulation techniques for the reduction and sensitivity analysis of complex environmental models”. *Environmental Modelling & Software*. 10.1016/j.envsoft.2011.11.003, / 34 1-4.

Ratto, M., A. Pagano ,P. Youngs. (2007). “State dependent parameter metamodelling and sensitivity analysis”. *Computer Physics Communications*. 10.1016/j.cpc.2007.07.011, / 177 (11). 863-876.

Razavi, S., B. A. Tolson ,D. H. Burns. (2012). “Review of surrogate modeling in water resources”. *Water Resources Research*. 10.1029/2011WR011527 /48 (7).

Renard, B., D. Kavetski, G. Kuczera, M. Thyer ,S. W. Frankss. (2010). “Understanding predictive uncertainty in hydrologic modeling: The challenge of identifying input and structural errors”. *Water Resources Research*. 10.1029/2009WR008328, / 46 (5).

Riedmiller, M. ,H. Braun (1993). A direct adaptive method for faster backpropagation learning: The RPROP algorithm. *Neural Networks, 1993., IEEE International Conference on*, IEEE. DOI: 10.1109/ICNN.1993.298623.

Rood, S. B. ,W. Tymensen (2001). *Recreational Flows for paddling along rivers in southern Alberta*. Government of Alberta, Lethbridge, AB, Canada.

Rudnyi, E. B. ,J. G. Korvinks. (2002). “Automatic Model Reduction for Transient Simulation of MEMS-based Devices”. *Sensors update*. 10.1002/seup.200211105 /11 (1). 3-33.

Russell, S. J. ,P. Norvig (2016). *Artificial intelligence: a modern approach*. Malaysia; Pearson Education Limited, Malaysia.

Schaap, M. G., F. J. Leij ,M. T. Van Genuchtens. (1998). "Neural network analysis for hierarchical prediction of soil hydraulic properties". *Soil Science Society of America Journal*. 10.2136/sssaj1998.03615995006200040001x, / 62 (4). 847-855.

Schewe, J., J. Heinke, D. Gerten, I. Haddeland, N. W. Arnell, D. B. Clark, R. Dankers, S. Eisner, B. M. Fekete ,F. J. Colón-Gonzálezs. (2014). "Multimodel assessment of water scarcity under climate change". *Proceedings of the National Academy of Sciences*. 10.1073/pnas.1222460110, / 111 (9). 3245-3250.

Schindler, D. W. ,W. F. Donahues. (2006). "An impending water crisis in Canada's western prairie provinces". *Proceedings of the National Academy of Sciences*. 10.1073/pnas.0601568103, / 103 (19). 7210-7216.

Schreinemachers, P. ,T. Bergers. (2011). "An agent-based simulation model of human–environment interactions in agricultural systems". *Environmental Modelling & Software*. 10.1016/j.envsoft.2011.02.004, / 26 (7). 845-859.

Selby, J. ,C. Hoffmanns. (2014). "Beyond scarcity: rethinking water, climate change and conflict in the Sudans". *Global Environmental Change*. 10.1016/j.gloenvcha.2014.01.008, / 29 360-370.

Shaw, A. R., H. Smith Sawyer, E. J. LeBoeuf, M. P. McDonald ,B. Hadjeriouas. (2017). "Hydropower Optimization Using Artificial Neural Network Surrogate Models of a High-Fidelity Hydrodynamics and Water Quality Model". *Water Resources Research*. doi.org/10.1002/2017WR021039, / 53 (11). 9444-9461.

Sheffield, J., K. M. Andreadis, E. F. Wood ,D. P. Lettenmaiers. (2009). "Global and continental drought in the second half of the twentieth century: Severity–area–duration analysis and temporal variability of large-scale events". *Journal of Climate*. / 22 (8). 1962-1981.

Shpyth, A. A.s. (1991). "An ex-post evaluation of enviromental impact assessment in Alberta: A case study of the Oldman River Dam". *Canadian Water Resources Journal*. 10.4296/cwrj1604367, / 16 (4). 367-379.

Siade, A. J., M. Putti ,W. W. G. Yehs. (2010). “Snapshot selection for groundwater model reduction using proper orthogonal decomposition”. *Water Resources Research*. 10.1029/2009WR008792, / 46 (8).

Simonovic, S. P. (2012). "General Systems Theory". *Managing water resources: methods and tools for a systems approach*. Routledge U.K. and USA 4**:** 65-111.

Smith, R. L., C. Tebaldi, D. Nychka ,L. O. Mearnss. (2009). “Bayesian modeling of uncertainty in ensembles of climate models”. *Journal of the American Statistical Association*. 10.1198/jasa.2009.0007, / 104 (485). 97-116.

Solomon, S., Qin, D., Manning, M., Chen, Z., Marquis, M., Averyt, K. B., ... & Miller, H. L. (2007). IPCC, 2007: *Climate Change 2007: The Physical Science Basis. Contribution of Working Group I to the Fourth Assessment. Report of the Intergovernmental Panel on Climate Change* (0521705967). Cambridge, United Kingdom and New York, NY, USA.

South Saskatchewan Regional Plan (2010). ISBN No. 978-0-7785-9165-8. Pub No. I/457. Printed July 2010.

Stainforth, D. A., T. E. Downing, R. Washington, A. Lopez ,M. News. (2007). “Issues in the interpretation of climate model ensembles to inform decisions”. *Philosophical Transactions of the Royal Society of London A: Mathematical, Physical and Engineering Sciences*. 10.1098/rsta.2007.2073, / 365 (1857). 2163-2177.

Sterman, J. D. (2000). *Business dynamics: systems thinking and modeling for a complex world*. McGraw-Hill Education, Boston, USA.

Stewart, I. T., D. R. Cayan ,M. D. Dettingers. (2005). “Changes toward earlier streamflow timing across western North America”. *Journal of climate*. / 18 (8). 1136-1155.

Sušnik, J., L. S. Vamvakeridou-Lyroudia, N. Baumert, J. Kloos, F. G. Renaud, I. La Jeunesse, B. Mabrouk, D. A. Savić, Z. Kapelan ,R. Ludwigs. (2015). “Interdisciplinary assessment of sea-level rise and climate change impacts on the lower Nile delta, Egypt”. *Science of the Total Environment*. 10.1016/j.scitotenv.2014.06.111, / 503-504 279-288.

Tanzeeba, S. ,T. Y. Gans. (2012). “Potential impact of climate change on the water availability of South Saskatchewan River Basin”. *Climatic Change*. 10.1007/s10584-011-0221-7, / 112 (2). 355-386.

The Global Water Partnership (2000). *Integrated Water Resources Management. (TAC background paper; no. 4)* Stockholm, Sweden The Global Water Partnership

Tilman, D.s. (1999). "Global environmental impacts of agricultural expansion: the need for sustainable and efficient practices". *Proceedings of the National Academy of Sciences*. 10.1073/pnas.96.11.5995, / 96 (11). 5995-6000.

Tranmer, M. ,M. Elliots. (2008). "Multiple linear regression". *The Cathie Marsh Centre for Census and Survey Research (CCSR)*. / 5 30-35.

Van Delden, H., M. Kirkby ,B. Hahn (2009). Towards a modelling framework for integrated assessment in arid and semi-arid regions. *International Congress on Modelling and Simulation. Modelling and Simulation Society of Australia and New Zealand and International Association for Mathematics and Computers in Simulation*, Leeds.

van der Merwe, R., T. K. Leen, Z. Lu, S. Frolov ,A. M. Baptistas. (2007). "Fast neural network surrogates for very high dimensional physics-based models in computational oceanography". *Neural Networks*. 10.1016/j.neunet.2007.04.023, / 20 (4). 462-478.

Vano, J. A., M. J. Scott, N. Voisin, C. O. Stöckle, A. F. Hamlet, K. E. Mickelson, M. M. Elsner ,D. P. Lettenmaiers. (2010). "Climate change impacts on water management and irrigated agriculture in the Yakima River Basin, Washington, USA". *Climatic Change*. 10.1007/s10584-010-9856-z, / 102 (1-2). 287-317.

Varela-Ortega, C., I. Blanco-Gutiérrez, C. H. Swartz ,T. E. Downings. (2011). "Balancing groundwater conservation and rural livelihoods under water and climate uncertainties: An integrated hydro-economic modeling framework". *Global Environmental Change*. 10.1016/j.gloenvcha.2010.12.001, / 21 (2). 604-619.

Vasseur, D. A., J. P. DeLong, B. Gilbert, H. S. Greig, C. D. Harley, K. S. McCann, V. Savage, T. D. Tunney ,M. I. O'Connors. (2014). "Increased temperature variation poses a greater risk to species than climate warming". *Proceedings of the Royal Society of London B: Biological Sciences*. / 281 (1779). 20132612.

Vicuna, S., J. A. Dracup, J. R. Lund, L. L. Dale ,E. P. Maurers. (2010). "Basin-scale water system operations with uncertain future climate conditions: Methodology and case studies". *Water Resources Research*. 10.1029/2009WR007838 /46 (4).

Vitousek, P. M., H. A. Mooney, J. Lubchenco ,J. M. Melillos. (1997). “Human domination of Earth's ecosystems”. *Science*. 10.1126/science.277.5325.494, / 277 (5325). 494-499.

Vörösmarty, C. J., P. Green, J. Salisbury ,R. B. Lammerss. (2000). “Global water resources: vulnerability from climate change and population growth”. *science*. 10.1126/science.289.5477.284, / 289 (5477). 284-288.

Vörösmarty, C. J., P. B. McIntyre, M. O. Gessner, D. Dudgeon, A. Prusevich, P. Green, S. Glidden, S. E. Bunn, C. A. Sullivan ,C. R. Liermanns. (2010). “Global threats to human water security and river biodiversity”. *Nature*. 10.1038/nature09440, / 467 (7315). 555.

Vörösmarty, C. J. ,D. Sahagians. (2000). “Anthropogenic disturbance of the terrestrial water cycle”. *AIBS Bulletin*. 10.1641/0006-3568(2000)050[0753:ADOTTW]2.0.CO;2, / 50 (9). 753-765.

Wada, Y., D. Wisser, S. Eisner, M. Flörke, D. Gerten, I. Haddeland, N. Hanasaki, Y. Masaki, F. T. Portmann ,T. Stackes. (2013). “Multimodel projections and uncertainties of irrigation water demand under climate change”. *Geophysical Research Letters*. 10.1002/grl.50686, / 40 (17). 4626-4632.

Wang, X.-j., J.-y. Zhang, S. Shahid, E.-h. Guan, Y.-x. Wu, J. Gao ,R.-m. Hes. (2016). “Adaptation to climate change impacts on water demand”. *Mitigation and Adaptation Strategies for Global Change*. 10.1007/s11027-014-9571-6, / 21 (1). 81-99.

Wang, X., Y. Sun, L. Song ,C. Meis. (2009). “An eco-environmental water demand based model for optimising water resources using hybrid genetic simulated annealing algorithms. Part I. Model development”. *Journal of environmental management*. 10.1016/j.jenvman.2009.02.008, / 90 (8). 2628-2635.

Werritty, A.s. (2002). “Living with uncertainty: climate change, river flows and water resource management in Scotland”. *Science of the Total Environment*. 10.1016/S0048-9697(02)00050-5, / 294 (1-3). 29-40.

Wheater, H. ,P. Gobers. (2013). “Water security in the Canadian Prairies: science and management challenges”. *Phil. Trans. R. Soc. A*. 10.1098/rsta.2012.0409, / 371 (2002). 20120409.

Wheater, H., A. Jakeman ,K. Bevens. (1993). “Progress and directions in rainfall-runoff modelling”. /,

Wheaton, E., S. Kulshreshtha, V. Wittrock ,G. Koshidas. (2008). “Dry times: hard lessons from the Canadian drought of 2001 and 2002”. *The Canadian Geographer/Le Géographe canadien*. / 52 (2). 241-262.

Wilby, R. L., C. W. Dawson ,E. M. Barrows. (2002). “SDSM—a decision support tool for the assessment of regional climate change impacts”. *Environmental Modelling & Software*. 10.1016/S1364-8152(01)00060-3, / 17 (2). 145-157.

Wiley, M. W. ,R. N. Palmers. (2008). “Estimating the impacts and uncertainty of climate change on a municipal water supply system”. *Journal of Water Resources Planning and Management*. 10.1061/(ASCE)0733-9496(2008)134:3(239), / 134 (3). 239-246.

Wu, W., G. C. Dandy ,H. R. Maiers. (2014). “Protocol for developing ANN models and its application to the assessment of the quality of the ANN model development process in drinking water quality modelling”. *Environmental Modelling & Software*. 10.1016/j.envsoft.2013.12.016, / 54 108-127.

Xue, J., D. Gui, J. Lei, F. Zeng, D. Mao ,Z. Zhangs. (2017). “Model development of a participatory Bayesian network for coupling ecosystem services into integrated water resources management”. *Journal of Hydrology*. 10.1016/j.jhydrol.2017.08.045, / 554 50-65.

Appendix

Data used in this study

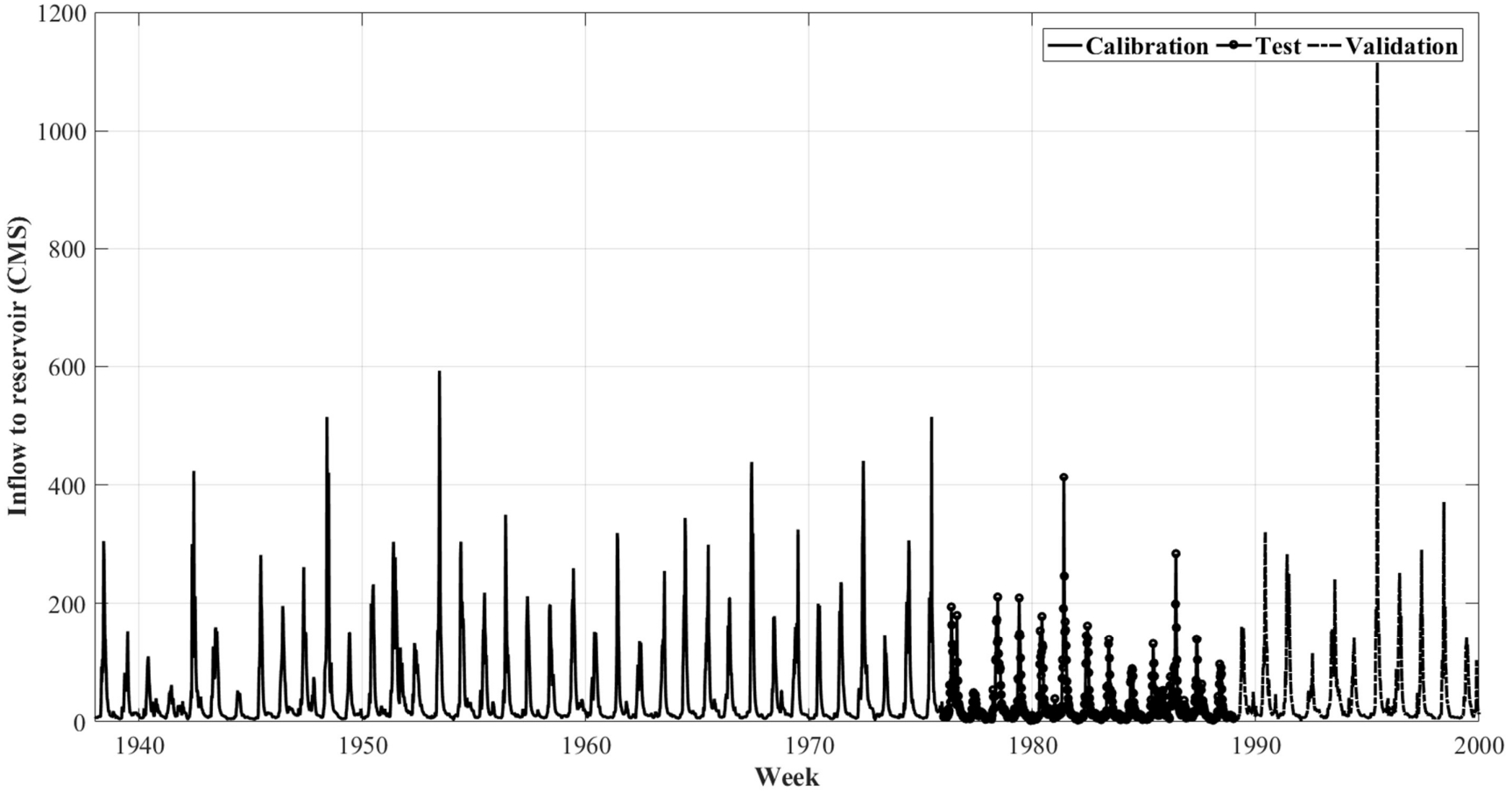

Fig. A1. Weekly WRMM inflow time series for 63 years spanning from January 1938 to December 2000.

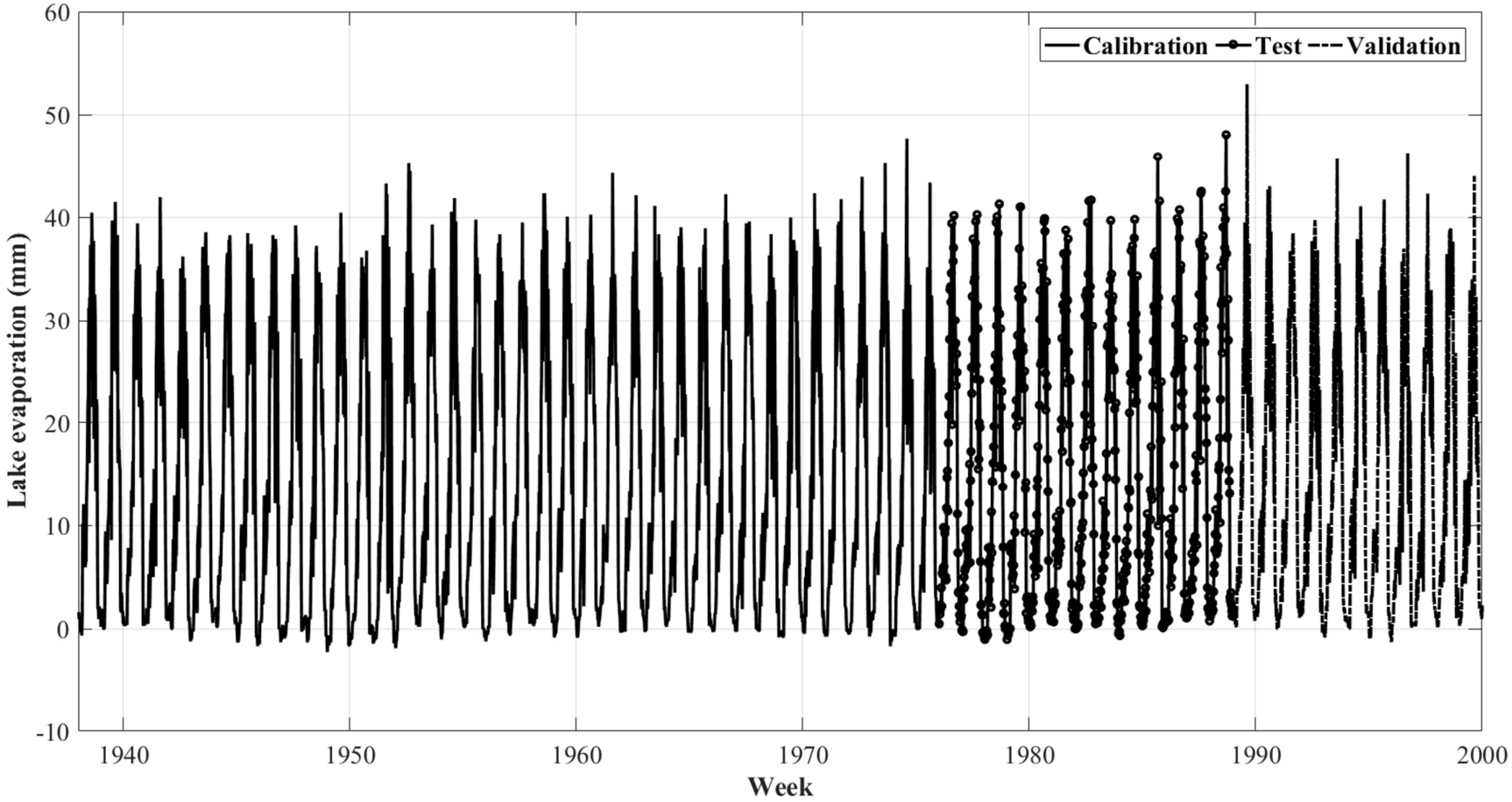

Fig. A2. Weekly WRMM Lake evaporation time series for 63 years spanning from January 1938 to December 2000.

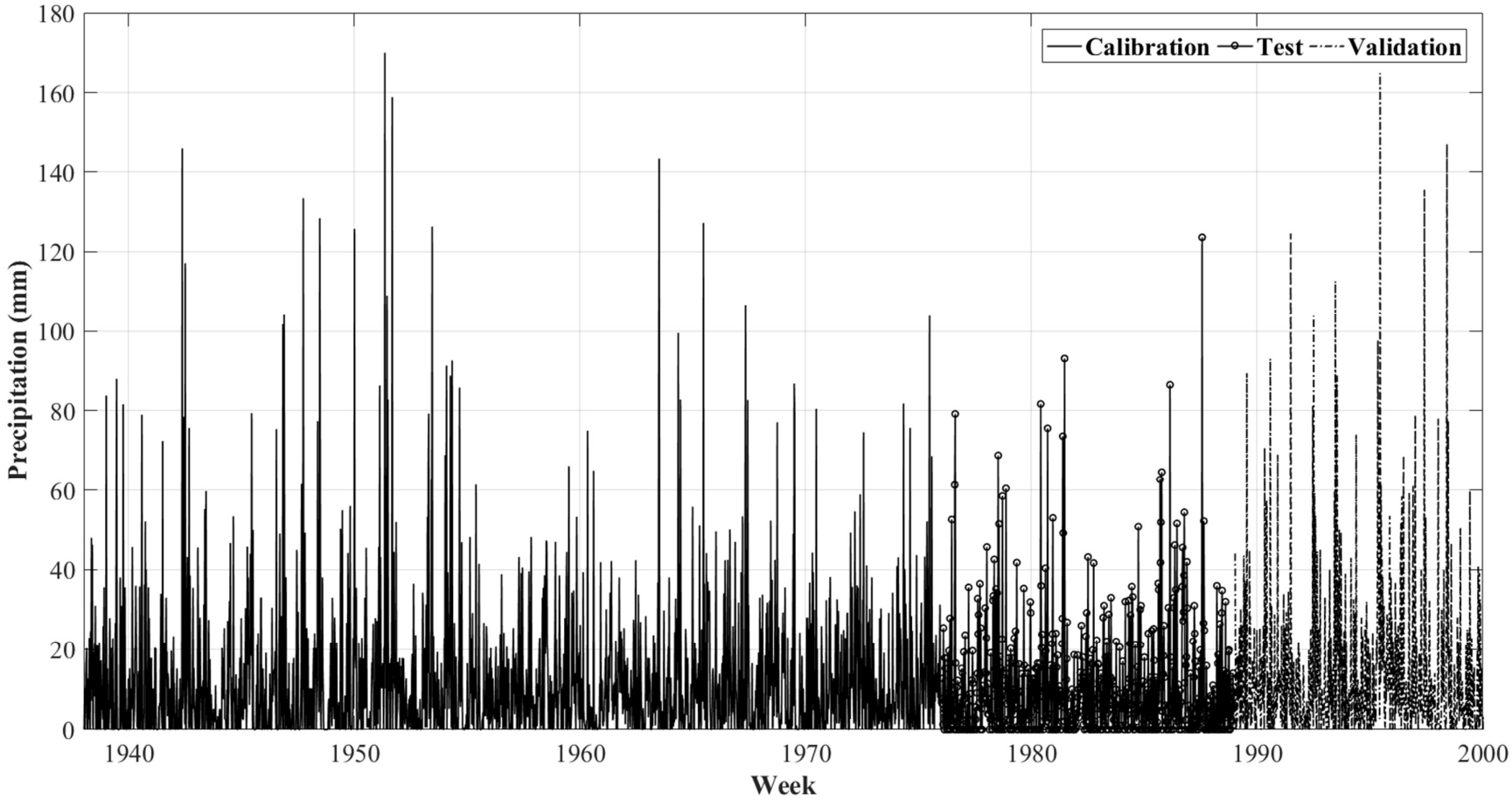

Fig. A3. Weekly WRMM Precipitation time series for 63 years spanning from January 1938 to December 2000.

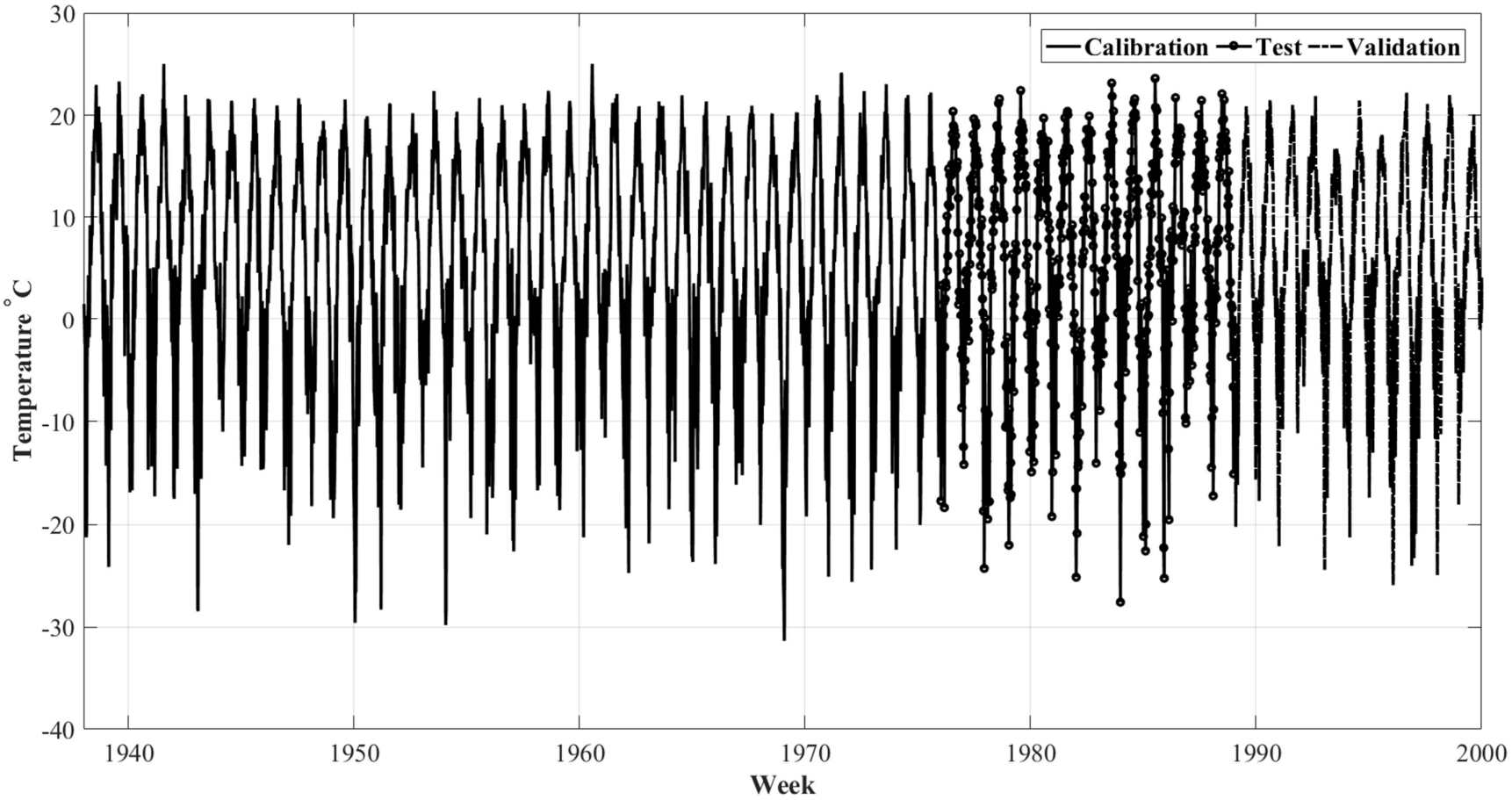

Fig. A4. Weekly Temperature time series for 63 years spanning from January 1938 to December 2000 from Environment Canada website.

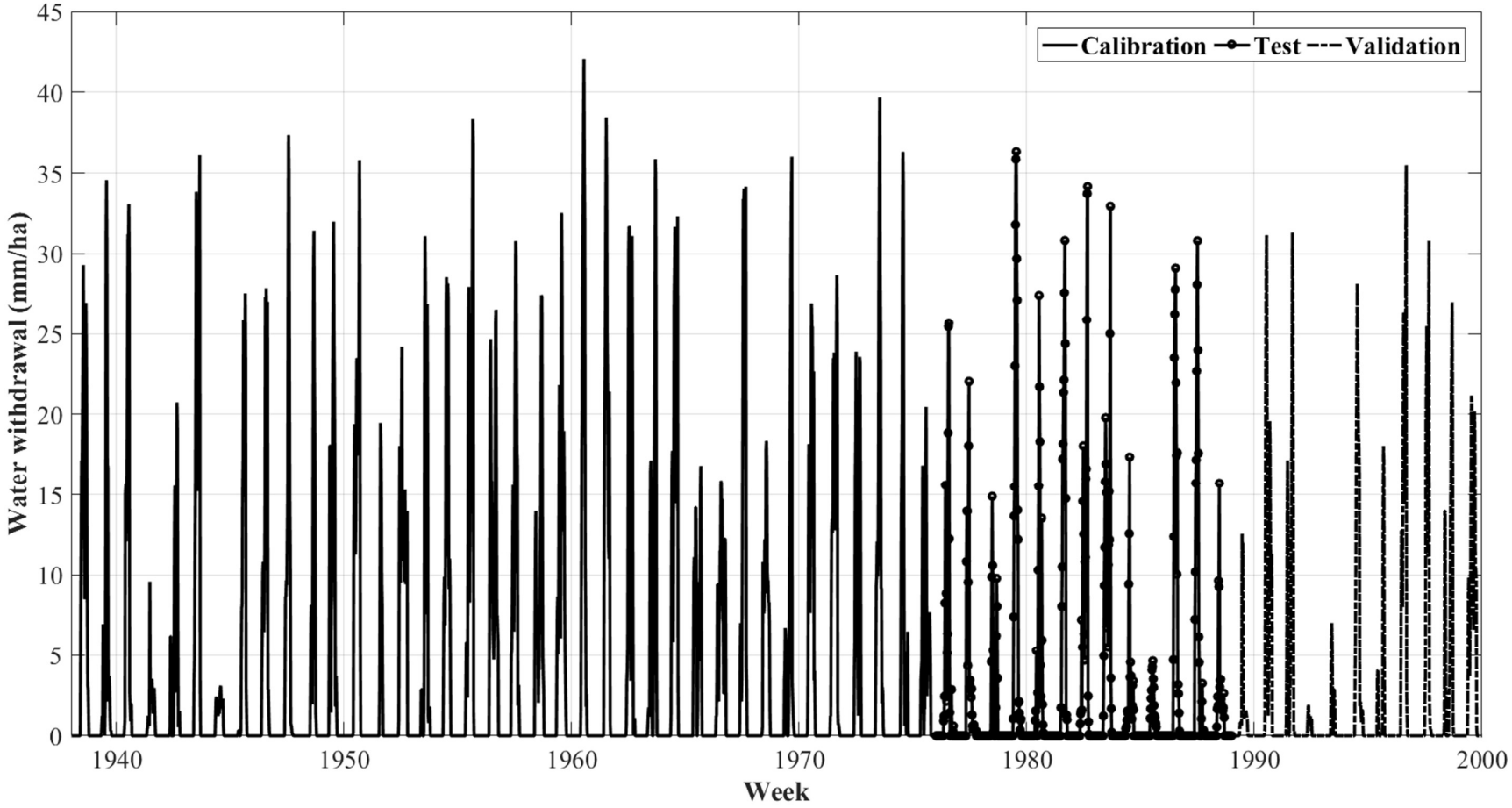

Fig. A5. Weekly WRMM water withdrawal time series for 63 years spanning from January 1938 to December 2000.

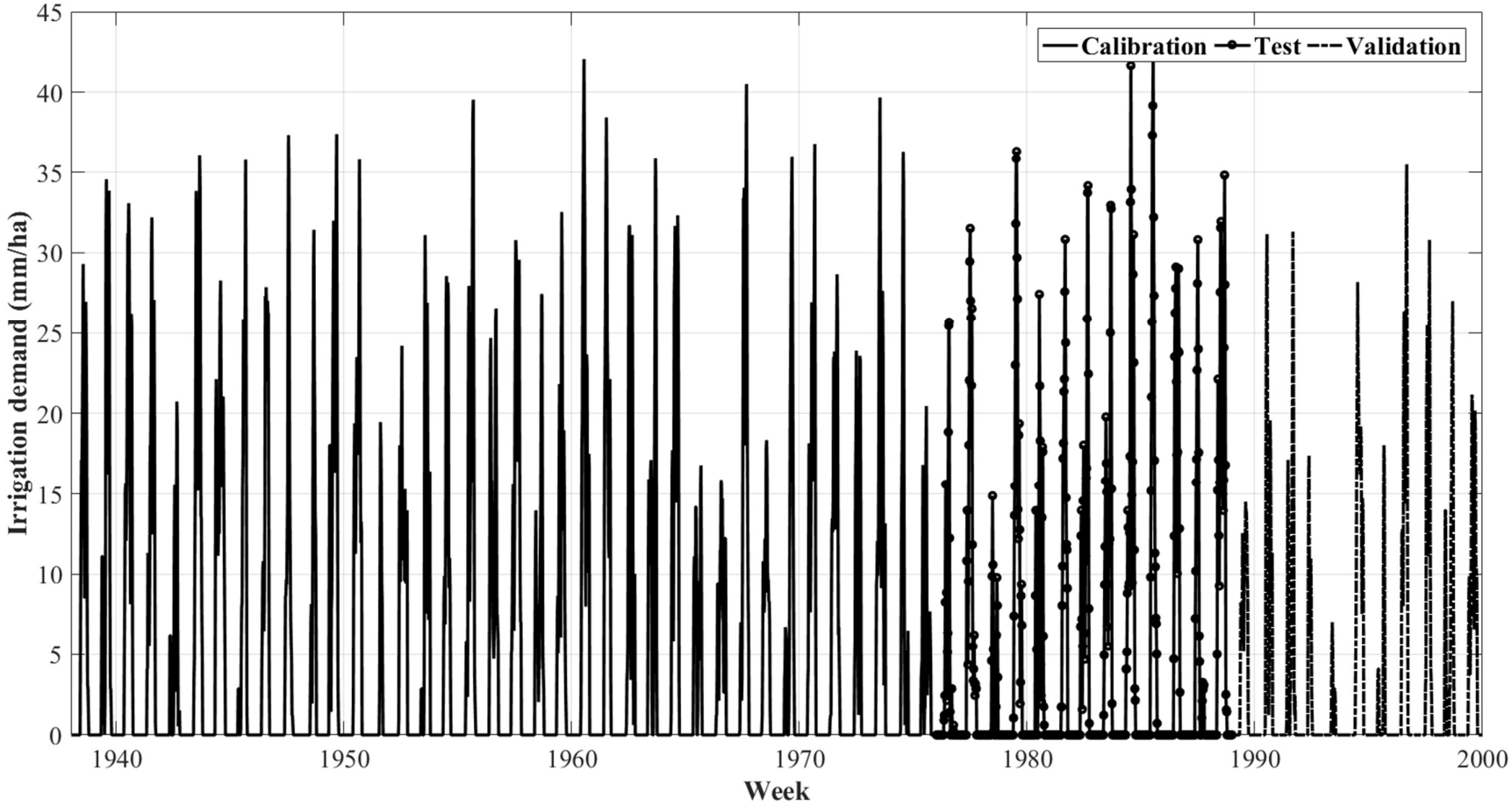

Fig. A6. Weekly WRMM irrigation demand time series for 63 years spanning from January 1938 to December 2000.

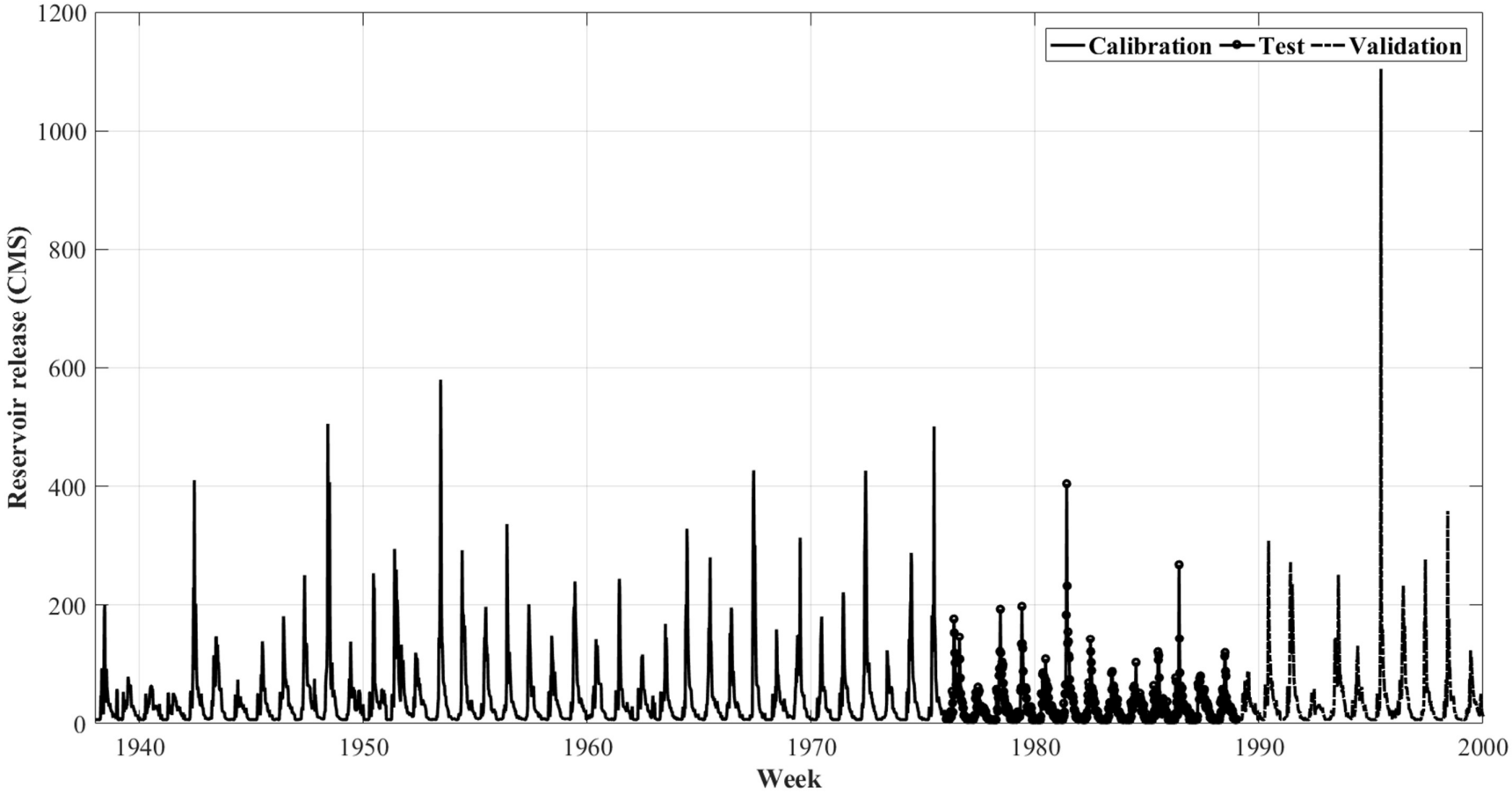

Fig. A7. Weekly WRMM reservoir release time series for 63 years spanning from January 1938 to December 2000.

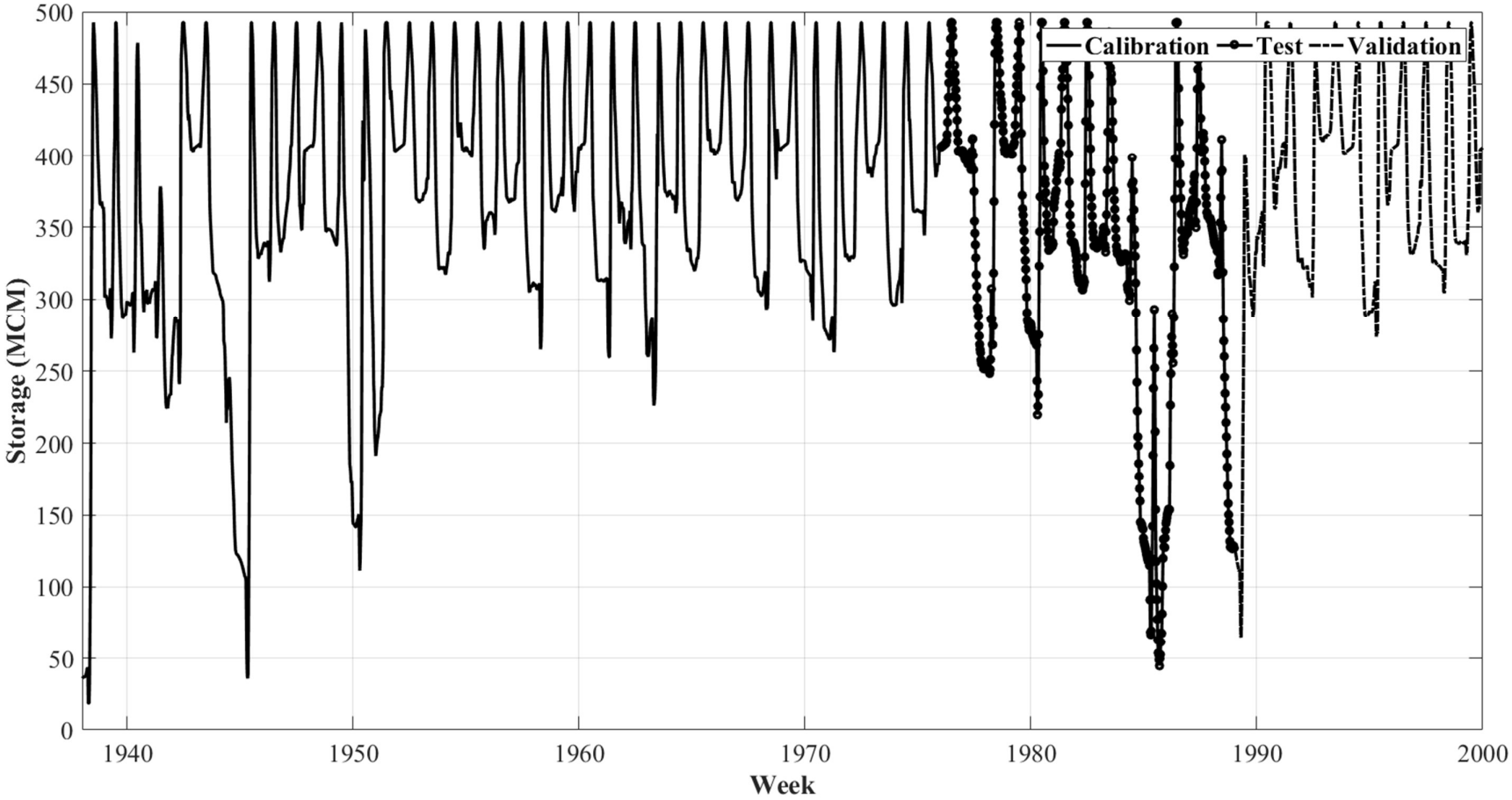

Fig. A8. Weekly WRMM storage time series for 63 years spanning from January 1938 to December 2000.